SIAM J. APPLIED DYNAMICAL SYSTEMS
Vol. 15, No. 2, pp. 655–712

A Geometric Approach to Stationary Defect Solutions in One Space Dimension*

A. Doelman†, P. van Heijster‡, and F. Xie§

Abstract. In this manuscript, we consider the impact of a small jump-type spatial heterogeneity on the existence of stationary localized patterns in a system of partial differential equations in one spatial dimension, i.e., defined on $\mathbb{R}$. This problem corresponds to analyzing a discontinuous and nonautonomous n-dimensional system, $\dot{u} = \begin{cases} f(u), & t \leq 0, \\ f(u) + \varepsilon g(u), & t > 0, \end{cases}$ under the assumption that the unperturbed system, i.e., the $\varepsilon \to 0$ limit system, possesses a heteroclinic orbit Γ that connects two hyperbolic equilibrium points (plus several additional nondegeneracy conditions). The unperturbed orbit Γ represents a localized structure in the PDE setting. We define the (pinned) *defect solution* Γ_ε as a heteroclinic solution to the perturbed system such that $\lim_{\varepsilon \to 0} \Gamma_\varepsilon = \Gamma$ (as graphs). We distinguish between three types of defect solutions: trivial, local, and global defect solutions. The main goal of this manuscript is to develop a comprehensive and asymptotically explicit theory of the existence of local defect solutions. We find that both the dimension of the problem as well as the nature of the linearized system near the endpoints of the heteroclinic orbit Γ have a remarkably rich impact on the existence of these local defect solutions. We first introduce the various concepts in the setting of planar systems ($n = 2$) and—for reasons of transparency of presentation—consider the three-dimensional problem in full detail. Then, we generalize our results to the n-dimensional problem, with special interest for the additional phenomena introduced by having $n \geq 4$. We complement the general approach by working out two explicit examples in full detail: (i) the existence of pinned local defect kink solutions in a heterogeneous Fisher–Kolmogorov equation ($n = 4$) and (ii) the existence of pinned local defect front and pulse solutions in a heterogeneous generalized FitzHugh–Nagumo system ($n = 6$).

Key words. defect solutions, heterogeneous media, discontinuous systems, heteroclinic orbits

AMS subject classifications. 34A34, 34A36, 34C37, 34E10, 35B20, 35B36, 35K57

DOI. 10.1137/15M1026742

1. Introduction.

In this manuscript, we develop a general geometrical theory on the impact of small jump-like defects, which we will call *weak defects*, on the existence of heteroclinic and homoclinic orbits in a general class of n-dimensional first order ordinary differential equations (ODEs). The weak defect appears as a small discontinuous, nonautonomous term

*Received by the editors June 18, 2015; accepted for publication (in revised form) by A. Scheel February 19, 2016; published electronically April 5, 2016.
http://www.siam.org/journals/siads/15-2/M102674.html

†Mathematisch Instituut, Leiden University, 2300 RA Leiden, the Netherlands (doelman@math.leidenuniv.nl).

‡School of Mathematical Sciences, Queensland University of Technology, Brisbane, QLD 4000, Australia (petrus.vanheijster@qut.edu.au). This author's work was supported by the Australian Research Council's Discovery Early Career Researcher Award funding scheme DE140100741.

§Department of Applied Mathematics, Donghua University, Shanghai 201620, People's Republic of China (fxie@dhu.edu.cn). The author's work was supported by the Natural Science Foundation of Shanghai under grant 15ZR1400800.

in the dynamical system

$$\dot{u} = \begin{cases} f(u), & t \leq 0, \\ f(u) + \varepsilon g(u), & t > 0, \end{cases} \tag{1.1}$$

where $u : \mathbb{R} \to \mathbb{R}^n$, ε is a small positive parameter, and $f(u), g(u) : \mathbb{R}^n \to \mathbb{R}^n$ are sufficiently smooth and $\mathcal{O}(1)$ with respect to ε.

System (1.1) represents a spatial dynamical system associated with a partial differential equation (PDE) with a small spatial jump-type heterogeneity in one space dimension x ($\in \mathbb{R}$) that appears as t in (1.1). There is extensive literature on the impact of spatial heterogeneities on the dynamics of PDEs; see, for instance, [2, 4, 14, 15, 16, 31, 36, 37, 40, 41, 45, 46, 47, 61, 64], where various types of defects are considered. For example, in [47] delta-function defects are used to model point-sources and the impact of these heterogeneities on fluxons is studied, while in [2, 4, 36, 61] the effect of step-function-like diffusion coefficients on traveling waves [4, 36, 61] and Turing patterns [2] supported by reaction-diffusion equations in one or more spatial dimensions is studied. For Turing patterns, it appears that the heterogeneity can act as a pattern selector, thus making the observed Turing patterns more robust [2]. In [15, 16, 40, 41], the effect of discontinuous, jump-type defects in the potential of a sine-Gordon equation is discussed. In these articles, several pinned waves are constructed and their stability is analyzed. This was one of the first times that the stability for pinned waves in heterogeneous media was rigorously proved. In [37, 45, 46], localized structures in heterogeneous Schrödinger equations are studied.

Recently, heterogeneous systems have been identified as offering promising future device applications, such as novel circuits for information storage and processing in both classical and quantum limits [24], a single flux quantum-based logic circuit [51], and artificial crystals for simulating and studying energy levels and band structures in large systems of spins [60]. Also, step-function-like defects have been used to describe the different production regimes of certain bone morphogenetic proteins for models of drosophila [62] and sea urchin [32] embryo development. While the above overview is far from complete, it signifies the importance of defect solutions and the attention they have recently started to get in the PDE literature.

The analysis in this manuscript is directly motivated by our previous study [31] of a heterogeneous generalized three-component FitzHugh–Nagumo (FHN) system

$$\begin{cases} U_t = \varepsilon^2 U_{xx} + U - U^3 - \varepsilon(\alpha V + \beta W + \gamma(x)), \\ \tau V_t = V_{xx} + U - V, \\ \theta W_t = D^2 W_{xx} + U - W \end{cases} \tag{1.2}$$

with $U, V, W : \mathbb{R} \times \mathbb{R}^+ \to \mathbb{R}, \alpha, \beta \in \mathbb{R}, D > 1, \tau, \theta > 0, 0 < \varepsilon \ll 1$. The spatial heterogeneity is modeled by a discontinuous, jump-like change in the parameter γ at $x = 0$,

$$\gamma(x) = \begin{cases} \gamma_1 & \text{for } x \leq 0\,, \\ \gamma_2 & \text{for } x > 0\,, \end{cases} \tag{1.3}$$

with $\gamma_{1,2} \in \mathbb{R}$. The original homogeneous three-component dimensional version of this model, i.e., $\gamma_1 = \gamma_2$, was proposed in [50, 58] to explore gas discharge phenomena (see [55] for a

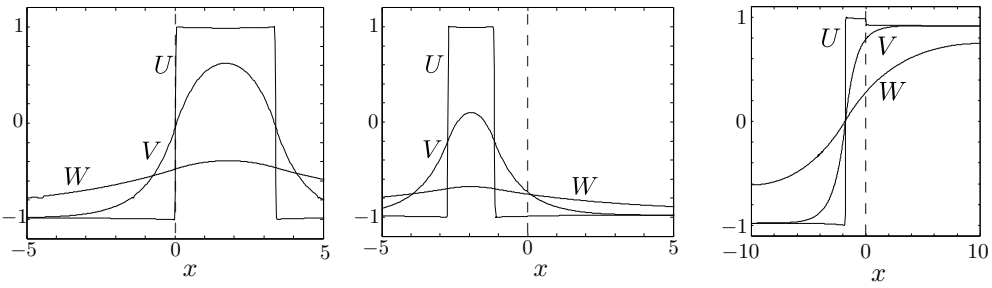

Figure 1. *Left panel: a global defect pulse (or 2-front) solution pinned with its back near the defect at $x = 0$ (indicated by the dashed line) supported by (1.2). The system parameters are as follows $(\alpha, \beta, D, \gamma_1, \gamma_2, \tau, \theta, \varepsilon) = (3, 2, 5, 2, 1, 1, 1, 0.01)$. Middle panel: a local defect pulse (or 2-front) solution pinned away from the defect supported by (1.2). The system parameters are the same as for the left panel and only the initial condition of the PDE was different. Right panel: a local defect 1-front solution pinned away from the defect supported by (1.2). The system parameters are as follows $(\alpha, \beta, D, \gamma_1, \gamma_2, \tau, \theta, \varepsilon) = (3, 2, 5, 0, 10, 1, 1, 0.01)$. The left panel and middle panel are both adapted from Figure 5 of [31] and are reproduced with permission.*

review article) and versions of it have been studied extensively since; see [5, 6, 7, 8, 9, 17, 29, 30, 33, 34, 49, 63] and references therein. The heterogeneous version (1.2) is studied in [31, 64]. In [31] it is shown that under certain conditions on the parameters and the spatial heterogeneity or defect (1.3), system (1.2) supports stable pinned stationary front and pulse solutions. These solutions are pinned with their front or back near the defect, i.e., near $x = 0$. In this manuscript, we call this type of defect solutions *global defect solutions* (see Definition 1.4 and Remark 1.5). See the left panel of Figure 1 for an example of a pinned global defect pulse solution of (1.2) with its back pinned near the defect. However, in [31] also another type of pinned localized defect solutions supported by (1.2) is identified, namely, defect solutions pinned away from the defect. Neither the existence nor the stability of this type of defect solutions, which we call *local defect solutions* in this manuscript (see Definition 1.4), can be studied with the approach of [31]. See the two right panels of Figure 1 for an example of a pinned local defect pulse solution (middle panel) and a pinned local defect front solution (right panel) supported by (1.2).

Besides pinning a solution, a defect may also *annihilate, rebound, penetrate,* or *split* a (traveling) solution, and it may correspond to a source (or sink) sending out (or absorbing) traveling waves; see, for example, [15, 16, 31, 42, 64]. We do not consider these phenomena in the current manuscript. Here, we focus on the most simple situation of a heterogeneously perturbed homogeneous system in one space dimension that supports a localized stationary solution of front or pulse type in the unperturbed homogeneous setting. In the homogeneous setting, the precise position of this front or pulse is not determined, due to the (assumed) translational symmetry of the PDE model. If such a front or pulse *survives* the effect of the heterogeneous perturbation, then it gets pinned at (a) very specific position(s)—as in the case of model problem (1.2); see Figure 1. The existence problem associated to these pinned, and thus stationary, defect solutions has the general form of (1.1), in which the one-dimensional spatial variable x plays the role of the time t. The specific structure of (1.1) implies that we choose to focus on a class of small heterogeneities of the type represented by (1.3): the defects considered here are of jump-type in the sense that there is a small difference between

the PDE system for $x \leq 0$ and that for $x > 0$, modeled by the term $\varepsilon g(u)$ that appears for $t > 0$ in (1.1); see also Remark 1.13 for a somewhat more general setting. Note that the perturbations modeled by $\varepsilon g(u)$ can be much richer than just a (small) jump in the value of a parameter—see, for instance, the upcoming examples (1.8) and (2.4). More specifically, to study pinned defect solutions supported by (1.2), we can cast (1.2) into the form of (1.1) with $n = 6$ (see (1.9) and, again, Remark 1.13).

This leads to the following question: can we develop a general theory for the persistence and/or existence of *defect solutions* supported by (1.1) for *generic perturbations* $\varepsilon g(u)$ under mild, generic, assumptions—see section 1.1—on the *unperturbed system*

$$\dot{u} = f(u), \qquad u(t) : \mathbb{R} \to \mathbb{R}^n? \tag{1.4}$$

While this appears to be a natural question, it has, to the best of our knowledge, not been considered in this generality in the ODE literature; see Remark 1.1.

Remark 1.1. The ODE/dynamical systems literature on discontinuous systems mainly concentrates on control problems, where the discontinuities are designed to regularize or stabilize solutions; see, for example, [10] and references therein. In particular, the *sliding motion* or *grazing flow* of trajectories along the discontinuity are studied (see, for example, [27, 44]), while the persistence of heteroclinic and homoclinic solutions are not discussed. Also, the discontinuities in these problems tend to lie in the dependent variable, see, for instance, [3], i.e., the system switches if the dependent variable crosses a particular value, so that the systems are actually autonomous. In contrast, the discontinuity in this manuscript lies in the independent variable, i.e., the system switches if the independent variable crosses a particular value, and it is thus truly nonautonomuous.

1.1. Problem setting, definitions, and assumptions. Before we go into the details of (partly) answering the question raised above, we discuss the *mild, generic, assumptions* mentioned above in more detail.

1.1.1. Assumptions on (1.4). The first generic assumption states that the unperturbed system (1.4) only has isolated hyperbolic equilibrium points.

Hypothesis H1. *System* (1.4) *only has isolated equilibrium points and all these isolated equilibrium points are hyperbolic in the sense that the Jacobians of the equilibrium points have no eigenvalues on the imaginary axis.*

We label these isolated hyperbolic equilibrium points $P_i, i = 1, 2, \ldots, N$, with N a positive integer (that may be $+\infty$). Since (1.4) is independent of ε, all the eigenvalues of the Jacobians of the equilibrium points are $\mathcal{O}(1)$ with respect to ε. Therefore, provided that ε is small enough, Hypothesis H1 and the implicit function theorem imply that the *fully perturbed system*

$$\dot{u} = f(u) + \varepsilon g(u), \qquad u(t) : \mathbb{R} \to \mathbb{R}^n, \tag{1.5}$$

also has N isolated hyperbolic equilibrium points P_i^ε with $\lim_{\varepsilon \to 0} P_i^\varepsilon = P_i$ for $i = 1, 2, \ldots, N$. In particular, all the eigenvalues of the Jacobians of the equilibrium points P_i^ε are also $\mathcal{O}(1)$ with respect to ε.

We are interested in solutions $\Gamma_\varepsilon(t)$ to (1.1) that are heteroclinic connections between a hyperbolic equilibrium point $P^- \in \{P_1, P_2, \ldots, P_N\}$ of the unperturbed system (1.4) and

a hyperbolic equilibrium point $P_\varepsilon^+ \in \{P_1^\varepsilon, P_2^\varepsilon, \dots, P_N^\varepsilon\}$ of the fully perturbed system (1.5), that can be seen as perturbations of an heteroclinic (or homiclinic) orbit $\Gamma(t)$ that connects P^- to $P^+ = \lim_{\varepsilon\to 0} P_\varepsilon^+$ in the unperturbed system (1.4). More specifically, we search for C^0-solutions $\Gamma_\varepsilon(t)$ of (1.1) with $\lim_{t\to-\infty} \Gamma_\varepsilon(t) = P^-$, and $\lim_{t\to\infty} \Gamma_\varepsilon(t) = P_\varepsilon^+$ such that the graph of the orbit of $\Gamma_\varepsilon(t)$ in the n-dimensional phase space of (1.1) is asymptotically close to that of Γ. That is, $\lim_{\varepsilon\to 0} dist(\Gamma_\varepsilon, \Gamma) = 0$, where we define the distance between the graphs of Γ and Γ_ε by

$$dist(\Gamma_\varepsilon, \Gamma) := \sup_{t\in\mathbb{R}} \left\{ \inf_{s\in\mathbb{R}} \|\Gamma(t) - \Gamma_\varepsilon(s)\| \right\}. \tag{1.6}$$

Note that here, and in the rest of the manuscript, we use $\|\cdot\|$ to denote the Euclidean norm in $\mathbb{R}^n$. We call this type of solution $\Gamma_\varepsilon(t)$ a *defect solution*. So, we assume that $\Gamma(t)$ is a heteroclinic (or homoclinic) orbit supported by the unperturbed system (1.4) connecting P^- and P^+. Moreover, we assume that this $\Gamma(t)$ is *minimaly nontransversal*. Note that $\Gamma(t)$ indeed corresponds to a localized structure of front or pulse type in the original, homogeneous, PDE setting and that $\Gamma_\varepsilon(t)$ can be seen as a pinned version of this localized structure in the heterogeneously perturbed model.

Hypothesis H2. *The unperturbed system (1.4) has a heteroclinic orbit Γ connecting the equilibrium point P^- with the equilibrium point P^+ in forward time and all the eigenvalues of the linearization around $P^\pm$ are simple. In other words, there is a $\Gamma \subset \mathcal{W}^u(P^-) \cap \mathcal{W}^s(P^+)$. Furthermore, we assume that this intersection is "minimally nontransversal." That is,*

- *if* $\dim(\mathcal{W}^u(P^-)) + \dim(\mathcal{W}^s(P^+)) \le n$, *then* $\dim(\mathcal{W}^u(P^-) \cap \mathcal{W}^s(P^+)) = 1$; *and*
- *if* $\dim(\mathcal{W}^u(P^-)) + \dim(\mathcal{W}^s(P^+)) = m > n$, *then* $\dim(\mathcal{W}^u(P^-) \cap \mathcal{W}^s(P^+)) = m - n$, *and the intersection is transversal.*

Of course, the stable and unstable manifolds must be smooth in a neighborhood of $\Gamma \subset \mathcal{W}^u(P^-) \cap \mathcal{W}^s(P^+)$. Moreover, observe that we a priori do not impose more explicit nontangency conditions on the way $\mathcal{W}^u(P^-)$ and $\mathcal{W}^s(P^+)$ intersect in the case that $\dim(\mathcal{W}^u(P^-)) + \dim(\mathcal{W}^s(P^+)) \le n$. This will come up, though, as an additional assumption in the statements of various of the upcoming theorems (see especially section 3). Also note that P^+ in Hypothesis H2 can in principle be equal to P^- such that we actually have a homoclinic orbit; see also Remark 1.11. Observe that Hypotheses H1 and H2 are both assumptions on (1.4) and therefore independent of the particulars of the perturbation $\varepsilon g(u)$. See also Remark 1.3.

The *minimally nontransversal* condition can be interpreted as the fact that the intersection of the manifolds is assumed to be *as generic as possible*: if $\dim(\mathcal{W}^u(P^-)) + \dim(\mathcal{W}^s(P^+)) \le n$, then the heteroclinic orbit Γ ($\subset \mathcal{W}^u(P^-) \cap \mathcal{W}^s(P^+)$) is isolated, while it is as low-dimensional as possible if $\dim(\mathcal{W}^u(P^-)) + \dim(\mathcal{W}^s(P^+)) > n$. For example, in the nongeneric case that a two-dimensional unstable manifold $\mathcal{W}^u(P^-)$ and a three-dimensional stable manifold $\mathcal{W}^s(P^+)$ intersect in a six-dimensional space to create a heteroclinic orbit Γ, we assume that this intersection is maximal generic. That is, near P^+, $\mathcal{W}^u(P^-) \not\subset \mathcal{W}^s(P^+)$ such that $\dim(\mathcal{W}^u(P^-) \cap \mathcal{W}^s(P^+)) \neq 2$. Similarly, if instead $\dim(\mathcal{W}^u(P^-)) = 5$, then $\dim(\mathcal{W}^u(P^-) \cap \mathcal{W}^s(P^+)) = 2$ and not 3.

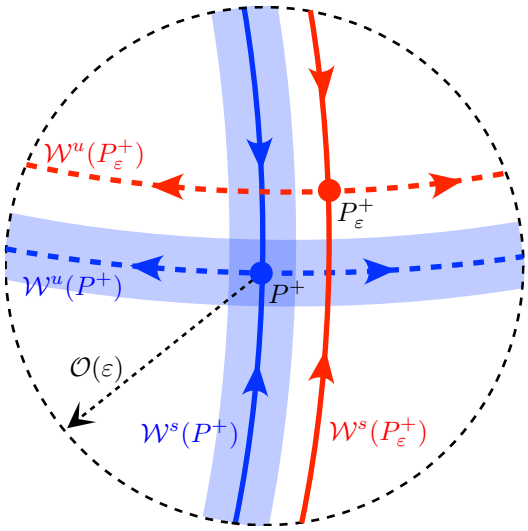

Figure 2. *For a generic perturbation, we have that* $dist(\mathcal{W}^{s,u}_{\text{loc}}(P^+), P_\varepsilon^+) = \mathcal{O}_s(\varepsilon)$ *near* P^+. *That is,* P_ε^+ *does not lie inside of the shaded blue regions (that have a width asymptotically smaller than* ε*). By Hypothesis* H1 *the stable and unstable manifolds of* P_ε^+ *and* P^+ *are locally parallel and consequently they do not intersect within an* $\mathcal{O}(\varepsilon)$ *neighborhood of* P_ε^+.

1.1.2. Assumptions on the perturbation $\varepsilon g(u)$. The perturbation $\varepsilon g(u)$ is assumed to be (asymptotically) generic such that the perturbed equilibrium point of interest P_ε^+ and the unperturbed local stable and unstable manifold of P^+ are not too close to each other.

Definition 1.2. *We call the perturbation* (1.1) *of* (1.4) *a(n) (asymptotically)* generic perturbation *near* P^+ *if the distance between* $\mathcal{W}^{s,u}_{\text{loc}}(P^+)$ *and* P_ε^+ *is strictly of order* ε *and not smaller, that is,*

$$dist(\mathcal{W}^{s,u}_{\text{loc}}(P^+), P_\varepsilon^+) = \inf_{x \in \mathcal{W}^{s,u}_{\text{loc}}(P^+)} \|x - P_\varepsilon^+\| = \mathcal{O}_s(\varepsilon)\,.$$

See Figure 2 for a graphical representation of a generic perturbation.

Hypothesis H3. *For* $\mathcal{W}^{s,u}(P^+) \neq n$, *we assume that the perturbation* $\varepsilon g(u)$ *of* (1.1) *is a generic perturbation near* P^+.

For $\mathcal{W}^{s,u}(P^+) = n$, every perturbation is a nongeneric perturbation according to Definition 1.2 since $d(\mathcal{W}^{s,u}_{\text{loc}}(P^+), P_\varepsilon^+) = 0$ in this case. Therefore, this particular case has to be excluded from Hypothesis H3. However, the results presented in this manuscript are actually straightforward to obtain in this case and the derived results hold independent of the particular form of the perturbation.

Since the equilibrium points P^+ and P_ε^+ are isolated and hyperbolic by Hypothesis H1, we have that $\mathcal{W}^s(P^+)$ and $\mathcal{W}^s(P_\varepsilon^+)$ are *locally parallel* near P_ε^+. That is, near P_ε^+—and to leading order in ε—$\mathcal{W}^s(P_\varepsilon^+)$ is a linear translation of $\mathcal{W}^s(P^+)$. Consequently, by Hypothesis H3 we have that $\mathcal{W}^s(P_\varepsilon^+)$ and $\mathcal{W}^s(P^+)$ do not intersect within an $\mathcal{O}(\varepsilon)$ neighborhood of P_ε^+. Similarly, also $\mathcal{W}^u(P^+)$ and $\mathcal{W}^u(P_\varepsilon^+)$ are *locally parallel* near P_ε^+ and do not intersect within an $\mathcal{O}(\varepsilon)$ neighborhood of P_ε^+. See Figure 2; $\mathcal{W}^s(P_\varepsilon^+)$ and $\mathcal{W}^s(P^+)$ do not intersect and similarly $\mathcal{W}^u(P_\varepsilon^+)$ and $\mathcal{W}^u(P^+)$ do not intersect near P^+/P_ε^+.

Remark 1.3. The assumptions as formulated in Hypotheses H1–H3 are stronger than necessary for establishing (most of) the results in the manuscript. For instance, it is certainly not necessary that all equilibrium points of (1.4) are hyperbolic, that all eigenvalues associated with the "endpoints" P^- and P^+ are simple and defect solutions will certainly exist in systems with nongeneric perturbations. See also Remark 1.13. Nevertheless, our present choice makes the analysis, and thus the presentation, as simple and transparent as possible.

1.1.3. Types of defect solutions. The goal of this manuscript is to derive necessary and sufficient conditions on the underlying systems for which defect solutions exist under the assumptions stated in Hypotheses H1–H3. We use (as much as possible) a *geometric approach* to construct these defect solutions. By definition, a defect solution lies in the intersection of $\mathcal{W}^u(P^-)$ and $\mathcal{W}^s(P_\varepsilon^+)$ of (1.1). For $t \leq 0$, $\mathcal{W}^u(P^-)$ of (1.1) is identical to $\mathcal{W}^u(P^-)$ of (1.4), while for $t > 0$, $\mathcal{W}^s(P_\varepsilon^+)$ of (1.1) is identical to $\mathcal{W}^s(P_\varepsilon^+)$ of (1.5). Therefore, we can restrict ourselves to studying the phase portraits of (1.4) and (1.5) to obtain qualitative information on defect solutions of (1.1). In particular, an intersection of a trajectory of $\mathcal{W}^u(P^-)$ of (1.4) and a trajectory of $\mathcal{W}^s(P_\varepsilon^+)$ of (1.5) yields a defect solution of (1.1) that can be obtained by concatenating the intersecting trajectories at $t = 0$. That is, we parametarize t in such a way that the *switch* between (1.4) and (1.5) occurs at the intersection point, which we call the *defect point* in the remainder of this manuscript. The location of the defect point in the phase portrait determines the type of the defect solution and we distinguish between three types of defect solutions.

Definition 1.4. *A defect solution* $\Gamma_\varepsilon(t)$ *is called*

- *a* trivial defect solution *if* $P^- = P^+$ *and*

$$\lim_{\varepsilon\to 0}\left(\sup_{t\in\mathbb{R}}\|\Gamma_\varepsilon(t) - P^+\|\right) = 0\,;$$

- *a* local defect solution *if either*

$$\lim_{\varepsilon\to 0}\left(\sup_{t>0}\|\Gamma_\varepsilon(t) - P^+\|\right) = 0 \qquad \text{or} \qquad \lim_{\varepsilon\to 0}\left(\sup_{t\leq 0}\|\Gamma_\varepsilon(t) - P^-\|\right) = 0\,; \tag{1.7}$$

  and, moreover we say that the defect occurs near P_ε^+ *if the first condition of* (1.7) *holds and the defect occurs near* P^- *if the second condition of* (1.7) *holds; and*

- *a* global defect solution *if*

$$\lim_{\varepsilon\to 0}\left(\sup_{t>0}\|\Gamma_\varepsilon(t) - P^+\|\right) > 0 \qquad \text{and} \qquad \lim_{\varepsilon\to 0}\left(\sup_{t\leq 0}\|\Gamma_\varepsilon(t) - P^-\|\right) > 0\,.$$

See Figure 3 for a schematic depiction of the three types of defect solutions discussed in Definition 1.7. In other words, for a trivial defect solution the *defect point* lies in the $o(1)$ neighborhood of P^+. For a local defect solution near P_ε^+ (P^-), the defect point lies in the $o(1)$ neighborhood of P^+ (P^-) and $O(1)$ away from P^- (P^+). So, if the *defect point* is (asymptotically) close to P_ε^+ but not (asymptotically) close to P^-, then we have a local defect solution near P_ε^+. A *defect point* $\mathcal{O}(1)$ away from both P_ε^+ and P^- yields a global defect solution. See, for example, Figure 5. However, observe that the distinction between local defect solutions and global defect solutions is not always unambiguous; see Remark 1.5.

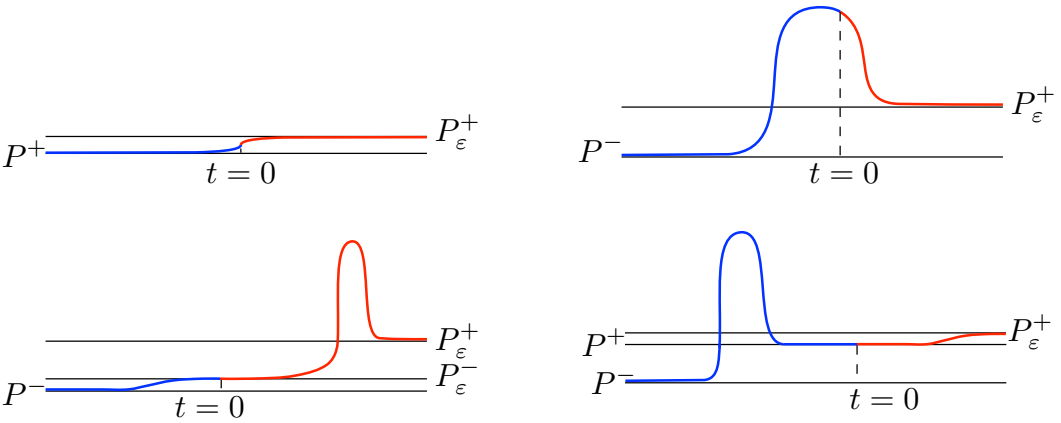

Figure 3. *Sketches of the three types of defect solutions described in Definition 1.4. Top left panel: a trivial defect solution connecting P^+ with P_ε^+. Top right panel: a global defect solution connecting P^- with P_ε^+. Bottom panels: a local defect solution near P^-, respectively, P_ε^+.*

We do not consider global defect solutions in the current manuscript. This is in general a very hard problem since it requires full control of the global flow of both (1.4) for $t \leq 0$ and (1.5) for $t > 0$ near the heteroclinic orbit Γ and this goes beyond the scope of this manuscript if $n \geq 3$; see Remark 1.6. However, see section 2.1 for an example of an explicit model with $n = 2$ for which the existence of countable many global defect solutions can be shown.

Remark 1.5. It is not always natural to make a precise distinction between global defect solutions and local defect solutions. For instance, there may be a continuous family of defect solutions ranging from being local to being global—see, for instance, the two-dimensional sketch given in Figure 8. In higher dimensions, there may be countably many distinct intersections $\mathcal{W}^u(P^-) \cap \mathcal{W}^s(P_\varepsilon^+)$ that also range between local and global; see Remark 3.7. Moreover, in systems in which also the unperturbed $t \leq 0$ part depends explicitly on ε—such as the ODE (1.9) associated (1.2) and more generally as described in Remark 1.13—one must also be more careful with this distinction. Nevertheless, Definition 1.4 is sufficiently clear to work with in the upcoming analysis.

Remark 1.6. In the case that we know that the unperturbed heteroclinic/homoclinic orbit Γ exists as a transversal intersection of $\mathcal{W}^u(P^-)$ and $\mathcal{W}^s(P^+)$, it follows (under general conditions) that $\mathcal{W}^u(P^-)$ and $\mathcal{W}^s(P_\varepsilon^+)$ may typically also intersect. In the most interesting and relevant case that $\dim(\mathcal{W}^u(P^-)) + \dim(\mathcal{W}^s(P^+)) = n$—see Remark 1.11 and section 3—this intersection will generically be zero-dimensional, i.e., it will consist of one or more points (see, for instance, Figure 7). In fact, the statement that there typically will be a discrete number of defect solutions—either local or global—may in principle be made rigorous under abstract conditions. However, controlling the position and the number of these points in the (global) case in which they are not close to either P^- or P^+ is in general a hard problem for which explicit information on the global character of $\mathcal{W}^u(P^-)$ and $\mathcal{W}^s(P^+)$ is required. These issues may be handled if the system is singularly perturbed [31]. Here, we refrain from going into the details.

1.2. Main results and outline. This is quite a long manuscript, in which we develop a comprehensive general theory on local defect solutions in n-dimensional systems of type (1.1) that satisfy Hypotheses H1–H3; see section 2 and especially section 3. Moreover, we apply the general theory to two explicit examples in section 4. The second example of those actually considers the three-component FHN system (1.2) and settles the issues that originally motivated this work. This second example also shows that the approach developed in sections 2 and 3 can, due to its geometric nature, also be applied to more general systems; see Remarks 1.3 and 1.13. Furthermore, it is also shown by this example that it can be possible to *control* the abstract twist conditions of the upcoming Theorem 1.9 and section 3 in an explicit (singular perturbed) setting.

First, we observe that a unique trivial defect solution of (1.1) generically exists for sufficiently small $\varepsilon > 0$ since $\mathcal{W}^s(P^+)$ and $\mathcal{W}^u(P^+)$ intersect transversally at P^+ and the local stable manifold of P_ε^+ lies close to $\mathcal{W}^s(P^+)$ such that the transversal intersection persists by the *local stable and unstable manifold theorem* (*e.g.*, [48]). See also Figure 2.

Lemma 1.7. *Assume that Hypothesis* H1 *holds. Then, for $\varepsilon > 0$ small enough, system* (1.1) *has a unique trivial defect solution $\Gamma_\varepsilon(t)$ connecting P^+ and P_ε^+, where $P^+ = \lim_{\varepsilon\to 0} P_\varepsilon^+$.*

The statement of Lemma 1.7 has already appeared in the literature; see, for example, [64]. However, we have not been able to find a proof of this (indeed somewhat straightforward) result in the literature, and for completeness of the presentation, we present a short geometric proof in section 2.3.

The existence of local defect solutions depends heavily on the local flow near the equilibrium point where the defect occurs and is therefore closely related to the nature of the heteroclinic (or homoclinic; see Remark 1.11) connections of (1.4) and (1.5) and the dimensions of the associated stable and unstable manifolds. In section 2.4, we prove the following result primarily by using a dimension counting argument and the fact that the (un)stable manifold and the perturbed (un)stable manifold are *locally parallel* and thus do not intersect in the vicinity of the equilibrium point of interest.

Theorem 1.8. *Assume that Hypotheses* H1–H3 *hold. Then, for $\varepsilon > 0$ small enough, a necessary condition for the existence of local defect solutions near P_ε^+ connecting P^- to P_ε^+ in* (1.1) *is*

$$\dim(\mathcal{W}^u(P^-)) \geq \dim(\mathcal{W}^u(P^+)).$$

Moreover, if $\dim(\mathcal{W}^u(P^-)) = \dim(\mathcal{W}^u(P^+))$*, then we necessarily also need* $\dim(\mathcal{W}^u(P^-)) > 1$ *for local defect solutions near P_ε^+ to exist.*

Finally, if

$$\dim(\mathcal{W}^u(P^-)) > \dim(\mathcal{W}^u(P^+)),$$

then the necessary condition is also sufficient and (1.1) *possesses a continuous family of local defect solutions near P_ε^+.*

Theorem 1.8 does not make exact statements about the existence of local defect solutions near P_ε^+ in the case that $\dim(\mathcal{W}^u(P^-)) = \dim(\mathcal{W}^u(P^+)) > 1$. Note that this is perhaps the most relevant case, since, for instance, all pinned PDE patterns of pulse type (homoclinics) fall under this case; see Remark 1.11. Moreover, also many of the front-type localized structures in the literature are of this type; see section 4. In this setting, the characteristics of the unstable eigenvalue of the Jacobian of P^+ with smallest real part is crucial to the existence of local

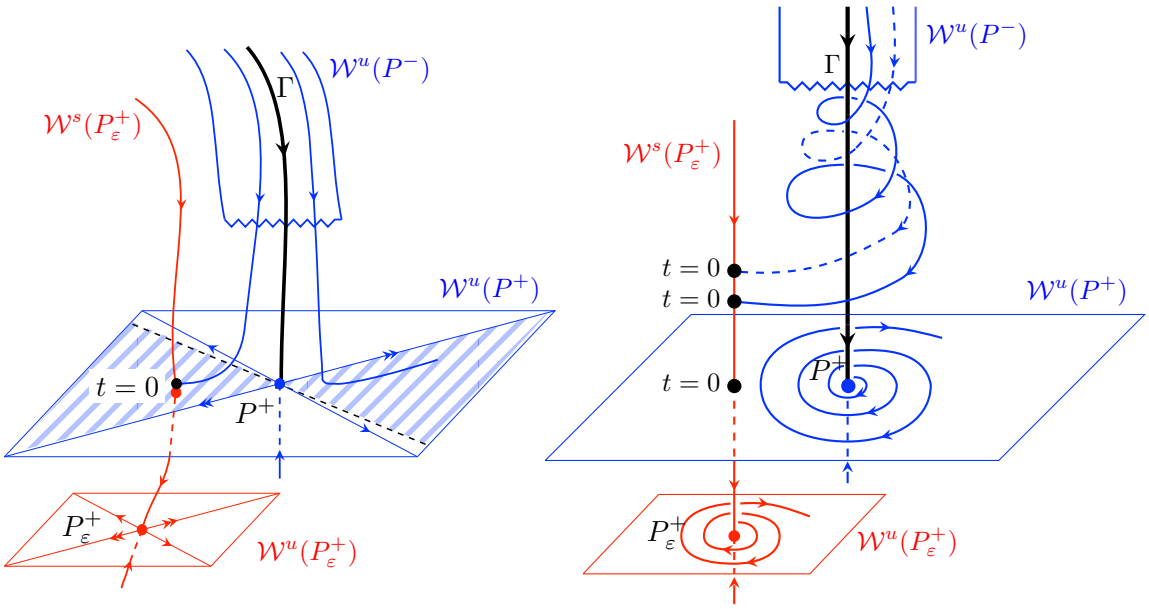

Figure 4. *Possible constructions of local defect solutions near P_ε^+ in three dimensions for* $\dim(\mathcal{W}^u(P^-)) = \dim(\mathcal{W}^u(P^+)) = 2$. *Left panel: the Jacobian of P^+ has two real positive eigenvalues and a local defect solution exists if a twist condition is met: if $\mathcal{W}^u(P^+) \cap \mathcal{W}^s(P_\varepsilon^+)$ lies in the cone (shaded region) covered by the forward flow of the local projection of $\mathcal{W}^u(P^-)$ near P^+ onto $\mathcal{W}^u(P^+)$, then a local defect solution near P_ε^+ exists. Right panel: the Jacobian of P^+ has a complex pair of eigenvalues with positive real part and countably many local defect solutions near P_ε^+ exist. See section 3.2 for the details behind this figure.*

defect solutions. We call this eigenvalue the *leading unstable eigenvalue* $\nu_{\ell+1}$; see also [35] and section 3.1.

Theorem 1.9. *Assume that Hypotheses* H1–H3 *and some transversality conditions hold and that*

$$\dim(\mathcal{W}^u(P^-)) = \dim(\mathcal{W}^u(P^+)) > 1.$$

If the leading unstable eigenvalue of the Jacobian of P^+ is complex valued, then, for $\varepsilon > 0$ small enough, system (1.4) *possesses countably many local defect solutions near P_ε^+.*

If the leading unstable eigenvalue of the Jacobian of P^+ is real valued, then, for $\varepsilon > 0$ small enough, system (1.4) *possesses at least one local defect solution near P_ε^+ as long as the (perturbed) system meets a twist condition.*

A geometric interpretation of the *twist condition* is given in the left panel of Figure 4. It should be noted that the twist condition is directly determined by the way $\mathcal{W}^u(P^-)$ twists around Γ as it *travels* from P^- to P^+. Thus, to explicitly validate such a condition, one needs to obtain information on the global behavior of $\mathcal{W}^u(P^-)$, which is in general a very hard problem—see, however, section 4.2 for an explicit example where we can obtain this information on the global behavior of $\mathcal{W}^u(P^-)$.

For the transparency of the presentation, we have kept the formulation and statement of Theorem 1.9 at a nonprecise, nontechnical level. In section 3, we provide and prove analytically precise statements on various subcases leading to, and extending, Theorem 1.9. More specifically, we quantify the *twist condition(s)* in terms of a normal form of the unperturbed system

(1.4). In section 3.2, we first analyze the $n = 3$ case in detail and carefully formulate and prove two results, Theorems 3.3 and 3.6, that together establish the statement of Theorem 1.9 for $n = 3$. Next, in section 3.3, we analyze general n-dimensional systems and establish Theorems 3.9 and 3.10, which together can be interpreted as (more carefully formulated versions of) Theorem 1.9. In section 3.3.2, we consider the impact of the strong unstable eigenvalues of the Jacobian of P^+, i.e., the nonleading unstable eigenvalues, on the existence of local defect solutions in n-dimensional systems (1.1) with $n \geq 4$. It is shown that there are various types of twist conditions, describing the existence of a unique local defect solution near P_ε^+ up to asymptotically many local defect solutions near P_ε^+; see in particular Theorems 3.11 and 3.12.

In section 4, we first consider stationary defect solutions to a heterogeneous perturbation of an extended Fisher–Kolmogorov (eFK) equation [11, 12, 53, 65]. Following [53], we bring the problem in its canonical form,

$$\frac{d^4u}{d\xi^4} + \beta\frac{d^2u}{d\xi^2} - u + u^3 = \begin{cases} 0, & \xi \leq 0, \\ \varepsilon g(u, u_\xi, u_{\xi\xi}, u_{\xi\xi\xi}), & \xi > 0, \end{cases} \tag{1.8}$$

where g is a sufficiently smooth function, $\beta < 0$, and $0 < \varepsilon \ll 1$. We utilize the result of this manuscript and [53] to prove the existence of countably many local defect solutions in the above problem.

Second, in section 4.2, we discuss the existence of local defect solutions in the generalized three-component FHN system (1.2) with a defect. Written as a system of six first order ODEs, it is given by

$$\begin{cases} u_\xi &= p\,, \\ p_\xi &= -u + u^3 + \varepsilon(\alpha v + \beta w + \gamma(\xi))\,, \\ v_\xi &= \varepsilon q\,, \\ q_\xi &= \varepsilon(v - u)\,, \\ w_\xi &= \frac{\varepsilon}{D} r\,, \\ r_\xi &= \frac{\varepsilon}{D}(w - u) \end{cases} \tag{1.9}$$

with $\xi := x/\varepsilon, \alpha, \beta \in \mathbb{R}, D > 1, 0 < \varepsilon \ll 1$, and $\gamma(\xi)$ as in (1.3). The dimensions of the unstable and stable manifolds of the equilibrium points of interest to us are equal and bigger than one and the corresponding eigenvalues are real valued. Although this system is not exactly of the type (1.1) (see Remark 1.13), we can apply the geometric approach of this manuscript and deduce that a *twist condition* decides about the existence of local defect solutions as shown in the right panel of Figure 1. Note that it is general very tricky to check the *twist conditions* since they are obtained from global information and they are based on the normal form of the unperturbed system (1.4). However, for the problem at hand we can use its singular perturbed nature to geometrically interpret these *twist conditions* to prove the existence of pinned local defect front solutions and pinned local defect pulse solutions.

We end the manuscript with a summary of the results and an outlook to future projects; see section 5.

Remark 1.10. Throughout this manuscript, we use the same color coding as is used in Figure 4. Blue trajectories represent trajectories on $\mathcal{W}^{s,u}(P^-)$ of the unperturbed problem (1.4), while red trajectories represent trajectories on $\mathcal{W}^{s,u}(P_\varepsilon^+)$ of the fully perturbed problem

(1.5). Intersections of these trajectories, i.e., defect points, give rise to defect solutions of (1.1). In the remainder of the manuscript, we no longer explicitly state the underlying systems where the stable and unstable manifolds belong to since it should be clear from the context, formulation, and/or color coding.

Remark 1.11. In Hypothesis H2, we assumed that (1.4) possesses a heteroclinic orbit Γ connecting P^- to P^+ in forward time. In the case that $P^+ = P^-$, we actually have a homoclinic orbit and we note that results on local defect solutions near P_ε^+ carry over. In particular, since $P^+ = P^-$, we have by default that $\dim(\mathcal{W}^u(P^-)) = \dim(\mathcal{W}^u(P^+))$. So, for the existence of local defect solutions near P_ε^+, we are always in the most interesting situation that $\dim(\mathcal{W}^u(P^-)) = \dim(\mathcal{W}^u(P^+))$, and the number of local defect solutions that (1.1) possess can range from zero to countably many; see Theorems 1.8 and 1.9.

Remark 1.12. The results of Theorems 1.8 and 1.9 about the existence of local defect solutions near P_ε^+ do not directly translate to the existence of local defect solutions near P^- by merely inverting time and the role of P^- and P^+, since Hypothesis H2 does not imply that the fully perturbed system (1.5) also possesses a heteroclinic orbit (see, for instance, the final example of section 2.1). On the other hand, and roughly speaking, Hypothesis H2 does provide the existence of an "almost" heteroclinic connection, up to $\mathcal{O}(\varepsilon)$ corrections. This orbit can also be the foundation on which local defect solutions near P^- may be built. We refrain from going into the details here—see also the discussion in section 5.

Remark 1.13. All results obtained in this manuscript for (1.1) can be generalized to hold for ε-dependent systems of the form

$$\dot{u} = \begin{cases} f(u;\varepsilon), & t \leq 0, \\ f(u;\varepsilon) + \varepsilon g(u;\varepsilon), & t > 0\,, \end{cases} \tag{1.10}$$

as long as $\dot{u} = f(u;\varepsilon), t \in \mathbb{R}$, fulfills Hypotheses H1 and H2 and as long as the perturbation $\varepsilon g(u;\varepsilon)$ is generic and such that the signs and order of the real parts of the eigenvalues of the Jacobian of the equilibrium points of $\dot{u} = f(u;\varepsilon)$ and $\dot{u} = f(u;\varepsilon) + \varepsilon g(u;\varepsilon)$ are the same. However, for clarity of the presentation, we decided to derive the results not for (1.10) but rather for the simpler system (1.1). Note that (1.9) is actually of the form of (1.10) and not of (1.1). We refer to section 4.2 for more details on this particular system (1.9).

2. Planar examples and preliminaries.

Before we prove the main results of this manuscript, we further demonstrate the complexity and subtle nature of the problem at hand by examining defect solutions to a particular perturbed planar Fisher–Kolmogorov/Petrovsky/Piskunov (KPP) equation [28, 43] and in general planar systems of ODEs. Afterward, we prove Lemma 1.7 concerning the existence and uniqueness of trivial defect solutions and Theorem 1.8 concerning local defect solutions near P_ε^+ for the situations where $\dim(\mathcal{W}^u(P^-)) \neq \dim(\mathcal{W}^u(P^+))$ or $\dim(\mathcal{W}^u(P^-)) = \dim(\mathcal{W}^u(P^+)) = 1$.

2.1. Global defect solutions in a perturbed stationary Fisher-KPP equation.

We consider a perturbation of the stationary Fisher-KPP equation to illustrate our geometric approach and the theme of the manuscript. Furthermore, we highlight the potential complexity of global defect solutions by showing that for specific perturbations the perturbed stationary Fisher-KPP equation supports arbitrary many global defect solutions.

Consider

$$\begin{pmatrix}\dot{u}\\ \dot{p}\end{pmatrix} = \begin{cases} \begin{pmatrix} p \\ u-u^2 \end{pmatrix}, & t \le 0, \\ \begin{pmatrix} p+\varepsilon g_1(u,p) \\ u-u^2+\varepsilon g_2(u,p) \end{pmatrix}, & t > 0, \end{cases} \tag{2.1}$$

where g_1 and g_2 are sufficiently smooth functions and ε is a small parameter. The unperturbed equation of (2.1) is given by

$$\begin{pmatrix}\dot{u}\\ \dot{p}\end{pmatrix} = \begin{pmatrix} p \\ u-u^2 \end{pmatrix}, \tag{2.2}$$

while the fully perturbed equation is given by

$$\begin{pmatrix}\dot{u}\\ \dot{p}\end{pmatrix} = \begin{pmatrix} p+\varepsilon g_1(u,p) \\ u-u^2+\varepsilon g_2(u,p) \end{pmatrix}. \tag{2.3}$$

Note that the ODE (2.1) is a bit more general than can be expected from the direct stationary ODE reduction of a Fisher-KPP equation with a general small jump-type heterogeneity

$$u_t = \frac{\partial^2 u}{\partial x^2} - u + u^2 - \begin{cases} 0, & x \le 0, \\ \varepsilon g_2(u, \frac{du}{dx}), & x > 0. \end{cases} \tag{2.4}$$

Thus, (2.1) corresponds to the stationary problem associated with (2.4) with $g_1(u,p) \equiv 0$.

The unperturbed equation (2.2) possesses an isolated homoclinic orbit Γ to the hyperbolic equilibrium point $P^- = P^+ = (0,0)$. Moreover, it possesses an isolated equilibrium point at $(1,0)$. Note that while Hypothesis H2 is satisfied, Hypothesis H1 is not satisfied since $(1,0)$ is not hyperbolic. However, we look for defect solutions asymptoting to the other equilibrium point (which is hyperbolic) and therefore the nonhyperbolic nature of $(1,0)$ is not important for the rersults to hold; see also Remark 1.3. So, if we assume that the perturbation is generic near the origin (see Definition 1.2), then the results of this manuscript establish that (2.1) always supports a unique trivial defect solution (see Lemma 1.7), while local defect solutions generically do not exist for this example since $\dim(\mathcal{W}^u(P^-)) = 1$ (see Theorem 1.8). A typical sketch of $\mathcal{W}^{s,u}(P^-)$ of (2.2) and $\mathcal{W}^{s,u}(P_\varepsilon^+)$ of (2.3) for a generic perturbation is shown in Figure 5. The manifolds $\mathcal{W}^u(P^-)$ and $\mathcal{W}^s(P_\varepsilon^+)$ intersect in two defect points; one yields a trivial defect solution, while the other one yields a global defect solution and local defect solutions do not exist.

As was already noticed, global defect solutions are extremely involved to study in the general case for general systems (1.1). However, for this problem one can use its underlying Hamiltonian structure to show the potential richness of global defect solutions. For example, for the nongeneric perturbation $g_1 = 0$ and $g_2 = -u + 2u^2$, system (2.1) has two global defect solutions. This can be seen from the fact that the fully perturbed system

$$\begin{pmatrix}\dot{u}\\ \dot{p}\end{pmatrix} = \begin{pmatrix} p \\ u-u^2+\varepsilon(2u^2-u) \end{pmatrix} \tag{2.5}$$

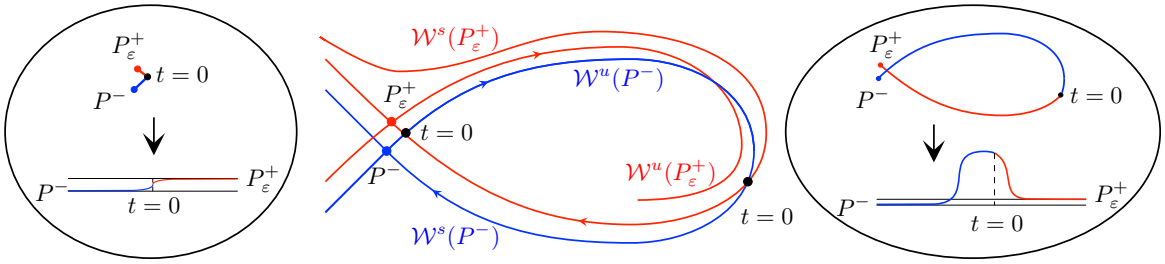

Figure 5. *Middle panel: a typical sketch of $\mathcal{W}^{s,u}(P^-)$ of (2.2) (blue) and $\mathcal{W}^{s,u}(P_\varepsilon^+)$ of (2.3) (red) for a generic perturbation. $\mathcal{W}^u(P^-)$ and $\mathcal{W}^s(P_\varepsilon^+)$ intersect twice (indicated by the black dots); one corresponds to a trivial defect solution of (2.1) (left panel) and one to a global defect solution of (2.1) (right panel).*

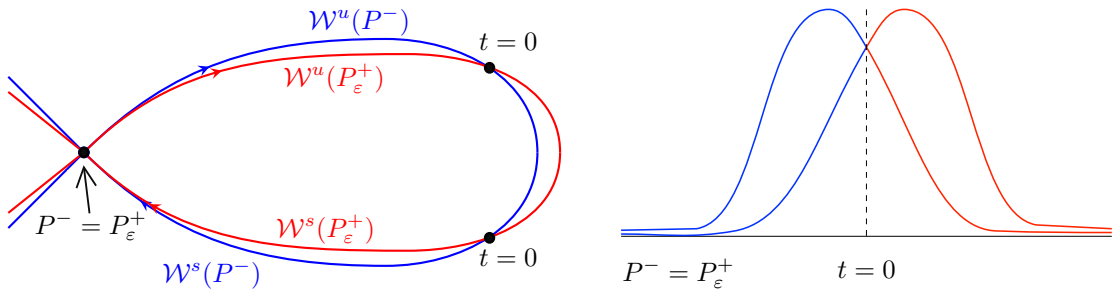

Figure 6. *Left panel: the stable and unstable manifold of P^- of (2.2) and the stable and unstable manifold of P_ε^+ of (2.5). Both defect points (indicated by the black dots) correspond to global defect solutions and these two global defect solutions are shown in the right panel.*

still has a homoclinic orbit to $(0,0)$ and this homoclinic orbit intersects the homoclinic orbit Γ of the unperturbed system (2.2) twice. Both intersections are far away from the origin yielding two global defect solutions. The left panel of Figure 6 shows the phase portraits of (2.2) and (2.5), and the two corresponding global defect solutions of (2.1) with $g_1 = 0$ and $g_2 = -u + 2u^2$ are shown in the right panel.

Actually, it can be shown by using the Hamiltonian structure of the problem that for a nongeneric perturbation of the form $g_1(u,p) = 0$ and $g_2(u,p) = -u + 2u^2 + p/N$ with $N > 0$, (2.1) supports many distinct global defect solutions. In particular, (2.1) supports an arbitrary, but finite, number of global defect solutions for increasing N. Note that the p-dependence of this particular perturbation breaks the reversibility symmetry of the original system and consequently the fully perturbed system (2.3) no longer possesses a homoclinic orbit. See Figure 7 for an example where six different global defect solutions exist: two global defect 1-pulse solutions, two global defect 2-pulse solutions, and two global defect 3-pulse solutions. One of these 3-pulse global defect solutions is shown in the right panel of Figure 7. Note that the fact that the perturbation (g_1, g_2) is nongeneric is irrelevant to the above observations: similar, but technically slightly more involved, examples can be given with generic perturbations.

2.2. Local defect solutions near P_ε^+ in planar systems. We mainly focus on local defect solutions near P_ε^+ in this manuscript, since the existence of trivial defect solutions is straightforward (see Lemma 1.7) and, as can be seen from the previous example, the analysis of global

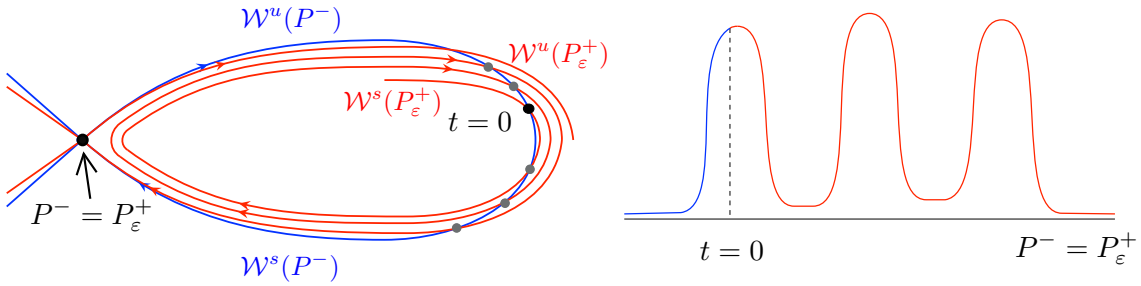

Figure 7. *Left panel: sketch of (2.1) with $g_1(u,p)=0$ and $g_2(u,p)=-u+2u^2+p/N$ for certain $N>0$. Six different defect points (indicated by the black and gray dots) yield six different global defect solutions. Right panel: the global defect 3-pulse solution created by the black defect point in the left panel.*

defect solutions requires the full control of the global flows of both (1.4) and (1.5) near the heteroclinic orbit Γ, which is a very hard problem in a general setting—see, however, [31] for an example of how this can be done in a singularly perturbed six-dimensional system associated with (1.2). See also Remark 1.12 and section 5 for a brief discussion of the existence of local defect solutions near P^-.

As can be seen from Theorems 1.8 and 1.9, the dimensions of $\mathcal{W}^u(P^-)$ and $\mathcal{W}^s(P_\varepsilon^+)$ play a crucial role in determining the (non)existence of local defect solutions near P_ε^+ in planar systems (as well as in systems with $n \geq 3$). By the hyperbolicity assumption in Hypothesis H1, we have that

$$\dim(\mathcal{W}^s(P_\varepsilon^+)) = \dim(\mathcal{W}^s(P^+)) = n - \dim(\mathcal{W}^u(P^+)). \tag{2.6}$$

Furthermore, by the assumption in Hypothesis H2 that the unperturbed system (1.4) supports a heteroclinic orbit Γ, we have

$$\dim(\mathcal{W}^u(P^-)) \geq 1 \qquad \text{and} \qquad \dim(\mathcal{W}^u(P^+)) \leq n-1\,. \tag{2.7}$$

The latter two statements, (2.6) and (2.7), are true for general n and do not hold only for planar systems. We distinguish between several cases:

- $\dim(\mathcal{W}^u(P^-)) > \dim(\mathcal{W}^u(P^+))$. For $\dim(\mathcal{W}^u(P^-)) > \dim(\mathcal{W}^u(P^+))$ and for a generic perturbation $\varepsilon g(u)$ with $\varepsilon > 0$ small enough, system (1.1) with $n = 2$ supports a continuous family of local defect solutions near P_ε^+. This result can be obtained from a simple *dimension counting* argument. Since $\dim(\mathcal{W}^u(P^-)) > \dim(\mathcal{W}^u(P^+))$, we have that $\dim(\mathcal{W}^u(P^-)) \in \{1,2\}$. If $\dim(\mathcal{W}^u(P^-)) = 2$, we have by (2.6) that $\dim(\mathcal{W}^s(P_\varepsilon^+)) \in \{1,2\}$. So, generically, the intersection $\mathcal{W}^u(P^-) \cap \mathcal{W}^s(P_\varepsilon^+)$ is at least one-dimensional. Since $\mathcal{W}^{s,u}(P^+)$ and $\mathcal{W}^{s,u}(P_\varepsilon^+)$ are *locally parallel* near P^+, $\mathcal{W}^u(P^+)$ and $\mathcal{W}^s(P_\varepsilon^+)$ actually intersect in an $\mathcal{O}(\varepsilon)$ neighborhood of P^+ (and P_ε^+). (This intersection actually creates the unique trivial defect solution connecting P^+ to P_ε^+; see Lemma 1.7.) Moreover, by Hypothesis H2 we know that Γ is minimally nontransversal and this guarantees that at least part of the one-dimensional intersection of $\mathcal{W}^u(P^-) \cap \mathcal{W}^s(P_\varepsilon^+)$ occurs near P_ε^+, creating a continuous family of local defect solutions near P_ε^+. A typical phase portrait in the case that the Jacobian of P^- has real eigenvalues and $\dim(\mathcal{W}^s(P_\varepsilon^+)) = 1$ is shown in Figure 8. If $\dim(\mathcal{W}^u(P^-)) = 1$, we have that

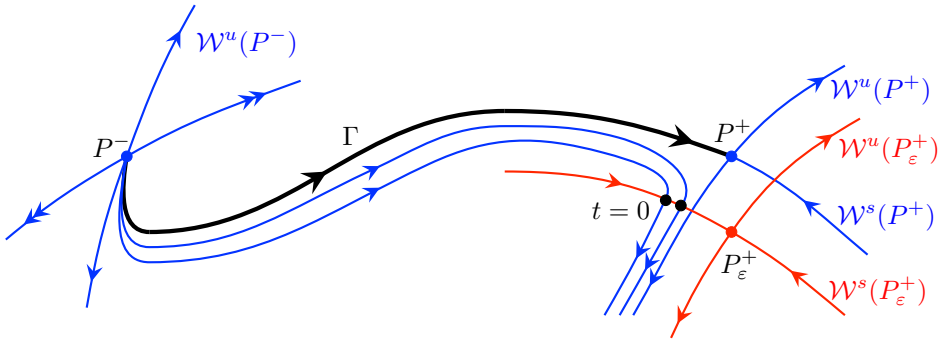

Figure 8. *For* $\dim(\mathcal{W}^u(P^-)) > \dim(\mathcal{W}^u(P^+))$ *there generically exist a continuous family of local defect solutions near* P_ε^+ *in a planar system. That is,* $\mathcal{W}^u(P^-)$ *and* $\mathcal{W}^s(P_\varepsilon^-)$ *intersect in a line (indicated by the black dots) near* P_ε^+*. Each of these intersections corresponds to a defect point creating a local defect solution. In this figure, we have* $\dim(\mathcal{W}^u(P^-)) = 2 > 1 = \dim(\mathcal{W}^u(P^+))$ *and we assume that the Jacobian of* P^- *has real eigenvalues.*

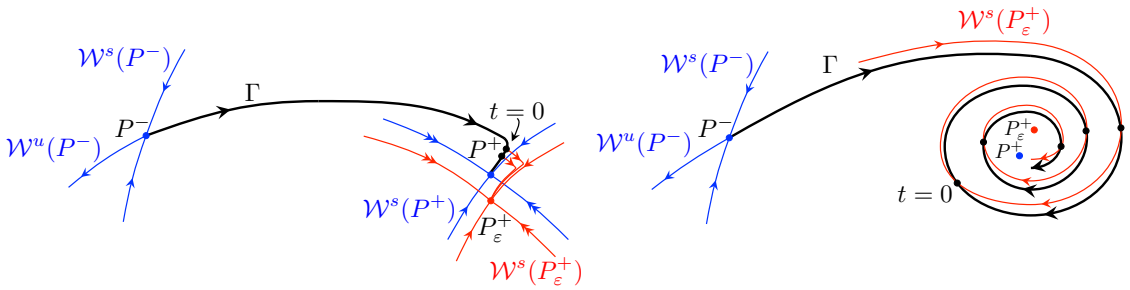

Figure 9. *For* $\dim(\mathcal{W}^u(P^-)) > \dim(\mathcal{W}^u(P^+))$ *there exists a continuous family of local defect solutions near* P_ε^+ *in a planar system. In this figure, we have* $\dim(\mathcal{W}^u(P^-)) = 1 > 0 = \dim(\mathcal{W}^u(P^+))$*. Left panel: the Jacobian of* P^+ *has two real negative simple eigenvalues. Right panel: the Jacobian of* P^+ *has a complex pair of eigenvalues with negative real part.*

$\dim(\mathcal{W}^u(P^+)) = 0$ and by (2.6) $\dim(\mathcal{W}^s(P^+)) = \dim(\mathcal{W}^s(P_\varepsilon^+)) = 2$. So, generically, the intersection $\mathcal{W}^u(P^-) \cap \mathcal{W}^s(P_\varepsilon^+)$ is one-dimensional. In fact, any point on $\mathcal{W}^u(P^-)$ that is $\mathcal{O}(\varepsilon)$ close to P^+ can be chosen as defect point since P_ε^+ is asymptotically stable. So, we again have a continuous family of local defect solutions. Two typical phase portraits are shown in in Figure 9.

- $\dim(\mathcal{W}^u(P^-)) < \dim(\mathcal{W}^u(P^+))$. This case is not possible in the planar setting by (2.7) with $n = 2$.
- $\dim(\mathcal{W}^u(P^-)) = \dim(\mathcal{W}^u(P^+))$. For the planar case it follows from (2.7) with $n = 2$ that we necessarily have that $\dim(\mathcal{W}^u(P^-)) = \dim(\mathcal{W}^u(P^+)) = 1$ (i.e., we are still in the case of Theorem 1.8). So, all equilibrium points of interest $\mathcal{W}^{u,s}(P^\pm)$ and $\mathcal{W}^{u,s}(P_\varepsilon^\pm)$ are saddles. In this case, for a generic perturbation with $\varepsilon > 0$ small enough, (1.1) with $n = 2$ does not support local defect solutions near P_ε^+. Generically, two one-dimensional manifolds intersect in a point in a two-dimensional space. However, the perturbation is assumed to be generic near P^+ and therefore the stable and unstable manifold of P^+ and P_ε^+ are *locally parallel*. So, $\mathcal{W}^s(P^+)$ and $\mathcal{W}^s(P_\varepsilon^+)$ generically do

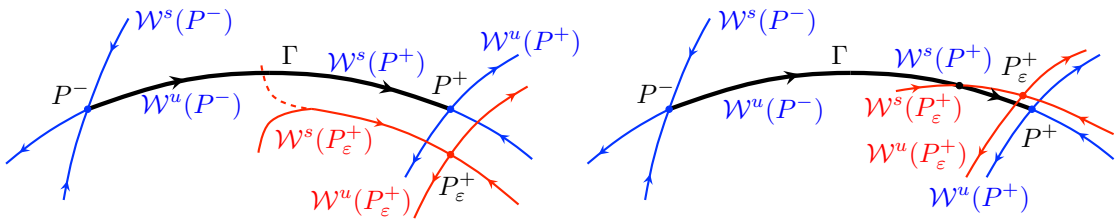

Figure 10. *Left panel: for* $\dim(\mathcal{W}^u(P^-)) = \dim(\mathcal{W}^u(P^+)) = 1$ *a generic perturbation does not lead to a local defect solution in a planar system near* P_ε^+ *since the stable and unstable manifolds of* P^+ *and* P_ε^+ *are locally parallel. Therefore,* Γ *cannot intersect with* $\mathcal{W}^s(P_\varepsilon^+)$ *near* P_ε^+*. A trivial defect solution connecting* P^+ *to* P_ε^+ *does exist since* $\mathcal{W}^u(P^+)$ *and* $\mathcal{W}^s(P_\varepsilon^+)$ *intersect for generic perturbations and also a global defect solution may exist (this is indicated by the red dotted trajectory). Right panel: in the case of* $\dim(\mathcal{W}^u(P^-)) = \dim(\mathcal{W}^u(P^+)) = 1$ *a nongeneric perturbation may lead to a local defect solution in a planar system.*

not intersect in a $\mathcal{O}(\varepsilon)$ neighborhood near P_ε^+ (see also Figure 2). Near P^+ we have that $\Gamma = \mathcal{W}^u(P^-) \subset \mathcal{W}^s(P^+)$. So, we also get that $\mathcal{W}^u(P^-)$ and $\mathcal{W}^s(P_\varepsilon^+)$ generically do not intersect in an $\mathcal{O}(\varepsilon)$ neighborhood near P_ε^+. Thus, local defect solutions near P_ε^+ generically do not exist in this case. See also the left panel of Figure 10. Observe that the perturbed Fisher-KPP equation (2.1) with a generic perturbation near the origin is an example of this case where $\dim(\mathcal{W}^u(P^-)) = \dim(\mathcal{W}^u(P^+)) = 1$; see Figure 5.

The existence of global defect solutions cannot be excluded (nor guaranteed). See the left panel of Figure 10. In the right panel of Figure 10 it is shown that local defect solutions may exist if Hypothesis H3 is dropped, i.e., if P_ε^+ can be sufficiently close to $\mathcal{W}^s_{\mathrm{loc}}(P^+)$.

2.3. Proof of Lemma 1.7. We now return to the n-dimensional setting and prove Lemma 1.7.

Proof. A trivial defect solution lies in the intersection of $\mathcal{W}^u(P^+)$ and $\mathcal{W}^s(P_\varepsilon^+)$ near P^+ and we distinguish two cases.

Case 1. $\dim(\mathcal{W}^u(P^+)) \in \{0, n\}$.

This is the trivial case, where the equilibrium points P^+ and P_ε^+ only have stable or unstable directions. If $\dim(\mathcal{W}^u(P^+)) = 0$, then the equilibrium point P^+ of (1.5) is asymptotically stable. That is, there exists a δ such that all points starting in a δ neighborhood of P^+ converge to P^+. For $\varepsilon = \varepsilon(\delta)$ small enough, P_ε^+ lies inside this δ neighborhood of P^+. Since P_ε^+ is also asymptotically stable it attracts points inside a $\tilde{\delta}$ neighborhood of P_ε^+, where $\tilde{\delta}$ is to leading order in ε equal to δ. Therefore, P^+ lies inside this $\tilde{\delta}$ neighborhood of P_ε^+ and there is a unique orbit $\overline{u}(t)$ in the fully perturbed system (1.5) starting at P^+ at $t = 0$ which tends to P_ε^+ for $t \to \infty$. The unique defect solution $\Gamma_\varepsilon(t)$ of (1.1) is now given by

$$\Gamma_\varepsilon(t) = \begin{cases} P^+, & t \le 0, \\ \overline{u}(t), & t > 0. \end{cases}$$

Similarly, if $\dim(\mathcal{W}^u(P^+)) = n$, then the equilibrium point P^+ of (1.4) has only unstable directions and we can choose ε small enough such that the unperturbed system (1.4) has a unique orbit $\underline{u}(t)$ starting at P_ε^+ at $t = 0$ which tends to P^+ for $t \to -\infty$. Consequently, (1.1)

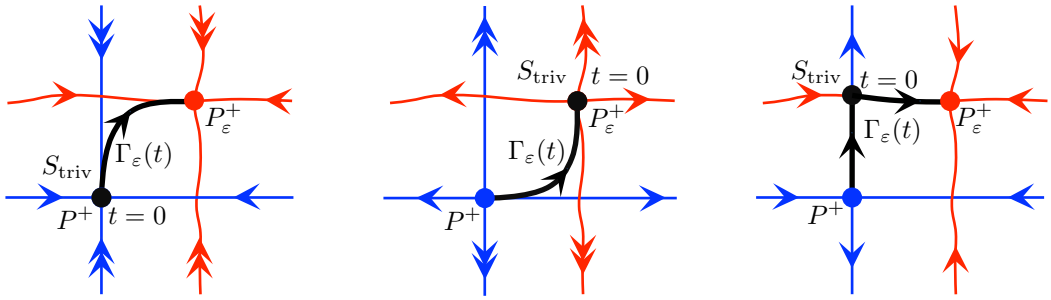

Figure 11. *Left two panels: trivial defect solutions in the planar case for* $\dim(\mathcal{W}^u(P^+)) = 0$ *(left) and* $\dim(\mathcal{W}^u(P^+)) = 2$ *(middle) in the case that the eigenvalues of the Jacobian of* P^+ *are real. In the case of complex or repeated eigenvalues, we obtain trivial defect solutions in a similar fashion. Right panel: a trivial defect solution in the planar case for* $\dim(\mathcal{W}^u(P^+)) = 1$*. The black dot indicates the defect point* S_{triv}*, where we switch from the unperturbed system (1.4) to the fully perturbed system (1.5). For convenience we already implicitly assumed that (1.1) has been transformed into its normal form (3.1) such that the unstable and stable manifolds are along the x-axis and the y-axis.*

has a unique defect solution $\Gamma_\varepsilon(t)$ given by

$$\Gamma_\varepsilon(t) = \begin{cases} \underline{u}(t), & t \le 0, \\ P_\varepsilon^+, & t > 0. \end{cases}$$

Case 2. $\dim(\mathcal{W}^u(P^+)) \notin \{0, n\}$.

The manifolds $\mathcal{W}^s(P^+)$ and $\mathcal{W}^u(P^+)$ intersect transversally and uniquely at P^+, and by the local stable and unstable manifold theorem (e.g., [48]), the stable and unstable manifolds of P_ε^+ are locally within the $\mathcal{O}(\varepsilon)$ neighborhood of those of P^+. Moreover, they are to leading order parallel. Therefore, generically the manifolds $\mathcal{W}^u(P^+)$ and $\mathcal{W}^s(P_\varepsilon^+)$ also intersect transversally in a uniquely defined (zero-dimensional) defect point $\mathcal{O}(\varepsilon)$ close to P^+ and P_ε^+. ■

See also Figure 11 for planar examples of both cases. As it turns out, the uniquely defined defect point that creates a trivial defect solution near P^+ is also important for the proofs of the (non)existence of local defect solutions near P_ε^+. Therefore, we label this defect point S_{triv} and it is indicated by the black dots in Figure 11.

2.4. Proof of Theorem 1.8. *Proof.* By Hypothesis H2, we know that the unperturbed system (1.4) possesses a heteroclinic orbit Γ connecting P^- and P^+. So, $\dim(\mathcal{W}^u(P^-)) \ge 1$ and $\dim(\mathcal{W}^s(P^+)) = \dim(\mathcal{W}^s(P_\varepsilon^+) \ge 1$. Moreover, since P^+ is assumed to be a hyperbolic equilibrium point, we also have that $\dim(\mathcal{W}^u(P^+)) \le n-1$. For convenience, we introduce $k^\pm$ and $\ell^\pm$ denoting the dimension of the unstable, respectively, stable, manifold of $P^\pm$. That is, $\dim(\mathcal{W}^u(P^\pm)) =: k^\pm$ and $\dim(\mathcal{W}^s(P^\pm)) =: \ell^\pm = n - k^\pm$.

We first prove the first statement of the theorem by showing that there are generically no local defect solutions near P_ε^+ if $\dim(\mathcal{W}^u(P^-)) = k^- < k^+ = \dim(\mathcal{W}^u(P^+))$. By the assumption that $P^\pm$ are hyperbolic equilibrium points, we have that

$$\dim(\mathcal{W}^u(P^-)) + \dim(\mathcal{W}^s(P^+)) = k^- + \ell^+ = n - (k^+ - k^-) < n$$

since $k^+ > k^-$. Therefore, the assumption that there exist a heteroclinic orbit Γ in the unperturbed system (1.4) is nongeneric (since generically two manifolds for which the sum of their dimensions is less than n do not intersect in n-dimensional space) and the minimally nontransversal assumption of Hypothesis H2 implies that Γ is one-dimensional and isolated.

Similarly, $\dim(\mathcal{W}^u(P^-)) + \dim(\mathcal{W}^s(P_\varepsilon^+)) < n$, since $\dim(\mathcal{W}^s(P^+)) = \dim(\mathcal{W}^s(P_\varepsilon^+))$. Moreover, since $\mathcal{W}^s(P^+)$ and $\mathcal{W}^s(P_\varepsilon^+)$ are locally parallel, $\mathcal{W}^u(P^-)$ and $\mathcal{W}^s(P_\varepsilon^+)$ generically do not intersect in an $\mathcal{O}(\varepsilon)$ neighborhood of P_ε^+: $\mathcal{W}^s(P_\varepsilon^+)$ is also translated from $\mathcal{W}^s(P^+)$ along the *missing* $(k^+ - k^-)$*-dimensions* and therefore $\mathcal{W}^u(P^-)$ and $\mathcal{W}^s(P_\varepsilon^+)$ do not intersect near P_ε^+. Hypothesis H3 is essential for the application of this argument—if Hypothesis H3 does not hold, counterexamples can be constructed along the lines of the right panel of Figure 10.

Next, we prove that there are no local defect solutions near P_ε^+ if $\dim(\mathcal{W}^u(P^-)) = k^- = k^+ = \dim(\mathcal{W}^u(P^+)) = 1$. In this case, in a small enough δ neighborhood near P^+ we have that $\Gamma = \mathcal{W}^u(P^-) \subset \mathcal{W}^s(P^+)$. That is, near P^+ the unstable manifold $\mathcal{W}^u(P^-)$ is completely contained in stable manifold $\mathcal{W}^s(P^+)$. By the hypotheses the perturbation is assumed to be generic and $\mathcal{W}^s(P_\varepsilon^+)$ and $\mathcal{W}^s(P^+)$ are locally parallel. Therefore, $\mathcal{W}^s(P^+)$ and $\mathcal{W}^s(P_\varepsilon^+)$ do not intersect within a ε neighborhood of P_ε^+ $(\varepsilon = \varepsilon(\delta))$. Consequently, since $\mathcal{W}^u(P^-) \subset \mathcal{W}^s(P^+)$ near P^+, $\mathcal{W}^u(P^-)$ and $\mathcal{W}^s(P_\varepsilon^+)$ do not intersect near P_ε^+.

Finally, we prove that (1.1) possesses a continuous family of local defect solutions near P_ε^+ if $\dim(\mathcal{W}^u(P^-)) = k^- > k^+ = \dim(\mathcal{W}^u(P^+))$. In this case, we have that $\dim(\mathcal{W}^u(P^-)) + \dim(\mathcal{W}^s(P_\varepsilon^+)) > n$. Therefore, generically $\mathcal{W}^u(P^-)$ and $\mathcal{W}^s(P_\varepsilon^+)$ intersect in a continuous family of orbits since $\mathcal{W}^s(P_\varepsilon^+)$ and $\mathcal{W}^u(P^-)$ are not parallel because $\mathcal{W}^s(P^+)$ and $\mathcal{W}^u(P^-)$ are not parallel.

To show that this continuous family exists near P_ε^+, we distinguish between two cases. First, if $\dim(\mathcal{W}^s(P^+)) = n$, we can choose an ε small enough such that there is a unique solution $\bar{u}(t)$ to the fully perturbed system (1.5) connecting P^+ at $t = 0$ to P_ε^+ for $t \to \infty$; see the proof of Lemma 1.7. Moreover, P_ε^+ attracts points inside a $\tilde{\delta}$ neighborhood around P_ε^+ and P^+ lies inside this $\tilde{\delta}$ neighborhood. Since there exists a heteroclinic orbit Γ in (1.4) connecting P^- and P^+, we have that part of $\mathcal{W}^u(P^-)$ gets arbitrarily close to P^+. Therefore, also part of $\mathcal{W}^u(P^-)$ lies inside the $\tilde{\delta}$ neighborhood around P_ε^+. We can create a continuous family of local defect solutions near P_ε^+ by parameterizing t such that we switch between the systems at any of these points on $\mathcal{W}^u(P^-)$ inside this $\tilde{\delta}$ neighborhood.

Second, if $0 < \dim(\mathcal{W}^s(P^+)) < n$, we have by the minimally nontransversal assumption of Hypothesis H3 that $\mathcal{W}^u(P^-)$ near P^+ is higher-dimensional than Γ. Moreover, $\mathcal{W}^u(P^+)$ and $\mathcal{W}^s(P_\varepsilon^+)$ intersect near P_ε^+ at S_{triv} (see the previous section). Consequently, there are trajectories in $\mathcal{W}^u(P^-)$ that get arbitrarily close to P^+ and then continue to follow the part of $\mathcal{W}^u(P^+)$ that intersects with $\mathcal{W}^s(P_\varepsilon^+)$. Therefore, these trajectories intersect $\mathcal{W}^s(P_\varepsilon^+)$ near S_{triv}, creating a continuous family of local defect solutions near P_ε^+. ∎

3. Local defect solutions for $\dim(\mathcal{W}^u(P^-)) = \dim(\mathcal{W}^u(P^+)) > 1$. In section 2.3, we showed the existence of unique trivial defect solutions and in section 2.4 the (non)existence of local defect solutions near P_ε^+ if $\dim(\mathcal{W}^u(P^-)) \neq \dim(\mathcal{W}^u(P^+))$ or $\dim(\mathcal{W}^u(P^-)) = \dim(\mathcal{W}^u(P^+)) = 1$. That is, we proved Lemma 1.7 and Theorem 1.8 of section 1.2. These proofs were primarily based on geometrical arguments. To prove the existence of local defect

solutions near P_ε^+ in the critical case $\dim(\mathcal{W}^u(P^-)) = \dim(\mathcal{W}^u(P^+)) > 1$, that is, to prove Theorem 1.9, we need a more analytical approach.

In order to do so, we first introduce an appropriate normal form for the unperturbed system (1.4); see section 3.1. Next, in section 3.2, we prove Theorem 1.9 for systems in three-dimensional space, since this is the lowest-dimensional, and therefore the most transparent, setting for which we can have $\dim(\mathcal{W}^u(P^-)) = \dim(\mathcal{W}^u(P^+)) > 1$ under the assumption that the unperturbed system (1.4) supports a heteroclinic orbit Γ connecting P^- to P^+. This lowest-dimensional case allows us to best explain and highlight the crucial aspects of the rather technical proofs. In section 3.3, we complete the proof of Theorem 1.9. In particular, we discuss how the results for $n = 3$ generalize to the general n-dimensional case.

3.1. Normal form of the unperturbed system (1.4). The defect point of local defect solutions near P_ε^+, i.e., the point where the switch between the two systems is made at $t = 0$, lies nearby P^+ and we assume, without loss of generality, that P^+ is located at the origin. Consequently, P_ε^+ lies in an ε neighborhood of the origin. Moreover, by assumption, P^+ is a hyperbolic equilibrium point of the unperturbed system (1.4), while P_ε^+ is a hyperbolic equilibrium point of the fully perturbed system (1.5). So, for u close to P^+, that is, $|u| = \mathcal{O}(\delta)$ with δ sufficiently small, we have

$$\dot{u} = f_u(0)u + \mathcal{O}(\delta^2)\,,$$

where $f_u(0)$ is the Jacobian of (1.4) at $P^+ = 0$.

To examine the *twist* of the unstable manifold coming from a far equilibrium point P^- near P^+ (see, for example, Figure 4), we need to separate the *leading eigenvalues* of $f_u(0)$ from the remaining eigenvalues, which we label the *strong eigenvalues* [35]. By Hypothesis H2 all the eigenvalues of $f_u(0)$ are simple, and we order the eigenvalues of $f_u(0)$ according to their real parts,

$$\Re(\nu_1) \leq \Re(\nu_2) \leq \cdots \leq \Re(\nu_\ell) < 0 < \Re(\nu_{\ell+1}) \leq \cdots \leq \Re(\nu_n)\,.$$

That is, $f_u(0)$ has ℓ stable eigenvalues and $k = n - \ell$ unstable eigenvalues. We single out the *leading stable eigenvalue(s)* ν^{ls} and the *leading unstable eigenvalue(s)* ν^{lu}, i.e., the stable, respectively, unstable, eigenvalues of $f_u(0)$ with real parts closest to zero. That is, $\nu^{ls} = \nu_\ell$ if ν_ℓ is real valued and $\nu_1^{ls} = \nu_\ell$ and $\nu_2^{ls} = \nu_{\ell-1}$ if ν_ℓ is complex valued and similar for ν^{lu}. The remaining eigenvalues are called *strong eigenvalues* and we introduce the real numbers $\lambda^{ss,uu}$ such that λ^{ss} is smaller than the real part of ν^{ls} but larger than the real parts of the strong stable eigenvalues. We define λ^{uu} in a similar fashion: λ^{uu} is larger than the real part of ν^{lu} but smaller than the real parts of the strong unstable eigenvalues. For example, if all eigenvalues are real valued, then we have the following ordering:

$$\begin{aligned}\Re(\nu_1) < \Re(\nu_2) < \cdots < \Re(\nu_{\ell-1}) < \lambda^{ss} < \Re(\nu_\ell = \nu^{ls}) < 0 < \Re(\nu_{\ell+1} = \nu^{lu}) < \lambda^{uu} \\ < \Re(\nu_{\ell+2}) \cdots < \Re(\nu_n)\,.\end{aligned}$$

Next, we choose local coordinates such that

$$u =: (x, y) =: (x^{ls}, x^{ss}, y^{lu}, y^{uu}) \in E^{ls} \oplus E^{ss} \oplus E^{lu} \oplus E^{uu}\,.$$

Here, E^{ls} is the stable eigenspace of $f_u(0)$ spanned by the eigenvector(s) belonging to the leading stable eigenvalue(s) ν^{ls} and E^{ss} the stable eigenspace of $f_u(0)$ spanned by the eigenvectors belonging to the strong stable eigenvalues with real parts less than λ^{ss}. Similarly, E^{lu} is the unstable eigenspace of $f_u(0)$ spanned by the eigenvector(s) belonging to the leading unstable eigenvalue(s) ν^{lu} and E^{uu} the unstable eigenspace of $f_u(0)$ spanned by the eigenvectors belonging to the strong unstable eigenvalues with real parts larger than λ^{uu}. Moreover, we denote the full stable eigenspace of $f_u(0)$ by E^s and the full unstable eigenspace by E^u. We thus have $E^s = E^{ls} \oplus E^{ss}$ and $E^u = E^{lu} \oplus E^{uu}$.

Lemma 3.1 (Proposition 3.1 of [35]). *There exists a smooth coordinate transformation $u \mapsto (x^{ls}, x^{ss}, y^{lu}, y^{uu})$ such that near the origin the unperturbed system (1.4) transforms into*

$$\begin{cases} \dot{x}^{ls} = A^{ls}x^{ls} + \mathcal{O}\left((|x^{ls}|^2 + |x^{ss}|)|y|\right), \\ \dot{x}^{ss} = A^{ss}x^{ss} + \mathcal{O}\left(|x^{ls}|^2 + |x^{ss}|(|x| + |y|)\right), \\ \dot{y}^{lu} = A^{lu}y^{lu} + \mathcal{O}\left((|y^{lu}|^2 + |y^{uu}|)|x|\right), \\ \dot{y}^{uu} = A^{uu}y^{uu} + \mathcal{O}\left(|y^{lu}|^2 + |y^{uu}|(|x| + |y|)\right), \end{cases} \tag{3.1}$$

where $x = (x^{ls}, x^{ss}) \in E^{ls} \oplus E^{ss} = E^s$, $y = (y^{lu}, y^{uu}) \in E^{lu} \oplus E^{uu} = E^u$, and $A^{ls,ss,lu,uu}$ are such that $\sigma(A^{ls}) = \nu^{ls}$ or $\{\nu_1^{ls}, \nu_2^{ls}\}$ (in the case that the leading stable eigenvalues are complex valued), $\sigma(A^{ss}) = \sigma(f_u(0)) \cap \{\Re(\nu) < \lambda^{ss}\}$, $\sigma(A^{lu}) = \nu^{lu}$ or $\{\nu_1^{lu}, \nu_2^{lu}\}$, and $\sigma(A^{uu}) = \sigma(f_u(0)) \cap \{\Re(\nu) > \lambda^{uu}\}$.

The proof of this lemma follows from a series of coordinate transformations; see, for example, [13, 35, 59] and references therein.

3.2. $n = 3$. In three dimensions, Hypotheses H1–H3 immediately imply that $\dim(\mathcal{W}^u(P^-)) = \dim(\mathcal{W}^u(P^+)) = 2$ and $\dim(\mathcal{W}^s(P^+)) = \dim(\mathcal{W}^s(P_\varepsilon^+)) = 1$. Thus, the Jacobians of P^+ and P_ε^+ have one negative real valued eigenvalue and two eigenvalues with positive real part. These two unstable eigenvalues with positive real part either are both real valued (and different by Hypothesis H2) or form a complex conjugate pair. Consequently, the general normal form as stated in Lemma 3.1 is too elaborate for the three-dimensional setting. For example, the eigenspace E^{ss} is always empty and, in addition, the eigenspace E^{uu} is empty in the case that the Jacobian of P^+ has two unstable complex conjugated eigenvalues. Therefore, and with a slight abuse of notation, we simplify the expression for the general n-dimensional normal form (3.1) to two different versions in three dimensions, each representing one of the two different possible configurations of the unstable eigenvalues of the Jacobian of P^+, which is still assumed to be located at the origin. We get

$$\begin{cases} \dot{x} = -\lambda_1 x + x h_1(x, y_1, y_2), \\ \dot{y_1} = \lambda_2 y_1 + y_1 h_2(x, y_1, y_2), \\ \dot{y_2} = \lambda_3 y_2 + y_2 h_3(x, y_1, y_2), \end{cases} \tag{3.2}$$

and

$$\begin{cases} \dot{x} = -\lambda_1 x + x h_4(x, y_1, y_2), \\ \dot{y_1} = \alpha y_1 + \beta y_2 + y_1 h_5(x, y_1, y_2) + y_2 h_6(x, y_1, y_2), \\ \dot{y_2} = -\beta y_1 + \alpha y_2 + y_1 h_7(x, y_1, y_2) + y_2 h_8(x, y_1, y_2), \end{cases} \tag{3.3}$$

where $\lambda_1 > 0$, and $\lambda_3 > \lambda_2 > 0$, $\alpha, \beta > 0$ such that $\alpha \pm i\beta = \nu_{2,3}$, and $h_j = \mathcal{O}(|x| + |y_1| + |y_2|)(j = 1, 2, \ldots, 8)$. Note that indeed both normal forms, including the existence and the magnitudes of the h_j's, can directly be obtained from (3.1) and [35] with $x^{ls} = x$, $x^{ss} \equiv 0$, and $y^{lu} = y_1$, $y^{uu} = y_2$ in the real case, while $y^{uu} \equiv 0$, $y^{lu} = (y_1, y_2)$ in the complex case. In fact, the results of Lemma 3.1 are stronger than used here. Furthermore, we use λ_i in (3.2) and (3.3) (and in the remainder of section 3) to denote the absolute magnitude of the real valued eigenvalues instead of ν_i used in the previous section; see in particular (3.1). That is, for $1 \leq i \leq \ell$ and ν_i real valued we have $0 < \lambda_i = -\nu_i$, while for $\ell + 1 \leq i \leq n$ and ν_i real valued we have $0 < \lambda_i = \nu_i$. The advantage of the current notation is that by default all λ_i's are positive.

Based on the normal forms (3.2) and (3.3) and by Hypotheses H1–H3, the heterogeneously perturbed system (1.1) with $n = 3$ can, near P^+, be written as

$$\begin{pmatrix} \dot{x} \\ \dot{y}_1 \\ \dot{y}_2 \end{pmatrix} = \begin{cases} \begin{pmatrix} -\lambda_1 x + x h_1(x, y_1, y_2) \\ \lambda_2 y_1 + y_1 h_2(x, y_1, y_2) \\ \lambda_3 y_2 + y_2 h_3(x, y_1, y_2) \end{pmatrix}, & t < 0, \\ \begin{pmatrix} -\lambda_1 x + x h_1(x, y_1, y_2) \\ \lambda_2 y_1 + y_1 h_2(x, y_1, y_2) \\ \lambda_3 y_2 + y_2 h_3(x, y_1, y_2) \end{pmatrix} + \varepsilon \begin{pmatrix} g_1(x, y_1, y_2) \\ g_2(x, y_1, y_2) \\ g_3(x, y_1, y_2) \end{pmatrix}, & t > 0, \end{cases} \tag{3.4}$$

or

$$\begin{pmatrix} \dot{x} \\ \dot{y}_1 \\ \dot{y}_2 \end{pmatrix} = \begin{cases} \begin{pmatrix} -\lambda_1 x + x h_4(x, y_1, y_2) \\ \alpha y_1 + \beta y_2 + y_1 h_5(x, y_1, y_2) + y_2 h_6(x, y_1, y_2) \\ -\beta y_1 + \alpha y_2 + y_1 h_7(x, y_1, y_2) + y_2 h_8(x, y_1, y_2) \end{pmatrix}, & t < 0, \\ \begin{pmatrix} -\lambda_1 x + x h_4(x, y_1, y_2) \\ \alpha y_1 + \beta y_2 + y_1 h_5(x, y_1, y_2) + y_2 h_6(x, y_1, y_2) \\ -\beta y_1 + \alpha y_2 + y_1 h_7(x, y_1, y_2) + y_2 h_8(x, y_1, y_2) \end{pmatrix} + \varepsilon \begin{pmatrix} g_4(x, y_1, y_2) \\ g_5(x, y_1, y_2) \\ g_6(x, y_1, y_2) \end{pmatrix}, & t > 0, \end{cases} \tag{3.5}$$

based on the nature of the unstable eigenvalues of the Jacobian of P^+. Here $g_i(x, y_1, y_2)$, $i = 1, 2, \ldots, 6$, are sufficiently smooth and of $\mathcal{O}(1)$ with respect to ε.

If a local defect solution $\Gamma_\varepsilon(t)$ near P^+_ε—which we shall denote by $\gamma_{ld}(t)$ from now on—exists, then by the definition of local defect solutions near P^+_ε (see Definition 1.4), the entire $\{t \geq 0\}$-part of $\gamma_{ld}(t)$ must approximate P^+_ε in the limit $\varepsilon \downarrow 0$. We define the asymptotic expression $\rho(\varepsilon)$ measuring the distance between the local defect solution $\gamma_{ld}(t)$ and the equilibrium point P^+_ε by

$$\rho(\varepsilon) = |\gamma_{ld}(0) - P^+_\varepsilon| \tag{3.6}$$

and conclude that, by definition, $\lim_{\varepsilon \downarrow 0} \rho(\varepsilon) = 0$.

In the unperturbed systems (3.2) and (3.3), the stable manifold $\mathcal{W}^s(P^+)$ is locally given by the x-axis: $\{y_1 = y_2 = 0\}$. Hence, by the existence of the heteroclinic connection Γ (Hypothesis H2), the two-dimensional manifold $\mathcal{W}^u(P^-)$ contains the x-axis near P^+. This

implies that for a δ small enough, $\mathcal{W}^u(P^-)$ intersects the $\{x = \delta\}$-plane transversally. Furthermore, the flow of systems (3.2) and (3.3) is dominated by their linear components in a $\mathcal{O}(\delta)$ neighborhood near the origin.

To enable the upcoming local analysis by which the existence of a local defect solution is established, we need to tune the choices of ε and the second small parameter $\delta > 0$. Note that δ is independent of ε since the unperturbed systems (3.2) and (3.3) are independent of ε. We choose δ small enough, so that $\mathcal{W}^u(P^-)$ intersects the $\{x = \delta\}$-plane transversally in a region in phase space where the flow is, to leading order in δ, linear. For a given choice of δ, we choose ε such that the jump of the potential local defect solution from the $t \leq 0$-subsystem to the $t > 0$-subsystem of (1.1) appears, in the normalized systems (3.4) and (3.5), with an x-coordinate that is sufficiently smaller than δ. That is, we assume that the heterogeneity starts playing a role only after γ_{ld} has passed through the $\{x = \delta\}$-plane—see, however, Remark 3.7 in section 3.2.2. Hence, for a given δ, we choose ε such that $\rho(\varepsilon)$ as defined in (3.6) is sufficiently small. Moreover, in the upcoming analysis we also want P_ε^+ to be within an $\mathcal{O}(\delta)$ neighborhood of P^+. Since $|P^+(\varepsilon)| = \mathcal{O}(\varepsilon)$, we thus also assume that ε is sufficiently small with respect to δ. With these choices of δ and ϵ, we define the bounded one-dimensional intersection $L_\delta \subset W^u(P^-) \cap \{x = \delta\}$; see also Figure 12.

Definition 3.2. *The bounded curve L_δ is determined by the transversal intersection of $\mathcal{W}^u(P^-)$ with the disc $\{x = \delta, \sqrt{y_1^2 + y_2^2} \leq \delta\}$.*

Note that $(\delta, 0, 0) \in L_\delta$, since $\mathcal{W}^s(P^+)$ coincides with the x-axis near P^+. Although the existence of L_δ follows by general geometrical considerations, its exact location, or more precisely, its orientation within the $\{x = \delta\}$-plane with respect to its *center* $(\delta, 0, 0)$, can be established only by obtaining a full control over the two-dimensional manifold $\mathcal{W}^u(P^-)$ as it travels from P^- to P^+, while *twisting* about Γ. This is in general a very hard problem (see, however, section 4.2). Nevertheless, by assuming that δ is small enough, we know that L_δ is, to leading order, a straight interval. So, there are constants K_1 and K_2, $(K_1, K_2) \neq (0, 0)$, such that L_δ is given by

$$L_\delta := \{(x, y_1, y_2) \mid x = \delta, \;\; K_1 y_1 + K_2 y_2 + \mathcal{O}(|y_1, y_2|^2) = 0, \;\; \sqrt{y_1^2 + y_2^2} \leq \delta\} \, . \tag{3.7}$$

Once again, even if one would have gone through all transformations by which the normal forms (3.2) and (3.3) can be obtained from the general unperturbed system (1.4), it is in general very hard to explicitly determine K_1 and K_2 for a given system. Moreover, in principle the choice of δ determines the exact values of K_1 and K_2, i.e., $K_{1,2} = K_{1,2}(\delta)$. Of course one can scale the K_j's in (3.7): in the subsequent analysis, we assume that the largest of the $|K_j|$'s—i.e., in absolute value—is scaled to one, so that the other is less than one in absolute value and thus at most $\mathcal{O}(1)$ with respect to δ, or smaller. That is, one of the K_j's may be asymptotically small in δ.

Note that the K_j's depend in a nontrivial way on δ in the case of the complex system (3.5), in which $\mathcal{W}^u(P^-)$ twists strongly as it approaches $\mathcal{W}^u(P^+)$ (see Figures 4 and 14). Nevertheless, we shall see that this is not a problem as the statement of upcoming Theorem 3.6 does not explicitly depend on K_1, K_2, and/or δ. However, in the real case the twist condition that establishes the (non)existence of local defect solutions near P_ε^+ is given in terms of K_1 and K_2; see Theorem 3.3. Although the twist condition depends on δ through

$K_{1,2}$, the existence or nonexistence of local defect solutions can of course not depend on the specific choice of the *artificial parameter* δ. For reasons closely related to this, one also needs to be extra careful with the relative magnitudes of δ and ε: the analysis in the upcoming sections will be of leading order in ε and we therefore assume that the K_j's are of $\mathcal{O}(1)$ with respect to ε. As a consequence, for instance, we find that the statement "for ε sufficiently small" may imply that $\varepsilon \ll \delta^{(\lambda_3-\lambda_2)/\lambda_1}$, which is the order of magnitude of K_1 (with K_2 scaled to 1). These issues are considered in detail in the next section; see in particular Corollary 3.4.

3.2.1. Case I: Distinct real unstable eigenvalues. We first prove the following special version of Theorem 1.9, in the case of a three-dimensional system with two real and distinct positive eigenvalues, and obtain an explicit version of the twist condition. However, it should be noted that the twist condition (3.8) is written in terms of the normalized system (3.4) and thus not in the general setting of (1.1).

Theorem 3.3. *Assume that Hypotheses* H1–H3 *hold and that the Jacobian of* P^+ *of system* (1.4) *with* $n = 3$ *has one negative and two distinct positive real eigenvalues. Let* ε *and* δ *be sufficiently small so that* $P_\varepsilon^+ = \varepsilon(x_\varepsilon^+, y_{1,\varepsilon}^+, y_{2,\varepsilon}^+)$ *with* $|(x_\varepsilon^+, y_{1,\varepsilon}^+, y_{2,\varepsilon}^+)| = \mathcal{O}(1)$ *with respect to* ε*, lies in a* δ *neighborhood of* P^+*, and is such that both* $K_1 \neq 0$ *and* $K_2 \neq 0$ (3.7)*. Then,* (3.4) *supports a unique local defect solution near* P_ε^+ *if and only if the following twist condition holds:*

$$K_1 y_{1,\varepsilon}^+ \left(K_1 y_{1,\varepsilon}^+ + K_2 y_{2,\varepsilon}^+ \right) < 0 \,. \tag{3.8}$$

Note that $K_1 = 0$ implies that $\mathcal{W}^u(P^-)$ is tangent to the $\{y_2 = 0\}$-plane. This yields that the two-dimensional manifolds $\mathcal{W}^u(P^-)$ and $\mathcal{W}^{s\oplus lu}(P^+)$—the manifold associated to $-\lambda_1 < 0$ and $\lambda_2 > 0$ and approximated by $E^s \oplus E^{lu}$—intersect nontransversally across the heteroclinic orbit Γ of Hypothesis H2 throughout the entire phase space of the unperturbed system (3.2). Similarly, $\mathcal{W}^u(P^-)$ and $\mathcal{W}^{s\oplus uu}(P^+)$—the manifold associated to $-\lambda_1 < 0$ and $\lambda_3 > 0$ and approximated by $E^s \oplus E^{uu}$—intersect nontransversally across Γ if $K_2 = 0$. Thus, the condition that both $K_1 \neq 0$ and $K_2 \neq 0$ is another nondegeneracy condition. Observe also that indeed both $K_1 \neq 0$ and $K_2 \neq 0$ if these intersections are both transversal.

Proof. The theorem will be proved by considering an $\mathcal{O}(\delta)$ neighborhood of P^+ $(= (0,0,0))$. By construction, this implies that all correction terms $|xh_k|$ and $|y_j h_k|$ in (3.2) are of $\mathcal{O}(\delta^2)$. For a given choice of δ, ε must be chosen such that $P_\varepsilon^+ = \varepsilon(x_\varepsilon^+, y_{1,\varepsilon}^+, y_{2,\varepsilon}^+)$ is in an $\mathcal{O}(\delta)$ neighborhood of P^+.

To establish the existence of a unique local defect solution near P_ε^+, we need to construct a solution $\gamma_{ld}(t) = (x_{ld}(t), y_{1,ld}(t), y_{2,ld}(t))$ of (3.4) with $\gamma_{ld}(0) \in \mathcal{W}^s(P_\varepsilon^+)$ such that there is a $\tau > 0$ for which $\gamma_{ld}(-\tau) \in L_\delta \subset \mathcal{W}^u(P^-)$; see Figure 12. By the $\mathcal{O}(\delta^2)$ bounds on the nonlinear terms in (3.2), we deduce that for $-\tau \leq t \leq 0$ and of $\mathcal{O}(1)$ with respect to δ, we can introduce the expressions $\xi_{ld}(t)$, $\eta_{1,ld}(t)$, and $\eta_{2,ld}(t)$, which are at most $\mathcal{O}(1)$ with respect to δ, such that $\gamma_{ld}(-\tau)$ can be written as

$$\begin{aligned} x_{ld}(-\tau) &= x_{ld}(0) e^{\lambda_1 \tau} \left(1 + \delta \xi_{ld}(-\tau)\right), \\ y_{1,ld}(-\tau) &= y_{1,ld}(0) e^{-\lambda_2 \tau} \left(1 + \delta \eta_{1,ld}(-\tau)\right), \\ y_{2,ld}(-\tau) &= y_{2,ld}(0) e^{-\lambda_3 \tau} \left(1 + \delta \eta_{2,ld}(-\tau)\right). \end{aligned} \tag{3.9}$$

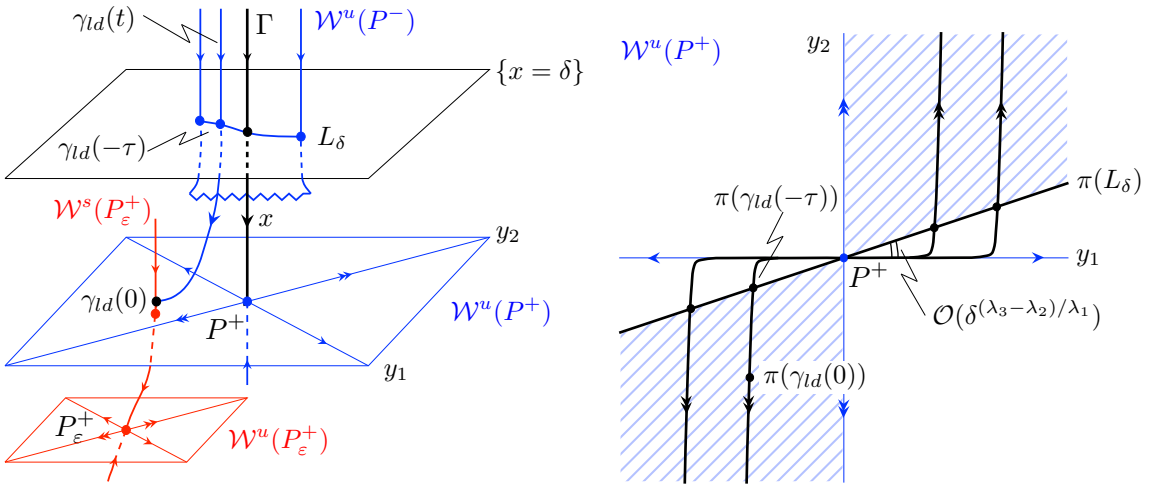

Figure 12. *Left panel: the bounded curve L_δ as intersection of $\mathcal{W}^u(P^-)$ and the $\{x=\delta\}$-plane and its role in the construction of potential local defect solutions $\gamma_{ld}(t)$. Right panel: the projection of $\gamma_{ld}(t)$ and L_δ near P^+ on the (y_1,y_2)-plane. After a projected orbit has passed through $\pi(L_\delta)$ it can only reach points in the shaded regions of the (y_1,y_2)-plane, i.e., points $\varepsilon(y_{1,\varepsilon}^+,y_{2,\varepsilon}^+)$ of $P_\varepsilon^+=\varepsilon(x_\varepsilon^+,y_{1,\varepsilon}^+,y_{2,\varepsilon}^+)$ that satisfy the twist condition (3.8). In particular, if the equilibrium point P_ε^+ is such that $\varepsilon(y_{1,\varepsilon}^+,y_{2,\varepsilon}^+)$ lies in one of the two white regions, then (3.4) (and thus (1.1)) does not possess local defect solutions near P_ε^+.*

Since the analysis takes place in an $\mathcal{O}(\delta)$ neighborhood of P^+, we know that $|x_{ld}(0)|$, $|y_{1,ld}(0)|$, and $|y_{2,ld}(0)|$ are at most of $\mathcal{O}(\delta)$. However, by Hypotheses H1 and H2 we know much more: $|P_\varepsilon^+|=\mathcal{O}(\varepsilon)$ and the one-dimensional manifold $\mathcal{W}^s(P_\varepsilon^+)$ is to leading order in ε parallel to the x-axis, i.e., to $\mathcal{W}^s(P^+)$. This implies that the norm of the y-coordinates of $\gamma_{ld}(0)$, $|(y_{1,ld}(0),y_{2,ld}(0))|$, is of $\mathcal{O}(\varepsilon)$. Moreover, since $|\gamma_{ld}(0)-P_\varepsilon^+|=\rho(\varepsilon)$—by the definition (3.6) of $\rho(\varepsilon)$—it follows that the distance between $(y_{1,ld}(0),y_{2,ld}(0))$ and the y-coordinates of P_ε^+ is at most $\mathcal{O}(\varepsilon\rho(\varepsilon))$ since $\mathcal{W}^s(P_\varepsilon^+)$ is parallel to the x-axis up to $\mathcal{O}(\varepsilon)$ corrections. Hence, we may introduce $\tilde{y}_{j,\varepsilon}^+$, with $|\tilde{y}_{j,,\varepsilon}^+|=\mathcal{O}(1)$ with respect to ε, such that

$$y_{j,ld}(0)=\varepsilon\left(y_{j,\varepsilon}^+ + \rho(\varepsilon)\tilde{y}_{j,\varepsilon}^+\right),\quad j=1,2. \tag{3.10}$$

Moreover, the evolution of the y-coordinates in (3.4) is dominated by the positive linear eigenvalues $\lambda_2,\lambda_3>0$ (especially for $t<0$). It thus follows that $|(y_{1,ld}(t),y_{2,ld}(t))|$ remains of $\mathcal{O}(\varepsilon)$ as it evolves in backward time. Hence, we can obtain a much more accurate approximation for the y-coordinates $(y_{1,ld}(t),y_{2,ld}(t))$ of $\gamma_{ld}(t)$ for $t<0$: there must be expressions $\tilde{\eta}_{1,ld}(-\tau)$ and $\tilde{\eta}_{2,ld}(-\tau)$—which are at most $\mathcal{O}(1)$ with respect to ε for $\tau>0$ of $\mathcal{O}(1)$ with respect to ε—so that the y-coordinates of $\gamma_{ld}(-\tau)$ can be written as

$$\begin{aligned} y_{1,ld}(-\tau)&=\varepsilon\left(y_{1,\varepsilon}^+ + \rho(\varepsilon)\tilde{y}_{1,\varepsilon}^+\right)e^{-\lambda_2\tau}\left(1+\varepsilon\tilde{\eta}_{1,ld}(-\tau)\right),\\ y_{2,ld}(-\tau)&=\varepsilon\left(y_{2,\varepsilon}^+ + \rho(\varepsilon)\tilde{y}_{2,\varepsilon}^+\right)e^{-\lambda_3\tau}\left(1+\varepsilon\tilde{\eta}_{2,ld}(-\tau)\right); \end{aligned} \tag{3.11}$$

see (3.10). Since we need that $\gamma_{ld}(-\tau)\in L_\delta$, we find by substitution of (3.11) into (3.7),

$$K_1\left(y_{1,\varepsilon}^+ + \rho(\varepsilon)\tilde{y}_{1,\varepsilon}^+\right)e^{-\lambda_2\tau}\left(1+\varepsilon\tilde{\eta}_{1,ld}(-\tau)\right)+K_2\left(y_{2,\varepsilon}^+ + \rho(\varepsilon)\tilde{y_,\varepsilon}_2^+\right)e^{-\lambda_3\tau}\left(1+\varepsilon\tilde{\eta}_{2,ld}(-\tau)\right)=\mathcal{O}(\varepsilon).$$

Note that we have divided out a factor ε, since the correction term of (3.7) is $\mathcal{O}(|y_1, y_2|^2) = \mathcal{O}(\varepsilon^2)$ and both y-components are of $\mathcal{O}(\varepsilon)$. Since $\rho(\varepsilon) \to 0$ as $\varepsilon \downarrow 0$ (3.6), we obtain for $\tau > 0$ of $\mathcal{O}(1)$ with respect to ε,

$$K_1 y_{1,\varepsilon}^+ + K_2 y_{2,\varepsilon}^+ e^{(\lambda_2 - \lambda_3)\tau} = 0, \tag{3.12}$$

where we note that $|(y_{1,\varepsilon}^+, y_{2,\varepsilon}^+)| = \mathcal{O}(1)$ with respect to ε and that $(y_{1,\varepsilon}^+, y_{2,\varepsilon}^+) \neq (0,0)$, by the assumption that the perturbation is generic; see Definition 1.2, Hypothesis H3, and Figure 2. Recall that $K_{1,2} = K_{1,2}(\delta)$ and that the largest K_j is scaled to one so that the other is less than or equal to one (in absolute value). In fact, it typically is not $\mathcal{O}(1)$ but asymptotically small in δ; see below and especially Corollary 3.4. Thus, we note that for a given choice of δ, condition (3.12) is indeed valid only under the assumption that ε is sufficiently small with respect to some decaying asymptotic function of δ.

To proceed, we employ the assumption that both $K_1 \neq 0$ and $K_2 \neq 0$. By considering the limits $\tau \gg 1$ and $0 < \tau \ll 1$ in (3.12), we conclude by the monotonic decay of $e^{(\lambda_2 - \lambda_3)\tau}$—recall that $\lambda_2 < \lambda_3$—that a unique local defect solution $\gamma_{ld}(t)$ near P_ε^+ exists if and only if the y-coordinates of P_ε^+ satisfy the following conditions:

$$\begin{aligned} K_1 y_{1,\varepsilon}^+ > 0: &\quad K_1 y_{1,\varepsilon}^+ + K_2 y_{2,\varepsilon}^+ < 0, \\ K_1 y_{1,\varepsilon}^+ < 0: &\quad K_1 y_{1,\varepsilon}^+ + K_2 y_{2,\varepsilon}^+ > 0. \end{aligned} \tag{3.13}$$

Note that the shaded regions in the right panel of Figure 12 correspond to those values of $(y_{1,\varepsilon}^+, y_{2,\varepsilon}^+)$ for which this condition holds.

Finally, we note that it also follows immediately from (3.12) that τ is indeed of $\mathcal{O}(1)$ magnitude with respect to ε. Through τ—and especially through the unique relation between τ and the x-coordinate $x_{ld}(t)$ of $\gamma_{ld}(t)$; see (3.9)—we may thus conclude that the defect point $\gamma_{ld}(0)$ is also defined uniquely if (3.13) holds. Since (3.13) is equivalent to (3.8), this completes the proof of Theorem 3.3; see also Remark 3.5. ∎

As the unstable manifold $\mathcal{W}^u(P^+)$ enters the neighborhood of P^+ in which (1.1) can be written as (3.4), it contains the x-axis since the unperturbed heteroclinic orbit $\Gamma(t)$ coincides with $\mathcal{W}^s(P^+)$ (= the x-axis). Moreover, the assumption that both $K_1 \neq 0$ and $K_2 \neq 0$ implies that it is tangent neither to the $\{y_2 = 0\}$-plane nor to the $\{y_1 = 0\}$-plane. That is, both the angles between $\mathcal{W}^u(P^-)$ and the $\{y_2 = 0\}$-plane and between $\mathcal{W}^u(P^-)$ and the $\{y_1 = 0\}$-plane remain bounded away from 0 outside any neighborhood of P^+. However, as soon as $\mathcal{W}^u(P^-)$ enters a region in which the flow of (3.4) is dominated by its linear part, it will be squeezed closer and closer to the $\{y_2 = 0\}$-plane since $\lambda_3 > \lambda_2$. A direct calculation, completely along the lines of the above proof of Theorem 3.3, shows that the intersection of $\mathcal{W}^u(P^-)$ with a $\{x = \delta\}$-plane, i.e., the (extension of the) curve L_δ, is asymptotically close to $\{y_2 = 0\}$-plane: the angle between the projection $\pi(L_\delta)$ on the (y_1, y_2)-plane and the y_1-axis is of $\mathcal{O}(\delta^{(\lambda_3 - \lambda_2)/\lambda_1})$; see the right-hand panel of Figure 12. More precisely, with K_2 scaled to one, it follows from a direct leading order analysis of (3.4) that

$$K_1(\delta) = \tilde{K}_1(\delta)\delta^{\frac{\lambda_3 - \lambda_2}{\lambda_1}} \quad \text{with} \quad \tilde{K}_1(0) \neq 0. \tag{3.14}$$

This provides a significant, but leading order, simplification of Theorem 3.3. In particular, while Theorem 3.3 is *asymptotically accurate* in δ, Corollary 3.4 only gives an $\mathcal{O}(1)$ result with respect to both ε and δ. See also Figure 13.

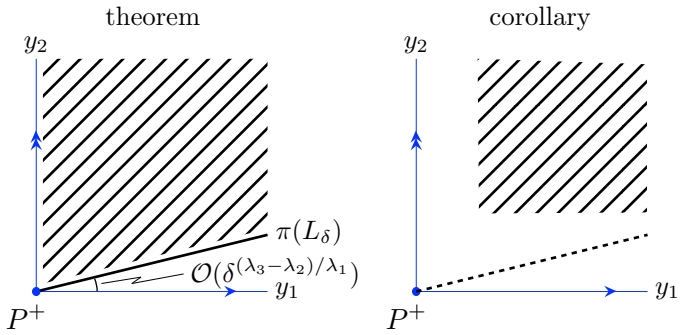

Figure 13. *Schematic representation of the difference between Theorem 3.3 and Corollary 3.4. While Theorem 3.3 gives a result up to corrections $\ll 1$ with respect to ε, Corollary 3.4 only yields results up to corrections $\ll 1$ with respect to δ*

Corollary 3.4. *Assume that Hypotheses H1–H3 hold and that the Jacobian of P^+ of system (1.4) with $n = 3$ has one negative and two distinct positive eigenvalues. Let ε and δ be sufficiently small and assume that both $K_1 \neq 0$ and $K_2 \neq 0$ (3.7) and that K_2 is scaled to one so that K_1 is given by (3.14). Then, (3.4) supports a unique local defect solution near P^+_ε if and only if $\tilde{K}_1(0)y^+_{1,\varepsilon}y^+_{2,\varepsilon} < 0$.*

Thus, the existence of local defect solutions can be established by a combination of direct information on the y-coordinates of P^+_ε and the sign of the expression $\tilde{K}_1(0)$ that encodes the accumulated nonlinear twisting of $\mathcal{W}^u(P^-)$ around the heteroclinic orbit $\Gamma(t)$ as it travels from P^- to the $\{x = \delta\}$-plane in the limit $\delta \to 0$. Note that the twist condition does not depend on δ, so that the existence of local defect indeed does not depend on the artificial parameter δ.

Proof. The statement of Corollary 3.4 follows immediately from that of Theorem 3.3 by setting $K_2 = 1$ and using (3.14) in twist condition (3.8). ∎

Remark 3.5. The asymptotic nature of the construction of Γ_ε from Γ ensures that the graph of Γ_ε indeed is asymptotically close to that of Γ, i.e., $\lim_{\varepsilon\to 0} dist(\Gamma, \Gamma_\varepsilon) = 0$; see (1.6). This is the case for all results established in this section.

3.2.2. Case II: Complex unstable eigenvalues. The situation in the case of a complex conjugate pair of unstable eigenvalues is very different from the real case, as could be seen from Theorem 1.9.

Theorem 3.6. *Assume that Hypotheses H1–H3 hold and that the Jacobian of the P^+ of system (1.4) with $n = 3$ has one negative eigenvalue and a pair of complex conjugate eigenvalues with positive real part. Then, for ε sufficiently small, (3.5) supports countably many distinct local defect solutions near P^+_ε.*

Proof. As in the real case, we look for a solution $\gamma^j_{ld}(t) = (x^j_{ld}(t), y^j_{1,ld}(t), y^j_{2,ld}(t))$ of (3.5) with $\gamma^j_{ld}(0) \in \mathcal{W}^s(P^+_\varepsilon)$ such that there is a $\tau_j > 0$ for which $\gamma^j_{ld}(-\tau_j) \in L_\delta \subset \mathcal{W}^u(P^-)$; see Figure 14. Following the approach of the real case, we first consider an $\mathcal{O}(\delta)$ neighborhood of P^+, which yields an approximation of the x-coordinate of γ^j_{ld} in terms of δ that is completely similar to (3.9),

$$x^j_{ld}(-\tau_j) = x^j_{ld}(0)e^{\lambda_1\tau_j}\left(1 + \delta\xi^j_{ld}(-\tau_j)\right).$$

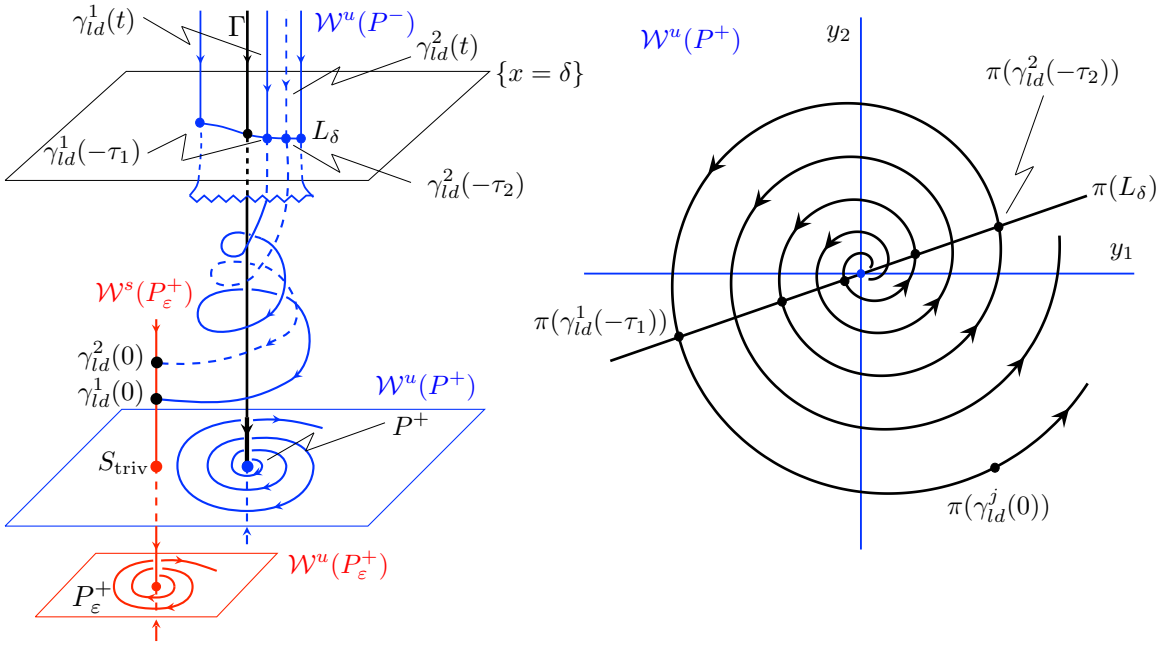

Figure 14. *The equivalent of Figure 12 in the case of complex unstable eigenvalues, indicating the existence of countably many isolated local defect solutions near* P^+_ε.

By exactly the same arguments as in the real case, we know that we can approximate the (y_1, y_2)-coordinates of γ^j_{ld} in terms the smallest asymptotic parameter ε and thus more accurately. Thus, we express the (y_1, y_2)-coordinates of $\gamma^j_{ld}(0)$ as in (3.10) in terms of the (y_1, y_2)-coordinates of $P^+_\varepsilon = \varepsilon(x^+_\varepsilon, y^+_{1,\varepsilon}, y^+_{2,\varepsilon})$, where we recall that $|(x^+_\varepsilon, y^+_{1,\varepsilon}, y^+_{2,\varepsilon})| = \mathcal{O}(1)$ with respect to ε, and $\rho(\varepsilon)$ (3.6). Moreover, we introduce the expressions $\tilde{\eta}^j_{1,ld}(t)$, and $\tilde{\eta}^j_{2,ld}(t)$—which are at most $\mathcal{O}(1)$ on a $\mathcal{O}(1)$ timescale, both with respect to ε—such that the (y_1, y_2)-coordinates of $\gamma^j_{ld}(-\tau_j)$ can be written as

(3.15)
$$y^j_{1,ld}(-\tau_j) = \varepsilon\left[\left(y^+_{1,\varepsilon}+\rho(\varepsilon)\tilde{y}^+_{1,\varepsilon}\right)\cos\beta\tau_j - \left(y^+_{2,\varepsilon}+\rho(\varepsilon)\tilde{y}^+_{2,\varepsilon}\right)\sin\beta\tau_j\right]e^{-\alpha\tau_j}\left(1+\varepsilon\tilde{\eta}^j_{1,ld}(-\tau_j)\right),$$
$$y^j_{2,ld}(-\tau_j) = \varepsilon\left[\left(y^+_{2,\varepsilon}+\rho(\varepsilon)\tilde{y}^+_{2,\varepsilon}\right)\cos\beta\tau_j + \left(y^+_{1,\varepsilon}+\rho(\varepsilon)\tilde{y}^+_{1,\varepsilon}\right)\sin\beta\tau_j\right]e^{-\alpha\tau_j}\left(1+\varepsilon\tilde{\eta}^j_{2,ld}(-\tau_j)\right),$$

as long as $\tau_j = \mathcal{O}(1)$ with respect to ε; cf. (3.11). Substitution of approximation (3.15) into (3.7) yields

$$\left[\left(K_1 y^+_{1,\varepsilon} + K_2 y^+_{2,\varepsilon}\right)\cos(\beta\tau_j) - \left(K_1 y^+_{2,\varepsilon} - K_2 y^+_{1,\varepsilon}\right)\sin(\beta\tau_j)\right]e^{-\alpha\tau_j} = \mathcal{O}(\varepsilon,\rho(\varepsilon)).$$

Since $\tau_j = \mathcal{O}(1)$, the above expression can, to leading order, be written as

$$R^+_{K,\varepsilon}\cos(\beta\tau_j + \theta^+_{K,\varepsilon}) = 0 \tag{3.16}$$

for some radius $R^+_{K,\varepsilon} > 0$ and some phase shift $\theta^+_{K,\varepsilon} \in [0, 2\pi)$. In fact,

$$R^+_{K,\varepsilon} = \sqrt{\left(K_1^2 + K_2^2\right)\left((y^+_{1,\varepsilon})^2 + (y^+_{2,\varepsilon})^2\right)},$$

and it follows that $R^+_{K,\varepsilon} > 0$ since $(K_1, K_2) \neq 0$ by Definition 3.2 and (3.7) and $(y^+_{1,\varepsilon}, y^+_{2,\varepsilon}) \neq (0,0)$ by Hypothesis H3. Since we assumed throughout the approximation analysis that $\tau_j = \mathcal{O}(1)$, we conclude that there are at least $\mathcal{O}(1)$ solutions τ_j of (3.16) and thus at least $\mathcal{O}(1)$ many distinct local defect solutions $\gamma^j_{ld}(t)$ of (3.5).

To understand that there must be countably many local defect solutions $\gamma^j_{ld}(t)$, we once again take a geometrical point of view and consider the two-dimensional manifold $\mathcal{L}_\delta$ spanned by the solutions $\gamma(t)$ of the unperturbed system (3.3) that satisfy $\gamma(0) \in L_\delta$. In forward time, $\mathcal{L}_\delta$ spirals *downward*—in the x-direction; see Figure 14, where decreasing x indeed corresponds to *going down*—to the $\{x = 0\}$-plane $\mathcal{W}^u(P^+)$. Since the y-coordinates of the solutions $\gamma(t) \subset \mathcal{L}_\delta$ expand and rotate uniformly in t, the manifold $\mathcal{L}_\delta$ accumulates on $\mathcal{W}^u(P^+)$—it cannot pass through it—with an exponentially decreasing distance in the x between successive twists. There is a direct connection between the above established $\mathcal{O}(1)$ many distinct local defect solutions $\gamma^j_{ld}(t)$ and orbits on $\mathcal{L}_\delta$: the $t \leq 0$ part of a local defect solution $\gamma^j_{ld}(t)$ corresponds, through a time shift of τ_j (determined by (3.16)), to the $t \leq \tau_j$ part of an orbit $\gamma(t) \subset \mathcal{L}_\delta$ that intersects the stable manifold $\mathcal{W}^s(P^+_\varepsilon)$ at $t = \tau_j$; (by definition of τ_j); see again Figure 14. A priori, the above analytic approximation approach is valid only up to $\mathcal{O}(1)$ values of τ_j. However, from the geometrical picture, which is also based on the leading order linear structure of (3.3), it follows that $\mathcal{L}_\delta$ must indeed intersect $\mathcal{W}^s(P^+_\varepsilon)$ countably many times, with intersections occurring at times $\tau_j \uparrow \infty$ as $j \to \infty$. Moreover, the intersections $\mathcal{L}_\delta \cap \mathcal{W}^s(P^+_\varepsilon)$ accumulate on the unique trivial defect point $S_{\text{triv}} = \mathcal{W}^s(P^+_\varepsilon) \cap \mathcal{W}^u(P^+)$ $(\subset \{x = 0\})$; see Figure 14.

Finally, it should be noted that the relative position of two-dimensional manifold $\mathcal{W}^u(P^+_\varepsilon)$ with respect to $\mathcal{W}^u(P^+)$ does not have an effect on the above geometrical arguments. Referring once again to Figure 14, in which $\mathcal{W}^u(P^+_\varepsilon)$ is sketched *below* $\mathcal{W}^u(P^+)$, also in the case that $\mathcal{W}^u(P^+_\varepsilon)$ is *above* $\mathcal{W}^u(P^+)$ there must be countably many intersections $\mathcal{L}_\delta \cap \mathcal{W}^s(P^+_\varepsilon)$. Here the somewhat loose *above* and *below* terminology refers to x^+_ε, the x-coordinate of P^+_ε being either positive or negative since $\mathcal{W}^u(P^+)$ is given by $\{x = 0\}$ locally near P^+ and $\mathcal{W}^u(P^+_\varepsilon)$ is to leading order parallel to $\mathcal{W}^u(P^+)$. In a $x^+_\varepsilon < 0$ *below* case, as sketched Figure 14, all local defect solutions $\gamma^j_{ld}(t)$ of (3.5) approach P^+_ε *from above*, i.e., along the $x > x^+_\varepsilon$-part of $\mathcal{W}^s(P^+_\varepsilon)$. In an $x^+_\varepsilon > 0$ *above* case, only the first finitely many $\gamma^j_{ld}(t)$'s approach P^+_ε *from above*, and all next local defect solutions $\gamma^j_{ld}(t)$ approach P^+_ε *from below*, i.e., along the $x < x^+_\varepsilon$-part of $\mathcal{W}^s(P^+_\varepsilon)$. ■

Remark 3.7. Of course the sketch in Figure 14 is an idealization, especially in the sense that the manifold $W^u(P^-)$ will also spiral around the unperturbed homoclinic orbit Γ, i.e., the x-axis, above the $\{x = \delta\}$-plane (which is not indicated in Figure 14). By the definition of δ—small enough so that the flow of (3.3) is dominated by its linear components—this will be the case for any choice of δ. This implies that it is in this case not possible to choose ε such that all intersections of $W^u(P^-)$ and $W^s(P^+_\varepsilon)$ take place *below* the $\{x = \delta\}$-plane. More precisely, the first intersection below $\{x = \delta\}$, indicated by $\pi(\gamma^1_{ld}(-\tau_1))$ in the right panel of Figure 14, is only the first intersection of $W^u(P^-)$ and $W^s(P^+_\varepsilon)$ *for this specific choice of* δ. Increasing δ will generate more, *earlier*, intersections. In fact, the first intersection of $W^u(P^-)$ and $W^s(P^+_\varepsilon)$, *if* there is such a first intersection, takes place at an $\mathcal{O}(1)$ distance from P^+ and is thus a global defect solution as defined in Definition 1.7. It is a priori also possible that the

intersections of $W^u(P^-)$ and $W^s(P_\varepsilon^+)$ also accumulate near P^-. Thus, it is not possible to make a sharp distinction between local and global defect solutions in this case.

3.3. $n > 3$. In this section, we again consider the critical setting $\dim(\mathcal{W}^u(P^-)) = \dim(\mathcal{W}^u(P^+)) > 1$ but now in the general n-dimensional case, $n > 3$. Although we find that equivalents of Theorems 3.3 and 3.6 also hold in dimension $n > 3$, we also show that due to the additional influences of the strong unstable spectrum there is an increasing potential richness in the structure, and thus number of local defect solutions near P_ε^+, as the dimension of system (1.1) increases.

Throughout this section, (1.4) is supposed to have the normal form structure of (3.1) near P^+. As in section 3.2, we work with modified versions of (3.1) according to the nature of the leading unstable eigenvalues. Also as in section 3.2, we perform our analysis in an $\mathcal{O}(\delta)$ neighborhood of P^+— which corresponds to $(x^{ls}, x^{ss}, y^{lu}, y^{uu}) \equiv (0,0,0,0)$ in (3.1)—and thus again introduce a second small parameter δ such that $P_\varepsilon^+ = \varepsilon(x_\varepsilon^{ls}, x_\varepsilon^{ss}, y_\varepsilon^{lu}, y_\varepsilon^{uu})$ lies inside this $\mathcal{O}(\delta)$ neighborhood. In particular, we choose ε such that $\rho(\varepsilon)$ as defined in (3.6) is sufficiently small compared to δ (if possible, see Remark 3.7).

Following section 3.1, we define k, with $1 < k < n$ by Hypothesis H2, as the dimension of $\mathcal{W}^u(P^-)$ $(= \dim(\mathcal{W}^u(P^+)))$ and $\ell = n - k$ as $\dim(\mathcal{W}^s(P^+))$. By Hypothesis H2 we know that the heteroclinic orbit Γ exists as an intersection of the k-dimensional manifold $\mathcal{W}^u(P^-)$ with the ℓ-dimensional manifold $\mathcal{W}^s(P^+)$. Moreover, by the assumption of *minimal nontransversality* we also know that $\dim(\mathcal{W}^u(P^-) \cap \mathcal{W}^s(P^+)) = 1$, i.e., that the one-dimensional curve Γ is the locally unique intersection of $\mathcal{W}^u(P^-)$ with $\mathcal{W}^s(P^+)$. Typically, $\Gamma(t)$ will approach P^+ along the eigendirection associated to the leading stable direction x^{ls}. By Hypothesis H2 all eigenvalues of the Jacobian of P^+ are simple. Hence, the x^{ls}-direction is one-dimensional if the leading stable eigenvalue ν_ℓ is real and two-dimensional if the leading stable eigenvalues ν_ℓ and $\nu_{\ell-1}$ form a complex conjugate pair; see section 3.1. By taking δ small enough, we may assume that $\Gamma(t)$ intersects the $(n-1)$-dimensional hyperplane $\{x^{ls} = \delta\}$, respectively, $\{x_1^{ls} = \delta\}$, transversally, if $\nu_\ell \in \mathbb{R}$, respectively, $\nu_\ell \notin \mathbb{R}$, since the flow of (3.1) is strongly dominated by the linear flow in an $\mathcal{O}(\delta)$ neighborhood of P^+. We now define the equivalent of the bounded one-dimensional curve L_δ in the two-dimensional plane $\{x = \delta\}$ of the three-dimensional problem (see Definition 3.2) in the general n-dimensional setting.

Definition 3.8. *The bounded $(k-1)$-dimensional manifold L_δ is determined by the transverse intersection of $\mathcal{W}^u(P^-)$ with either the hyperplane $\{x^{ls} = \delta\}$ or $\{x_1^{ls} = \delta\}$, inside the cylinder $\sqrt{|y^{lu}|^2 + |y^{uu}|^2} \leq \delta\}$.*

In the nongeneric case in which $\Gamma(t)$ approaches P^+ along one of the faster x^{ss}-directions, the definition of L_δ can be adapted by choosing a hyperplane of intersection transversal to $\Gamma(t)$'s direction of approach. In other words, the assumption that $\Gamma(t)$ approaches P^+ along the leading stable direction x^{ls}-direction is not a restriction, but for transparency of presentation we refrain from going into the details of the nongeneric situation. Due to the exponentially strong *squeezing* in all strong stable x^{ss}-directions near $\Gamma(t)$ (in an $\mathcal{O}(\delta)$ neighborhood of P^+), all x^{ss}-coordinates of L_δ may be assumed to be exponentially close in δ to the intersection point $\Gamma_\delta \stackrel{\text{def}}{=} \Gamma \cap \{x^{ls} = \delta\}$, or $\Gamma_\delta \stackrel{\text{def}}{=} \Gamma \cap \{x_1^{ls} = \delta\}$. Since $\Gamma(t) \subset \mathcal{W}^s(P^+)$ and $\mathcal{W}^s(P^+) = \{y^{ly} = 0, y^{uu} = 0\}$ locally near P^+ (3.1), we conclude that Γ_δ, up to exponentially small correction, can be written as $\Gamma_\delta = (x_\delta, 0, 0)$ with either $x_\delta = (x_\delta^{ls}, x_\delta^{ss}) = (\delta, 0) \in E^{ls} \oplus E^{ss}$ or

$x_\delta = ((\delta, 0), 0) \in E^{ls} \oplus E^{ss}$. In the latter case one may need to tune δ in such a way that the (spiraling) x_2^{ls}-coordinate of $\Gamma(t) \cap \{x_1^{ls} = \delta\}$ is exactly 0.

Thus, we can now approximate L_δ in a way similar to the three-dimensional case (3.7): there are $K^{lu} \in \mathbb{R}$ or $\mathbb{R}^2$ and $K^{uu} \in \mathbb{R}^{k-1}$ or $\mathbb{R}^{k-2}$ with $(K^{lu}, K^{uu}) \neq (0,0)$, such that L_δ is given, up to exponentially small corrections with respect to δ in the x-coordinates, by

$$L_\delta = \{(x_\delta, y^{lu}, y^{uu}) \in E^s \oplus E^{lu} \oplus E^{uu} \mid K^{lu} y^{lu} + K^{uu} y^{uu} + \mathcal{O}(|y^{lu}, y^{uu}|^2) = 0, \quad \sqrt{|y^{lu}|^2 + |y^{uu}|^2} \leq \delta\}, \tag{3.17}$$

where $K^{uu}y^{uu}$, respectively, $K^{lu}y^{lu}$, denote the standard inner products in $\mathbb{R}^2$ (if $K^{lu} \in \mathbb{R}^2$), respectively, in $\mathbb{R}^{k-1}$ and with x_δ as introduced above. That is, depending on the leading stable eigenvalue, $x_\delta = (\delta, 0) \in E^{ls} \oplus E^{ss}$ or $x_\delta = ((\delta, 0), 0) \in E^{ls} \oplus E^{ss}$. As in the case $n = 3$, we assume that the largest of the coefficients K_j^{uu} and K_j^{lu} of (3.17)—in absolute value—is scaled to 1, so that we may use in the subsequent analysis that all K_j^{uu}'s and K_j^{lu}'s are either of $\mathcal{O}(1)$ with respect to δ and ≤ 1 (in absolute value) or asymptotically small in δ; see section 3.3.2.

3.3.1. Direct n-dimensional generalizations of Theorems 3.3 and 3.6. Like in the case $n = 3$, we first consider the situation in which the leading unstable eigenvalue $\nu_{\ell+1}$ (section 3.1) is real (and simple by Hypothesis H2). Since the decomposition of the stable x-direction into $x = (x^{ls}, x^{ss})$ is less relevant for the upcoming analysis, we rewrite and simplify normal form (3.1) and consider the following perturbed system in this section,

$$\begin{pmatrix} \dot{x} \\ \dot{y}^{lu} \\ \dot{y}^{uu} \end{pmatrix} = \begin{cases} \begin{pmatrix} A^s x + \mathcal{O}\left(|x|(|x| + |y|)\right) \\ \lambda_{\ell+1} y^{lu} + \mathcal{O}\left(|x||y|\right) \\ A^{uu} y^{uu} + \mathcal{O}\left(|y|(|x| + |y|)\right) \end{pmatrix}, & t < 0, \\ \begin{pmatrix} A^s x + \mathcal{O}\left(|x|(|x| + |y|)\right) \\ \lambda_{\ell+1} y^{lu} + \mathcal{O}\left(|x||y|\right) \\ A^{uu} y^{uu} + \mathcal{O}\left(|y|(|x| + |y|)\right) \end{pmatrix} + \varepsilon \begin{pmatrix} g^s(x,y) \\ g^{lu}(x,y) \\ g^{uu}(x,y) \end{pmatrix}, & t > 0, \end{cases} \tag{3.18}$$

with $x \in E^s$, $y^{lu} \in E^{lu}$ and $y^{uu} \in E^{uu}$, $A^{s,uu}$ such that $\sigma(A^s) = \sigma(f_u(0)) \cap \{\Re(\nu) < 0\}$ and $\sigma(A^{uu}) = \sigma(f_u(0)) \cap \{\Re(\nu) > \lambda^{uu}\}$ and $g^{s,lu,uu}$ sufficiently smooth and $\mathcal{O}(1)$ with respect to ε. Moreover, we have explicitly used that $\lambda_{\ell+1}$ $(=\nu_{\ell+1})$ is real and simple (so that the y^{lu}-direction is indeed one-dimensional).

We now follow the same approach as in section 3.2: we establish the existence of a local defect solution near $P_\varepsilon^+ = \varepsilon(x_\varepsilon^+, y_\varepsilon^{+,lu}, y_\varepsilon^{+,uu})$ in the coordinates of (3.18) by constructing a solution $\gamma_{ld}(t) = (x_{ld}(t), y_{ld}^{lu}(t), y_{ld}^{uu}(t))$ of (3.18) that has $\gamma_{ld}(0) \in \mathcal{W}^s(P_\varepsilon^+)$ such that there is a $\tau > 0$ for which $\gamma_{ld}(-\tau) \in L_\delta$. By Hypotheses H1–H3 we know that $\mathcal{W}^s(P_\varepsilon^+)$ is locally parallel to $\mathcal{W}^s(P^+)$ $(= \{y^{lu} = 0, y^{uu} = 0\}$ near $P^+ = (0,0,0))$ up to $\mathcal{O}(\varepsilon)$ corrections, which implies that we can approximate the y-coordinates of the initial condition $\gamma_{ld}(0)$ by the y-coordinates of P_ε^+ in a way completely similar to (3.10),

$$y_{ld}^{lu}(0) = \varepsilon\left(y_\varepsilon^{+,lu} + \rho(\varepsilon)\tilde{y}_\varepsilon^{+,lu}\right), \; y_{ld}^{uu}(0) = \varepsilon\left(y_\varepsilon^{+,uu} + \rho(\varepsilon)\tilde{y}_\varepsilon^{+,uu}\right). \tag{3.19}$$

Given the strong dominance of the linear terms in (3.18) and following the arguments presented in section 3.2, we may conclude that we again can approximate the y-coordinates of $\gamma_{ld}(-\tau)$ in terms of ε and that there are thus smooth expressions $\tilde{\eta}^{lu}_{ld}(t)$ and $\tilde{\eta}^{uu}_{j,ld}(t)$, $j = 1, \dots, k-1$, that are at most $\mathcal{O}(1)$ with respect to ε, so that the y-coordinates of $\gamma_{ld}(t)$ can be written as

$$\begin{aligned} y^{lu}_{ld}(-\tau) &= \varepsilon \left(y^{+,lu}_{\varepsilon} + \rho(\varepsilon) \tilde{y}^{+,lu}_{\varepsilon} \right) \left(1 + \delta \tilde{\eta}^{lu}_{ld}(-\tau) \right) e^{-\lambda_{\ell+1}\tau}, \\ y^{uu}_{ld}(-\tau) &= \varepsilon e^{-A^{uu}\tau} \left[\left(\operatorname{diag}(1 + \delta \tilde{\eta}^{uu}_{j,ld}(-\tau) \right) \left(y^{+,uu}_{\varepsilon} + \rho(\varepsilon) \tilde{y}^{+,uu}_{\varepsilon} \right) \right] \end{aligned} \tag{3.20}$$

as long as $\tau = \mathcal{O}(1)$ with respect to ε. Here, $\operatorname{diag}(\cdot)$ represents a diagonal matrix. Substitution of (3.20) into (3.17) yields

$$K^{lu} e^{-\lambda_{\ell+1}\tau} y^{+,lu}_{\varepsilon} + K^{uu} e^{-A^{uu}\tau} y^{+,uu}_{\varepsilon} = \mathcal{O}(\varepsilon, \rho(\varepsilon)).$$

In other words, to leading order in ε, we have that

$$K^{lu} y^{+,lu}_{\varepsilon} + K^{uu} e^{-(A^{uu} - \lambda_{\ell+1}\mathrm{Id})\tau} y^{+,uu}_{\varepsilon} = 0 \tag{3.21}$$

with Id the identity matrix. Similar to the $n = 3$ case, we now need to assume that both $K^{lu} \neq 0$ and $K^{uu} \neq 0$, i.e., that L_δ is not tangent to either the $\{y^{lu} = 0\}$-hyperplane or the $\{y^{uu} = 0\}$-axis (3.17). Note that this is equivalent to assuming that $\mathcal{W}^u(P^-)$ is tangent to neither $\mathcal{W}^{s\oplus uu}(P^+)$—the manifold approximated by $E^s \oplus E^{uu}$—nor $\mathcal{W}^{s\oplus lu}(P^+)$ the manifold associated to $E^s \oplus E^{lu}$. By construction, $0 < \lambda_{\ell+1} < \Re(\lambda_j)$, $j = \ell + 2, \dots, n$, yielding that $|e^{-(A^{uu} - \lambda_{\ell+1}\mathrm{Id})\tau} y^{+,uu}_{\varepsilon}|$ can be made arbitrarily small by taking τ large enough. Thus, completely similar to the $n = 3$ case, we conclude by considering $0 < \tau$ small enough and large enough that there indeed are values of τ for which (3.21) holds if

$$K^{lu} y^{+,lu}_{\varepsilon} \left(K^{lu} y^{+,lu}_{\varepsilon} + K^{uu} y^{+,uu}_{\varepsilon} \right) < 0. \tag{3.22}$$

Hence, we have established an n-dimensional generalization of Theorem 3.3.

Theorem 3.9. *Assume that Hypotheses* H1–H3 *hold, that* $\dim(\mathcal{W}^u(P^-)) = \dim(\mathcal{W}^u(P^+)) > 1$, *and that the Jacobian of* P^+ *of system* (1.4) *has a real leading unstable eigenvalue. Let* ε *and* δ *be sufficiently small so that* $P^+_\varepsilon = \varepsilon(x^+_\varepsilon, y^{+,lu}_\varepsilon, y^{+,uu}_\varepsilon)$ *with* $|(x^+_\varepsilon, y^{+,lu}_\varepsilon, y^{+,uu}_\varepsilon)| = \mathcal{O}(1)$ *with respect to* ε *lies in a* δ *neighborhood of* P^+ *and such that both* $K^{lu} \neq 0$ $(\in \mathbb{R})$ *and* $K^{uu} \neq 0$ $(\in \mathbb{R}^{k-1})$ (3.17). *Then,* (3.18) *supports at least one local defect solution near* P^+_ε *if the twist condition* (3.21) *holds.*

Notice though that there is also a significant difference between Theorem 3.3 and its n-dimensional generalization: for $n = 3$, a local defect solution near P^+_ε is *uniquely* determined *if and only if* twist condition (3.8) holds, while in Theorem 3.9, *at least one* local defect solution near P^+_ε exists *if* (3.21) holds. This is due to monotonically decreasing term $|K_2 y^+_{2,\varepsilon} e^{(\lambda_2 - \lambda_3)\tau}|$ in (3.12), while the corresponding term $|K^{uu} e^{-(A^{uu} - \lambda_{\ell+1}\mathrm{Id})\tau} y^{+,uu}_\varepsilon|$ in (3.21) is in general not monotonically decreasing; see section 3.3.2. Moreover, like in Theorem 3.3, twist condition (3.21) is asymptotically accurate in δ and thus depends explicitly on the *artificial* parameter δ through $K^{lu,uu} = K^{lu,uu}(\delta)$. In section 3.3.2, we present two n-dimensional generalizations of Corollorary 3.4 in which the twist conditions are leading order in both ε and δ and thus do not depend explicitly on δ.

There is a more direct equivalence between the three- and the n-dimensional case if the leading unstable eigendirection is spanned by a pair of complex conjugate eigenvalues $\nu_{\ell+1}$ and $\nu_{\ell+2}$. The matrix A^{lu} can be brought in standard form (cf. (3.5) by introducing $\alpha_{\ell+1} = \Re(\nu_{\ell+1}) > 0$ and $\beta_{\ell+1} = \Im(\nu_{\ell+1}) > 0$, i.e., $\nu_{\ell+1,\ell+2} = \alpha_{\ell+1} \pm i\beta_{\ell+1}$. Hence, we consider the perturbed system,

$$
\begin{pmatrix} \dot{x} \\ \dot{y}_1^{lu} \\ \dot{y}_2^{lu} \\ \dot{y}^{uu} \end{pmatrix} = \begin{cases} \begin{pmatrix} A^s x + \mathcal{O}\left(|x|(|x|+|y|)\right) \\ \alpha_{\ell+1} y_1^{lu} + \beta_{\ell+1} y_2^{lu} + \mathcal{O}\left(|x||y|\right) \\ -\beta_{\ell+1} y_1^{lu} + \alpha_{\ell+1} y_2^{lu} + \mathcal{O}\left(|x||y|\right) \\ A^{uu} y^{uu} + \mathcal{O}\left(|y|(|x|+|y|)\right) \end{pmatrix}, & t < 0, \\ \begin{pmatrix} A^s x + \mathcal{O}\left(|x|(|x|+|y|)\right) \\ \alpha_{\ell+1} y_1^{lu} + \beta_{\ell+1} y_2^{lu} + \mathcal{O}\left(|x||y|\right) \\ -\beta_{\ell+1} y_1^{lu} + \alpha_{\ell+1} y_2^{lu} + \mathcal{O}\left(|x||y|\right) \\ A^{uu} y^{uu} + \mathcal{O}\left(|y|(|x|+|y|)\right) \end{pmatrix} + \varepsilon \begin{pmatrix} g^s(x,y) \\ g_1^{lu}(x,y) \\ g_2^{lu}(x,y) \\ g^{uu}(x,y) \end{pmatrix}, & t > 0, \end{cases} \tag{3.23}
$$

with $x \in E^s$, $(y_1^{lu}, y_2^{lu}) \in E^{lu}$ and $y^{uu} \in E^{uu}$, $A^{s,uu}$ such that $\sigma(A^s) = \sigma(f_u(0)) \cap \{\Re(\nu) < 0\}$ and $\sigma(A^{uu}) = \sigma(f_u(0)) \cap \{\Re(\nu) > \lambda^{uu}\}$ and $g^{s,lu,uu}$ sufficiently smooth and $\mathcal{O}(1)$ with respect to ε. We establish the following direct generalization of Theorem 3.6.

Theorem 3.10. *Assume that Hypotheses* H1–H3 *hold, that* $\dim(\mathcal{W}^u(P^-)) = \dim(\mathcal{W}^u(P^+)) = k > 1$, *and that the leading unstable eigenvalues of the Jacobian of system* (1.4) *at* P^+ *form a complex conjugate pair. Let* ε *and* δ *be sufficiently small so that* $P_\varepsilon^+ = \varepsilon(x_\varepsilon^+, y_{1,\varepsilon}^{+,lu}, y_{2,\varepsilon}^{+,lu}, y_\varepsilon^{+,uu})$ *with* $|(x_\varepsilon^+, y_{1,\varepsilon}^{+,lu}, y_{2,\varepsilon}^{+,lu}, y_\varepsilon^{+,uu})| = \mathcal{O}(1)$ *with respect to* ε *and lies in a* δ *neighborhood of* P^+, *and such that* $K^{lu} \neq 0$ $(\in \mathbb{R}^2)$ *if* $k > 2$ (3.17). *Then,* (3.23) *supports countably many distinct local defect solutions near* P_ε^+.

There is one additional generic assumption in this theorem compared to Theorem 3.6: in the case that there are strong unstable y^{uu}-directions, i.e., if $k > 2$, K^{lu} must be unequal to zero, which implies that L_δ cannot be tangent to $\{y^{uu} = 0\}$ (3.17), i.e., $W^u(P^-)$ cannot be tangent to the manifold $\mathcal{W}^{s\oplus lu}(P^+)$ (which is tangent to $E^s \oplus E^{lu}$).

Proof. We follow the approach developed for the proofs of Theorems 3.3, 3.6, and 3.9. Skipping some of the details, we immediately observe that there exist smooth $\mathcal{O}(1)$ expressions $\tilde{\eta}_{1,ld}^{lu}(t)$, $\tilde{\eta}_{2,ld}^{lu}(t)$, and $\tilde{\eta}_{j,ld}^{uu}(t)$, $j = 1, \ldots, k-2$, such that for $\tau = \mathcal{O}(1)$ with respect to ε, the y-coordinates of a local defect solution $\gamma_{ld}(t)$ at $t = -\tau < 0$ can be written as

$$
\begin{aligned}
y_{1,ld}^{lu}(-\tau) &= \left(y_{1,ld}^{lu}(0)\cos\beta_{\ell+1}\tau - y_{2,ld}^{lu}(0)\sin\beta_{\ell+1}\tau\right)\left(1 + \delta\tilde{\eta}_{1,ld}^{lu}(-\tau)\right)e^{-\alpha_{\ell+1}\tau}, \\
y_{2,ld}^{lu}(-\tau) &= \left(y_{2,ld}^{lu}(0)\cos\beta_{\ell+1}\tau + y_{1,ld}^{lu}(0)\sin\beta_{\ell+1}\tau\right)\left(1 + \delta\tilde{\eta}_{2,ld}^{lu}(-\tau)\right)e^{-\alpha_{\ell+1}\tau}, \\
y_{ld}^{uu}(-\tau) &= e^{-A^{uu}\tau}\left[\left(\mathrm{diag}(1 + \delta\tilde{\eta}_{j,ld}^{uu}(-\tau)\right)y_{ld}^{uu}(0)\right],
\end{aligned} \tag{3.24}
$$

where we know that we once again have the approximations

$$
y_{j,ld}^{lu}(0) = \varepsilon\left(y_{j,\varepsilon}^{+,lu} + \rho(\varepsilon)\tilde{y}_{j,\varepsilon}^{+,lu}\right),\ j = 1,2,\ \ y_{ld}^{uu}(0) = \varepsilon\left(y_\varepsilon^{+,uu} + \rho(\varepsilon)\tilde{y}_\varepsilon^{+,uu}\right); \tag{3.25}
$$

cf. (3.19). Plugging this into (3.17) yields

$$\left[\left(K_1^{lu}y_{1,\varepsilon}^{+,lu}+K_2^{lu}y_{2,\varepsilon}^{+,lu}\right)\cos(\beta_{\ell+1}\tau)-\left(K_1^{lu}y_{1,\varepsilon}^{+,lu}-K_2^{lu}y_{2,\varepsilon}^{+,lu}\right)\sin(\beta_{\ell+1}\tau)\right]e^{-\alpha_{\ell+1}\tau}$$
$$=-K^{uu}e^{-A^{uu}\tau}y_\varepsilon^{+,uu}+\mathcal{O}(\varepsilon)\,,$$

where $(K_1^{lu},K_2^{lu})\in\mathbb{R}^2$ and $K^{uu}\in\mathbb{R}^{k-2}$. By defining

$$R_{K,\varepsilon}^{+,lu}=\sqrt{\left((K_1^{lu})^2+(K_2^{lu})^2\right)\left((y_{1,\varepsilon}^{+,lu})^2+(y_{2,\varepsilon}^{+,lu})^2\right)},$$

this is to leading order equivalent to

$$R_{K,\varepsilon}^{+,lu}\cos(\beta_{\ell+1}\tau+\theta_{K,\varepsilon}^{+,lu})=-K^{uu}e^{-(A^{uu}-\alpha_{\ell+1}\mathrm{Id})\tau}y_\varepsilon^{+,uu} \tag{3.26}$$

for some phase shift $\theta_{K,\varepsilon}^{+}\in[0,2\pi)$; see (3.16) and (3.21). By definition of the leading unstable eigenvalues, we know that $|e^{-(A^{uu}-\alpha_{\ell+1}\mathrm{Id})\tau}y_\varepsilon^{+,uu}|$ becomes arbitrarily small for τ large enough. Hence, we may conclude that (3.26) has $\mathcal{O}(1)$ many discrete solutions τ_j *if* $R_{K,\varepsilon}^{+,lu}>0$. It follows from Hypothesis H3 that $((y_{1,\varepsilon}^{+,lu})^2+(y_{2,\varepsilon}^{+,lu})^2)>0$, but in general we only know that $(K^{lu},K^{uu})\neq(0,0)\in\mathbb{R}^2\times\mathbb{R}^{k-2}$; see Definition 3.8 and (3.17). To obtain Theorem 3.10 from (3.26), it is necessary that $R_{K,\varepsilon}^{+,lu}>0$ and we thus need to assume that $(K_1^{lu},K_2^{lu})\neq(0,0)\in\mathbb{R}^2$. This implies that we need to assume that $\mathcal{W}^u(P^-)$ is not asymptotically close to the full two-dimensional leading unstable eigenspace E^{lu} of P^+. Also since we know that (K^{lu},K^{uu}) cannot be equal to $(0,0)$, this additional assumption only needs to be imposed if the y^{uu}-direction exists, i.e., if the number of unstable eigendirections k exceeds 2, the number of leading eigendirections. See also the proof of Theorem 3.6, in which indeed $k=2$.

Finally, since τ must be $\mathcal{O}(1)$ with respect to δ, we only established the existence of arbitrarily but $\mathcal{O}(1)$ many local defect solutions $\gamma_{ld}(t)$ by our analytic approximation approach. The existence of countably many local defect solutions near P_ε^+ follows by a similar geometric extension of the analytic arguments as in the proof of Theorem 3.6. ∎

3.3.2. The impact of the strong unstable spectrum. In the three-dimensional setting there is a sharp distinction between either having one unique local defect solution—if a twist condition holds—or having countably many isolated local defect solutions; see Theorems 3.3 and 3.6. In this section, we show that in the n-dimensional setting, the situation is much less strongly separated between these two extreme cases. In fact, we show that the gap between the statements of the n-dimensional generalizations of Theorems 3.3 and 3.6, i.e., Theorems 3.9 and 3.10, can be bridged by considering several natural and thus generic subcases associated to the relative richness of the strong unstable spectrum for $n>3$ (compared to $n=3$).

We first consider the *extreme* case in which all k unstable eigenvalues ν_j, $j=\ell+1,\dots,\ell+k=n$ of P^+ are real ($\nu_j=\lambda_j$ for all $j=\ell+1,\dots,n$). Then, it is natural to decompose the y-directions in normal form (3.1) into $(y_1,y_2,\dots,y_k)$, where $y_1=y^{lu}$ and $(y_2,\dots,y_k)=y^{uu}$. In these coordinates, the approximation (3.17) of L_δ is given by

$$L_\delta=\{(x_\delta,y)\,|\,K_1y_1+K_2y_2+\cdots+K_ky_k+\mathcal{O}(|y|^2)=0\} \tag{3.27}$$

(cf. (3.2)), where we once again note that the coefficients K_j, $j = 1, \dots, k$, depend on δ. The upcoming theorem establishes that Theorem 3.9 with twist condition (3.21) is only a special case of a more general situation in which there can be up to $k-1$ distinct local defect solutions near P_ε^+ if certain *generalized twist conditions* are satisfied. Although it is in principle possible to derive these generalized twist conditions explicitly, we refrain from going into the full analytic details; see, however, Corollaries 3.13 and 3.14.

Theorem 3.11. *Assume that Hypotheses* H1–H3 *hold, that* $\dim(\mathcal{W}^u(P^-)) = \dim(\mathcal{W}^u(P^+)) = k > 1$, *and that all* k *unstable eigenvalues* $\nu_j = \lambda_j$, $j = \ell+1, \dots, \ell+k = n$, *of the Jacobian of* (1.4) *at* P^+ *are real and distinct. Let* ε *and* δ *be sufficiently small so that* $P_\varepsilon^+ = \varepsilon(x_\varepsilon^+, y_{1,\varepsilon}^+, y_{2,\varepsilon}^+, \dots, y_{k,\varepsilon}^+)$ *with* $|(x_\varepsilon^+, y_{1,\varepsilon}^+, y_{2,\varepsilon}^+, \dots, y_{k,\varepsilon}^+)| = \mathcal{O}(1)$ *with respect to* ε *and lies in a* δ *neighborhood of* P^+ *and let* $K = (K_1, K_2, \dots, K_k) \in \mathbb{R}^k$ *determine the leading order approximation of* L_δ (3.27). *Then, for* $j \in \{0, 1, \dots, k-1\}$, *there exist open regions* Ω_j *in the* $3k$*-dimensional space of parameters spanned by* $(y_{1,\varepsilon}^+, y_{2,\varepsilon}^+, \dots, y_{k,\varepsilon}^+)$, $(K_1, K_2, \dots, K_k)$, *and* $(\lambda_{\ell+1}, \lambda_{\ell+2}, \dots, \lambda_n)$, *such that system* (1.1) *has* j *distinct local defect solutions near* P_ε^+.

In the left panel of Figure 15, a sketch of a possible configuration as described by this Theorem is given in the unstable k-dimensional y-space for $k = 3$—compare to the right panel of Figure 12 for a similar two-dimensional sketch of the $k = 2$ case. The relative configuration of the two-dimensional manifold $\pi(L_\delta)$ and the point $\pi(\gamma_{ld}(0))$—with $\gamma_{ld}(0) \in W^s(P_\varepsilon^+)$—is chosen such that the projected orbit of (3.18) through $\gamma_{ld}(0)$ intersects $\pi(L_\delta)$ twice in backward time. These two intersections correspond to two different local defect solutions $\gamma_{ld}(t)$, the maximal possible number of local defect solutions for $k = 3$ by the above theorem. See again the right panel of Figure 12 for the $k = 2$ case, where there can be only one such intersection as described by Theorem 3.3.

Proof. Following the same approach as in the proofs of the preceding theorems and using the y-coordinates $(y^{lu}, y^{uu}) = (y_1, y_2, \dots, y_k)$, (3.27) yields the existence condition for local defect solutions

$$K_1 y_{1,\varepsilon}^+ e^{-\lambda_{\ell+1}\tau} + \cdots + K_k y_{k,\varepsilon}^+ e^{-\lambda_n \tau} = 0$$

up to $\mathcal{O}(\varepsilon, \rho(\varepsilon))$ corrections. Here, the $y_{j,\varepsilon}^+$'s are the y-coordinates of $P_\varepsilon^+ = \varepsilon(x_\varepsilon^+, y_{1,\varepsilon}^+, \dots, y_{k,\varepsilon}^+)$. This can be written as

$$\sum_{i=1}^{k-1} \kappa_i e^{\mu_i \tau} = -\kappa_k \tag{3.28}$$

with $\kappa_i = K_i y_{i,\varepsilon}^+, i = 1, \dots, k$, and $\mu_i = \lambda_n - \lambda_{\ell+i} > 0$, $i = 1, \dots, k-1$. Note that $\mu_1 > \mu_2 > \cdots > \mu_{k-1} > 0$. The statement of the theorem then follows by a straightforward induction-type analysis of existence condition (3.28). We first consider

$$\kappa_{k-1} e^{\mu_{k-1}\tau} = -\kappa_k, \tag{3.29}$$

which is in essence equivalent to the existence condition (3.12) that led to Theorem 3.3. Clearly this expression can have either one zero or no zeroes. Without loss of generality we can assume that $\kappa_k < 0$, so that (3.29) has a solution $\tau_{*,1} > 0$ if $0 < \kappa_{k-1} < -\kappa_k$ (recall that $\mu_{k-1} > 0$). The extended expression

$$\kappa_{k-2} e^{\mu_{k-2}\tau} + \kappa_{k-1} e^{\mu_{k-1}\tau} = -\kappa_k \tag{3.30}$$

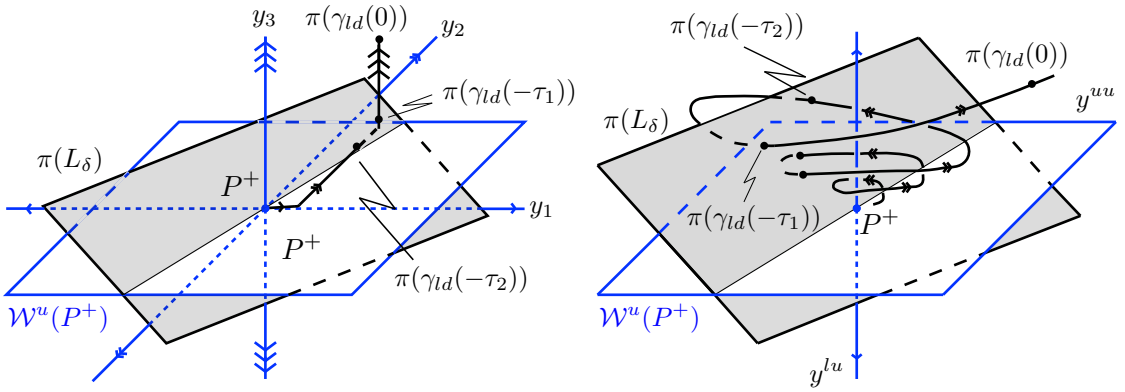

Figure 15. *Sketches of the projected flow of (3.18) near P^+ in the case of a real unstable leading eigenvalue for $k = 3$. Left panel: all three unstable eigenvalues are real and there can be up to two local defect solutions near P^+_ε. Right panel: the two-dimensional strong unstable spectrum consists of a pair of complex conjugate eigenvalues and there can be many distinct local defect solutions, but always finitely many. Compare to the right panel of Figure 12, where $k = 2$ and there can at most be a unique local defect solution. See Remark 3.16 for a brief discussion on the (lack of) asymptotic accuracy of these sketches.*

can have maximally two zeroes. The second zero appears by taking $\kappa_{k-2} < 0$ close enough to zero: the zero $\tau_{*,1}$ of (3.29) persists as perturbed zero of (3.30) since the effect of the difference $\kappa_{k-2}e^{\mu_{k-2}\tau_{*,1}}$ between (3.30) and (3.29) for $\tau = \tau_{*,1}$ can be made as small as necessary. Moreover, the left-hand side of (3.30) is smaller than $-\kappa_k$. Since $\mu_{k-2} > \mu_{k-1}$, the term $\kappa_{k-2}e^{\mu_{k-2}\tau} < 0$ dominates for large τ. Note that here the magnitude of τ is measured with respect to δ—the coefficients K_j of (3.27) depend on δ—which can thus be considered $\mathcal{O}(1)$ with respect to ε (as is necessary for the validity of the applied arguments). So, the left-hand side of (3.30) must cross the line $-\kappa_k$ once more, i.e., (3.30) can have a second zero at $\tau = \tau_{*,2} > \tau_{*,1} > 0$. A Descartes rule of signs type argument shows that (3.30) cannot have more than two roots. The statement of the theorem now follows by induction. ∎

The next theorem considers the case in which there is a pair of complex conjugate eigenvalues within the strong unstable y^{uu} direction and it bridges the gap between Theorem 3.11, in which there can be up to $k-1$ local defects, and Theorem 3.10, which established the existence of countably many local defect solutions.

Theorem 3.12. *Assume that Hypotheses H1–H3 hold, that* $\dim(\mathcal{W}^u(P^-)) = \dim(\mathcal{W}^u(P^+)) = k > 1$, *and that the Jacobian of P^+ of system (1.4) has a real leading unstable eigenvalue and at least one pair of complex conjugate unstable eigenvalues. Let ε and δ be small enough. Then, there are a finite number j of local defect solutions near P^+_ε to system (1.1). However, for any $j = 0, 1, 2, \ldots$ there are open regions in the parameter space spanned by the y-coordinates of P^+_ε, the K-coordinates that describe L_δ, and the unstable eigenvalues $\nu_{\ell+i}$ associated to P^+ for which (1.1) has exactly j distinct local defect solutions.*

In the right panel of Figure 15, a sketch of the configuration described by Theorem 3.12 is given for $k = 3$, that is, in the case of three unstable eigenvalues. The projected orbit through $\pi(\gamma_{ld}(0))$ spirals down—in backward time—to the $\{y^{lu} = 0\}$-plane. Since the strong unstable spectrum consists of complex valued eigenvalues, the rate of the contraction of the spiraling orbit is stronger than the rate at which it approaches the $\{y^{lu} = 0\}$-plane. As a

consequence, there are only a finite number of intersections: as $|\tau|$ becomes too large, the orbit is exponentially close to the y^{lu}-axis and no longer intersects $\pi(L_\delta)$—see also Remark 3.16. Note that in the alternative case of a pair of leading complex conjugate unstable eigenvalues and one real strong unstable eigenvalue, the rate of contraction of the spiral would be so weak, compared to the approach to $\{y^{lu} = 0\}$, that the extent of the downward spiraling orbit would remain so wide that it would keep on intersecting the $\pi(L_\delta)$ manifold as τ becomes more and more negative. This is the situation as described by Theorem 3.10; see also the right panel of Figure 14 for a two-dimensional sketch of this situation.

Proof. For simplicity we only consider the case in which the eigenvalues associated to the weakest unstable direction within the y^{uu}-coordinates form a complex conjugate pair. All other possible cases follow in essence by the same arguments. Following the proofs of Theorems 3.6 and 3.10, we introduce $\alpha_{\ell+2}$ and $\beta_{\ell+2}$ by setting $\lambda_{\ell+2,\ell+3} = \alpha_{\ell+2} \pm i\beta_{\ell+2}$—recall that the leading eigenvalue $\lambda_{\ell+1}$ is real. Moreover, we decompose the y-directions in normal form (3.1) into (y_1, y_2, y_3, y^{uuu}), where $y_1 = y^{lu}$ and $(y_2, y_3, y^{uuu}) = y^{uu}$ (with $y^{uuu} \in \mathbb{R}^{k-3}$). In these coordinates, the y-coordinates of P_ε^+ are given by $\varepsilon(y_{1,\varepsilon}^+, y_{2,\varepsilon}^+, y_{3,\varepsilon}^+, y_\varepsilon^{+,uuu})$ and the equivalent of approximation (3.17) of L_δ by

$$L_\delta = \{(x_\delta, y) \,|\, K_1 y_1 + K_2 y_2 + K_3 y_3 + K^{uuu} y^{uuu} + \mathcal{O}(|y|^2) = 0\}.$$

Still following the proofs of Theorems 3.6 and 3.10, we conclude that local defect solutions near P_ε^+ exist if the following condition holds:

$$K_1 e^{(\alpha_{\ell+2}-\lambda_{\ell+1})\tau} + R_{K,\varepsilon}^+ \cos(\beta_{\ell+2}\tau + \theta_{K,\varepsilon}^+) + K^{uuu} e^{-(A^{uuu}-\alpha_{\ell+2}\mathrm{Id})\tau} y_\varepsilon^{+,uuu} = 0, \tag{3.31}$$

where

$$R_{K,\varepsilon}^+ = \sqrt{\left(K_2^2 + K_3^2\right)\left((y_{2,\varepsilon}^+)^2 + (y_{3,\varepsilon}^+)^2\right)},$$

and $\theta_{K,\varepsilon}^+ \in [0, 2\pi)$ is a certain phase shift. By definition, we know that $\alpha_{\ell+2} - \lambda_{\ell+1} > 0$, while $|e^{-(A^{uuu}-\alpha_{\ell+2}\mathrm{Id})\tau} y_\varepsilon^{+,uuu}|$ will become arbitrarily small by taking τ large enough. We rewrite (3.31) as

$$\cos(\beta_{\ell+2}\tau + \theta_{K,\varepsilon}^+) = -\frac{K_1}{R_{K,\varepsilon}^+} e^{(\alpha_{\ell+2}-\lambda_{\ell+1})\tau} - \frac{K^{uuu}}{R_{K,\varepsilon}^+} e^{-(A^{uuu}-\alpha_{\ell+2}\mathrm{Id})\tau} y_\varepsilon^{+,uuu} \tag{3.32}$$

to conclude that there can indeed be only finitely many solutions τ of (3.31) since the absolute value of the right-hand side of (3.31) is larger than one for τ large enough. However, by choosing $\frac{K_1}{R_{K,\varepsilon}^+}$ small enough, we also see that this number can become arbitrarily large; see also Figure 16. ∎

We finally consider leading order simplifications of Theorems 3.9, 3.11, and 3.12 that do not depend on the artificial small parameter δ, i.e., we derive generalizations of Corollary 3.4 in section 3.2. As in the first part of section 3.2, and especially as in the formulation and proof of Theorem 3.3, we did not consider the fact that the manifold L_δ will be *squeezed* against the (hyper)plane associated to the strongest unstable direction. As usual, we have to distinguish between two cases.

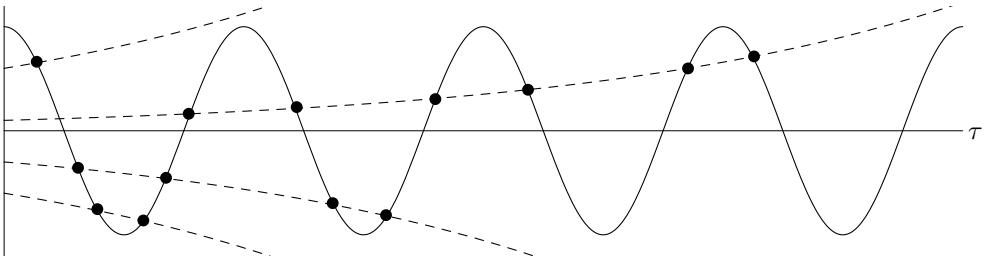

Figure 16. *The variation in the number of possible local defect solutions near P_ε^+ in the case of strong complex valued unstable eigenvalues as represented by the zeroes of (3.32) and indicated by various choices of the coefficients in (3.32).*

If the strongest unstable eigenvalue $\nu_n = \lambda_n > 0$ is real, we can decouple the y^n-direction from the other y^{uu} directions in normal form (3.18), i.e., decompose $y^{uu} \in \mathbb{R}^{k-1}$ into $(y^{iuu}, y_n) \in \mathbb{R}^{k-2} \times \mathbb{R}$, and thus also write the leading order approximation (3.17) of L_δ as

$$K^{lu} y^{lu} + K^{iuu} y^{iuu} + K_n y_n + \mathcal{O}(|y|^2) = 0 \tag{3.33}$$

with $K_n^{lu,iuu} = K_n^{lu,iuu}(\delta)$. Scaling K_n to 1, and thus assuming it is unequal to zero, it is straightforward to deduce that

$$K^{lu}(\delta) = \mathcal{O}(\delta^{\frac{\lambda_n - \lambda_{\ell+1}}{\lambda_\ell}}) \ll 1, \ |K^{iuu}|(\delta) = \mathcal{O}(\delta^{\frac{\lambda_n - \lambda_{n-1}}{\lambda_\ell}}) \ll 1\,. \tag{3.34}$$

Here, either $-\lambda_\ell = \nu_\ell = \nu^{ls} < 0$ if the leading stable eigenvalue of P^+ is real or $-\lambda_\ell = \alpha_\ell = \Re(\nu_{\ell,\ell-1}) < 0$ if the leading stable eigenvalues form a complex conjugate pair; see the definition/construction of L_δ at the beginning of section 3.3. Similarly, if the strongest unstable eigenvalue associated to the y^{iuu}-coordinates is real, then $\lambda_{n-1} = \nu_{n-1} > 0$, or if it is associated to a pair of complex conjugate eigenvalues, then $\lambda_{n-1} = \alpha_{n-1} = \Re(\nu_{n-1,n-2}) > 0$. Directly along the lines of Corollary 3.4, this yields the following leading order simplification of Theorem 3.9 and especially of twist condition (3.22) that does not explicitly depend on δ.

Corollary 3.13. *Assume that Hypotheses H1–H3 hold, that* $\dim(\mathcal{W}^u(P^-)) = \dim(\mathcal{W}^u(P^+)) = k > 1$, *and that the Jacobian of P^+ of system (1.4) has a real leading unstable eigenvalue $\nu_{\ell+1} = \lambda_{\ell+1}$ and a real most unstable eigenvalue $\nu_n = \lambda_n$. Let ε and δ be sufficiently small so that both $K^{lu} \neq 0$ and $K_n \neq 0$ in (3.33) and that K_n is scaled to 1 so that K^{lu} can be written as*

$$K^{lu}(\delta) = \tilde{K}^{lu}(\delta)\delta^{\frac{\lambda_n - \lambda_{\ell+1}}{\lambda_\ell}} \quad \text{with} \quad \tilde{K}^{lu}(0) \neq 0$$

(cf. (3.14)). Then, (3.18) supports at least one local defect solution near P_ε^+ if $\tilde{K}^{lu}(0) y_{\ell+1,\varepsilon}^+ y_{n,\varepsilon}^+ < 0$, where $\varepsilon y_{\ell+1,\varepsilon}^+$ and $\varepsilon y_{n,\varepsilon}^+$ are the $y_{\ell+1}$- and y_n-coordinates of P_ε^+.

By the same arguments, it is also possible to determine a very explicit δ-independent version of the twist condition that establishes the existence of the maximal number of $k-1$ distinct local defect solutions if all unstable eigenvalues associated to P^+ are real (cf. Theorem 3.11).

Corollary 3.14. *Assume that Hypotheses H1–H3 hold, that* $\dim(\mathcal{W}^u(P^-)) = \dim(\mathcal{W}^u(P^+)) = k > 1$, *and that all* k *unstable eigenvalues* $\nu_j = \lambda_j$, $j = \ell+1, \dots, \ell+k = n$, *of the Jacobian of* (1.4) *at* P^+ *are real. Let* ε *and* δ *be sufficiently small so that* $P_\varepsilon^+ = \varepsilon(x_\varepsilon^+, y_{1,\varepsilon}^+, y_{2,\varepsilon}^+, \dots, y_{k,\varepsilon}^+)$ *with* $|(x_\varepsilon^+, y_{1,\varepsilon}^{+,lu}, y_{2,\varepsilon}^{+,lu}, y_\varepsilon^{+,uu})| = \mathcal{O}(1)$ *with respect to* ε *and lies in a* δ *neighborhood of* P^+, *and such that* $K_1 \neq 0$, $K_2 \neq 0$, …, $K_k \neq 0$ *determine the leading order approximation of* L_δ (3.27). *Assume that* $K_k \neq 0$ *and that it is scaled to one, so that* $K_j(\delta)$ *can be written as*

$$K_j(\delta) = \tilde{K}_j(\delta)\delta^{\frac{\lambda_n - \lambda_{\ell+j}}{\lambda_\ell}} \quad \text{with} \quad \tilde{K}_j(0) \neq 0, \quad j = 1, \dots, k-1.$$

Then, system (1.1) *has* $k-1$ *distinct local defect solutions near* P_ε^+ *if*

$$\operatorname{sign}\{\tilde{K}_{k-1}(0) y_{k-1,\varepsilon}^+\} = -1 \quad \text{and} \quad \operatorname{sign}\{\tilde{K}_i(0) y_{i,\varepsilon}^+\} \neq \operatorname{sign}\{\tilde{K}_{i+1}(0) y_{i+1,\varepsilon}^+\}, i = 1, 2, \dots k-2.$$

Note that since all unstable eigenvalues are real we have $K_1 \ll K_2 \ll \cdots \ll K_{k-1} \ll 1$ and the proof of this corollary follows along exactly the induction-type lines as the proof of Theorem 3.11.

In the case that strongest unstable eigenvalues $\nu_{n,n-1}$ form a pair of complex conjugate eigenvalues, the y^{uu} directions in normal form (3.18) can be decoupled into (y^{iuu}, y_{n-1}, y_n), where the strongest linear growth is determined by $\alpha_n = \Re(\nu_{n,n-1}) > \Re(\nu_j)$, $j \leq n-2$. Completely similar to (3.33), L_δ can now be approximated by

$$K^{lu} y^{lu} + K^{iuu} y^{iuu} + K_{n-1} y_{n-1} + K_n y_n + \mathcal{O}(|y|^2) = 0,$$

where $K_{n,n-1}(\delta) = \mathcal{O}(1)$, $K^{lu}(\delta) = \mathcal{O}(\delta^{(\alpha_n - \lambda_{\ell+1})/\lambda_\ell}) \ll 1$, and $|K^{iuu}|(\delta) = \mathcal{O}(\delta^{(\alpha_n - \lambda_{n-2})/\lambda_\ell}) \ll 1$, with $\lambda_\ell, \lambda_{n-2} > 0$ defined exactly as $\lambda_\ell, \lambda_{n-1}$ in (3.34). Thus, it follows that in this case L_δ is given by

$$K_{n-1} y_{n-1} + K_n y_n = \mathcal{O}(\delta^\sigma) \tag{3.35}$$

for some $\sigma > 0$. Following the arguments of the proofs of Theorems 3.6, 3.12, and 3.10, we conclude that the existence of local defect solutions near P_ε^+ corresponds directly to finding zeroes of the very simple expression

$$R_{K,\varepsilon}^+ \cos(\beta_{\ell+2}\tau + \theta_{K,\varepsilon}^+) = \mathcal{O}(\delta^\sigma) \tag{3.36}$$

for certain expressions $R_{K,\varepsilon}^+ > 0$ and $\theta_{K,\varepsilon}^+$ (cf. (3.31)) *as long as* $\tau = \mathcal{O}(1)$ *with respect to* δ. Note that the right-hand side of (3.36) becomes unbounded for τ (logarithmically) large in δ; see the proof of Theorem 3.12 and Figure 16. Thus, we conclude that in this case (3.36) has asymptotically but finitely many solutions.

Corollary 3.15. *Assume that Hypotheses H1–H3 hold, that* $\dim(\mathcal{W}^u(P^-)) = \dim(\mathcal{W}^u(P^+)) = k > 1$, *and that the Jacobian of* P^+ *of system* (1.4) *has a real leading unstable eigenvalue* $\lambda_{\ell+1}$ *and a complex conjugate pair of most unstable eigenvalues. Then, for* ε *and* δ *small enough,* (3.18) *supports asymptotically (in* δ*) but finitely many local defect solutions near* P_ε^+.

Note that the fact that the number of local defect solutions depends on δ indicates that it is not possible to make a sharp distinction between local defect solutions and global defect solutions—as in the case of Theorems 3.6 and 3.10 and as discussed in Remark 3.7.

Remark 3.16. The sketches presented in Figure 15 indeed are rough indications of the relevant geometric structures. It follows from the above arguments that the L_δ *plane* in the left panel of Figure 15 must be asymptotically close to the $\{y_3 = 0\}$-plane (see the angle in the right panel of Figure 12), while the L_δ plane should be perpendicular—in leading order in δ—to the $\{y^{lu} = 0\}$-plane in the right panel (cf. (3.35)). Moreover, it follows from Corollary 3.15 that the number of intersections of the sketched (projected) orbit and L_δ—which is 4 in the right panel of Figure 15—should be asymptotically large in δ.

4. Examples. In this section, we consider defect solutions for two explicit examples. In section 4.1, we consider the eFK equation and in section 4.2 the perturbed generalized FHN model (1.2) mentioned in the introduction. For both systems of equations there are results in the literature on the existence of heteroclinic and homoclinic orbits. In particular, both the eFK equation and the FHN model support kink or front solutions and pulse solutions. Both cases are of the most relevant and interesting type in which $\dim(\mathcal{W}^u(P^-)) = \dim(\mathcal{W}^u(P^+)) = k > 1$. The eFK example is a four-dimensional system with $k = 2$. We consider the situation in which both limit points P^- and P^+ have a complex conjugate pair of stable and unstable eigenvalues. So, section 4.1 presents a (rather straightforward) application of Theorem 3.10.

This is certainly not the case for the example in section 4.2. Here, both a two-component simplification and the three-component FHN model (1.2) are considered. In both cases, all eigenvalues associated to the limit points P^+ and P^- are real. Moreover, the dimensions of the stable and unstable manifolds $\mathcal{W}^{s,u}(P^{+,-})$ are all the same. So, in section 4.2, we consider a four-dimensional system with $k = \ell = 2$ and a six-dimensional system with $k = \ell = 3$. However, these systems are not exactly of the type (1.1), since the unperturbed system (1.4) also depends explicitly on ε; see (1.2). Although this means that we need to be a bit more careful, this is not a serious problem: the form of (1.1) was chosen as simple as possible to keep the presentation of our approach as simple as possible. The precise form of the dynamical system is not essential, though the geometric structures near the equilibrium points are (as we show in section 4.2). See also Remark 1.13. Nevertheless, we cannot present a direct application of Theorem 3.9 in section 4.2: to establish the (non)existence of local defect solutions in (1.2) we need to evaluate the twist conditions of Theorem 3.9 in terms of the normal form of (1.2). However, since we do not bring (1.2) in normal form, the core of section 4.2 is dedicated to unraveling the twists of the unstable manifold $\mathcal{W}^u(P^-)$ geometrically as it travels from P^- to P^+. The singularly perturbed structure of (1.2) plays a crucial role in this analysis.

4.1. The eFK equation. The eFK equation is a higher order extension of the classical Fisher-KPP equation and is for $h > 0$ given by

$$\frac{\partial u}{\partial t} = -h\frac{\partial^4 u}{\partial \xi^4} + \frac{\partial^2 u}{\partial \xi^2} + u - u^3, \quad h > 0; \tag{4.1}$$

see [11, 12, 53, 65]. By the simple rescaling $\xi \to h^{1/4}\xi$ [53], the stationary problem associated to (4.1) can be written as

$$\frac{d^4u}{d\xi^4} + \beta\frac{d^2u}{d\xi^2} - u + u^3 = 0, \tag{4.2}$$

where $\beta = -1/\sqrt{h} < 0$. Here, we consider for $0 < \varepsilon \ll 1$ small a very general heterogeneous perturbation of (4.2), and thus of (4.1),

$$\frac{d^4u}{d\xi^4} + \beta\frac{d^2u}{d\xi^2} - u + u^3 = \begin{cases} 0, & \xi \le 0, \\ \varepsilon g(u, u_\xi, u_{\xi\xi}, u_{\xi\xi\xi}), & \xi > 0, \end{cases} \tag{4.3}$$

where g is assumed to be smooth enough and $\mathcal{O}(1)$ with respect to ε. Writing (4.3) in the dynamical system form of (1.1) yields

$$\begin{pmatrix} \dot u \\ \dot p \\ \dot q \\ \dot r \end{pmatrix} = \begin{cases} \begin{pmatrix} p \\ q \\ r \\ u - u^3 - \beta q \end{pmatrix}, & \xi \le 0, \\ \begin{pmatrix} p \\ q \\ r \\ u - u^3 - \beta q \end{pmatrix} + \varepsilon \begin{pmatrix} 0 \\ 0 \\ 0 \\ g(u,p,q,r) \end{pmatrix}, & \xi > 0, \end{cases} \tag{4.4}$$

where we have introduced $p = u_\xi, q = u_{\xi\xi}$, and $r = u_{\xi\xi\xi}$. The unperturbed system, system (4.4) with $\varepsilon = 0$, has three equilibrium points $P^0 = (0,0,0,0)$ and $P^\pm = (\pm 1, 0, 0, 0)$. The latter two equilibrium points $P^\pm$ are hyperbolic for all $\beta < 0$. Consequently, we immediately obtain the following result from Lemma 1.7.

Corollary 4.1. *For $\beta < 0$ and ε small enough there exists a unique trivial defect solution in (4.4) that connects P^- to P^-_ε and a unique trivial defect solution that connects P^+ to P^+_ε.*

For $\beta \in (-2\sqrt{2}, 0)$, $P^\pm = (\pm 1, 0, 0, 0)$ are of saddle-focus type. That is, the eigenvalues $\nu_j^\pm$, $j = 1, \dots, 4$, appear in two complex conjugate pairs, one pair with positive real part and the other pair with negative real part. So, $\dim(\mathcal{W}^u(P^\pm)) = \dim(\mathcal{W}^s(P^\pm)) = 2$. The kinks and pulses considered in this manuscript are heteroclinic and homoclinic connections between two of the $P^\pm$'s and are thus given by the intersections of a two-dimensional stable manifold with a two-dimensional unstable manifold. The basic kink solution is odd as a function of ξ with respect to its midpoint and has only one zero.

Theorem 4.2. *Let $\varepsilon = 0$ and $\beta \in (-2\sqrt{2}, 0)$ in the stationary homogeneous eFK system (4.4). Then, there is an isolated heteroclinic solution $\Gamma_1 = (u_1, p_1, q_1, r_1)$ that connects P^- to P^+; the u-component $u_1(\xi - \xi_*)$ of Γ_1 corresponds to a translational family of kink solutions of (4.2) that have one unique zero at the midpoint $\xi = \xi_*$ and that are odd as a function of ξ with respect to this midpoint $\xi = \xi_*$.*

This is a reformulation of Theorem 5.1.1 in [53], in which also a constructive proof is presented; see also [52] for the original result. It follows immediately from the proof in [53]

that Γ_1 is isolated, i.e., that the intersection $\mathcal{W}^u(P^-) \cap \mathcal{W}^s(P^+)$ is one-dimensional and thus minimally nontransversal; see Hypothesis H2.

The equilibrium points $P^\pm$ persist in heterogeneously perturbed system (4.4),

$$P_\varepsilon^\pm = (\pm 1 + \varepsilon g(\pm 1, 0, 0, 0) + \mathcal{O}(\varepsilon^2), 0, 0, 0). \tag{4.5}$$

Clearly, all assumptions in Hypothesis H2 can be satisfied for any $\beta \in (-2\sqrt{2}, 0)$ by choosing ε sufficiently small. However, we need to impose the additional assumption $g(1,0,0,0) \neq 0$ to satisfy Hypothesis H3: if $g(1,0,0,0) = 0$, then $|P^\pm - P_\varepsilon^\pm| = \mathcal{O}(\varepsilon^2)$ (4.5), which implies that the perturbation term in (4.2) is not generic in the sense of Definition 1.2. The fact that the perturbation term is generic if $g(1,0,0,0) \neq 0$ follows by a straightforward computation of the linear approximations of the stable and unstable manifolds $\mathcal{W}^{s,u}(P^\pm)$.

Thus, for $\beta \in (-2\sqrt{2}, 0)$ and $g(1,0,0,0) \neq 0$ we are in a situation in which Theorem 3.10 can directly be applied. Moreover, since $k = 2$ we do not need to consider the additional condition $K^{lu} \neq 0$ of Theorem 3.10 and consequently it is not necessary to bring (4.4) in its normal form.

Theorem 4.3. *Let $\beta \in (-2\sqrt{2}, 0)$ and $g(1,0,0,0) \neq 0$. Then, for $\varepsilon > 0$ small enough, the stationary perturbed heterogeneous eFK system (4.4) supports countably many local defect kink solutions that connect P^- to P_ε^+.*

Although it is obvious from the definition of a local defect solution near P_ε^+ (see (1.7)), it may be useful to notice explicitly that the midpoint ξ_* of the unperturbed $\xi \leq 0$ part of the u-component of a local defect kink (see Theorem 4.2) must satisfy $\xi_* < 0$: the *jump* to the perturbed system occurs only in the oscillatory tail of $u_1(\xi)$ close to $u = 1$, the u-component of P^+.

There exist many other results on the existence of kink-type and pulse-type solutions to eFK-type equations; see [39, 53] and the references therein. If the limit points $P^\pm$ are of saddle-focus type, one can again apply Theorem 3.10 in a straightforward fashion. Thus, each of the unperturbed kink solutions $\Gamma_{2j+1}(\xi)$ that connect P^- to P^+ and that have $2j+1$ zeroes in their u-components [53] persists as a family of countably many local defect kink solutions in (4.4) connecting P^- to P_ε^+. The reversed orbits $\Gamma_{2j+1}(-\xi)$ persist as families of local defect kink solutions connecting P^+ to P_ε^- (under the alternative additional assumption that $g(-1,0,0,0) \neq 0$). The same is true for the unperturbed homoclinic pulse solutions of [39, 53], if the limit points are of saddle-focus type.

Simple monotone (in the u-component) kink solutions also exist in (4.2) for $\beta < -2\sqrt{2}$, when all eigenvalues of the equilibrium points $P^\pm$ are real [53]. From the point of view of the unperturbed eFK equations, these kinks are much simpler. However, to establish their persistence as local defect solutions in (4.4) is a much harder problem: one needs to check the twist conditions of Theorem 3.9 and one thus needs to obtain analytical control of the manifold $\mathcal{W}^u(P^-)$ as it travels from P^- to P^+. Note that this may in principle be possible with the help of the constructive methods of [53]. However, we refrain from considering this substantial and nontrivial problem: we consider an equivalent problem in the context of the perturbed generalized FHN model (1.2) in the upcoming section.

4.2. The perturbed generalized FHN model.

In this section, we discuss local defect solutions to two types of perturbed FHN equations: the three-component model (1.2) as

discussed in section 1 and its reduced two-component model

$$\begin{cases} U_t = \varepsilon^2 U_{xx} + U - U^3 - \varepsilon(\alpha V + \gamma(x)), \\ \tau V_t = V_{xx} + U - V \end{cases} \tag{4.6}$$

with $(x,t) \in (\mathbb{R}, \mathbb{R}^+), \alpha \in \mathbb{R}, \tau > 0, 0 < \varepsilon \ll 1$, and $\gamma(x)$ as in (1.3). The latter two-component model can be obtained from the former three-component model by setting $\beta = 0$ in (1.2) and observing that (U,V) dynamics is now independent of the W dynamics, or by letting $D \to \infty$ and observing that the second inhibitor W becomes a constant and can be incorporated into γ for the U equation.

The dynamics of the two-component model (4.6) is less interesting compared to the dynamics of the three-component model (1.2); see, for example, [9, 17, 34]. However, it is also significantly easier to study geometrically and most of the ideas of the proofs carry over from the two-component system (4.6) to the three-component system (1.2). Therefore, we decided to focus on the two-component system in this section and we only sketch the changes in the proofs of the generalization to the three-component system.

For the three-component system (1.2), the associated ODE for the existence of stationary defect solutions is six-dimensional and given by (1.9). For the two-component system (4.6), the associated ODE is four-dimensional. Written in the fast coordinate $\xi = x/\varepsilon$, it is given by

$$\begin{cases} u_\xi = p\,, \\ p_\xi = -u + u^3 + \varepsilon(\alpha v + \gamma(\xi))\,, \\ v_\xi = \varepsilon q\,, \\ q_\xi = \varepsilon(v - u)\,. \end{cases} \tag{4.7}$$

Both ODE systems (4.7) and (1.9) are not exactly of the type (1.1), since the unperturbed system for $\xi \le 0$—i.e., $\dot u = f(u)$ in (1.1)/(1.4) —depends explicitly on ε here. However, this does not have an impact on the approach of this manuscript since all conditions of Remark 1.13 hold; see the next section.

4.2.1. Homogeneous case. In the homogeneous case $\gamma(\xi) \equiv \gamma$, both the 2ℓ-component ODE systems—(1.9) for $\ell = 3$ and (4.7) for $\ell = 2$—possess two hyperbolic equilibrium points,

$$\begin{aligned} \ell = 2: &\quad P_1^\gamma = (u_\gamma^-, 0, u_\gamma^-, 0)^t\,, && P_2^\gamma = (u_\gamma^+, 0, u_\gamma^+, 0)^t\,, \\ \ell = 3: &\quad P_1^\gamma = (u_\gamma^-, 0, u_\gamma^-, 0, u_\gamma^-, 0)^t\,, && P_2^\gamma = (u_\gamma^+, 0, u_\gamma^+, 0, u_\gamma^+, 0)^t\,, \end{aligned} \tag{4.8}$$

where

$$\ell = 2: u_\gamma^\pm = \pm 1 \mp \tfrac{1}{2}\varepsilon(\alpha \pm \gamma) + \mathcal{O}(\varepsilon^2)\,, \quad \ell = 3: u_\gamma^\pm = \pm 1 \mp \tfrac{1}{2}\varepsilon(\alpha + \beta \pm \gamma) + \mathcal{O}(\varepsilon^2)\,. \tag{4.9}$$

There exists a third equilibrium point in both systems that is $\mathcal{O}(\varepsilon)$ close to the origin. However, these equilibrium points are unstable in the PDE sense and are therefore not of interest to us [17]. It is a matter of straightforward linear algebra to show that $\dim(\mathcal{W}^u(P_1^\gamma)) = \dim(\mathcal{W}^u(P_2^\gamma)) = \dim(\mathcal{W}^s(P_1^\gamma)) = \dim(\mathcal{W}^s(P_1^\gamma)) = \ell$ for $\ell = 2, 3$ and that all eigenvalues associated to the linearization around $P_{1,2}^\gamma$ are real and simple. In other words, the situation we consider here is the most interesting and most critical type, as determined in the previous

sections. For the upcoming analysis, we need more precise information on the linearizations around $P^\gamma_{1,2}$.

Lemma 4.4. *Let $\lambda_j(P^\gamma_{1,2}) \in \mathbb{R}$ and $v_j(P^\gamma_{1,2}) \in \mathbb{R}^{2\ell}$, $j = 1, 2, \dots, 2\ell$, be the eigenvalues, respectively, eigenvectors, associated to the linearizations around $P^\gamma_{1,2}$ for $\ell = 2, 3$. Then*

- $\ell = 2 : \lambda_4(P^\gamma_{1,2}) < \lambda_3(P^\gamma_{1,2}) < 0 < \lambda_2(P^\gamma_{1,2}) < \lambda_1(P^\gamma_{1,2})$ *with*

$$\lambda_{1,4}(P^\gamma_1) = \pm\sqrt{2}\left(1 - \tfrac{3}{4}(\alpha-\gamma)\varepsilon + \mathcal{O}(\varepsilon^2)\right), \quad \lambda_{1,4}(P^\gamma_2) = \pm\sqrt{2}\left(1 - \tfrac{3}{4}(\alpha+\gamma)\varepsilon + \mathcal{O}(\varepsilon^2)\right),$$
$$\lambda_{2,3}(P^\gamma_1) = \pm\varepsilon\left(1 + \tfrac{\alpha}{4}\varepsilon + \mathcal{O}(\varepsilon)\right), \qquad \lambda_{2,3}(P^\gamma_2) = \pm\varepsilon\left(1 + \tfrac{\alpha}{4}\varepsilon + \mathcal{O}(\varepsilon)\right),$$

and

$$v_{1,4}(P^\gamma_1) = \left(1, \pm\sqrt{2}\left(1 - \tfrac{3}{4}(\alpha-\gamma)\varepsilon\right), 0, \mp\tfrac{1}{2}\varepsilon\sqrt{2}\right) + \mathcal{O}(\varepsilon^2),$$
$$v_{1,4}(P^\gamma_2) = \left(1, \pm\sqrt{2}\left(1 - \tfrac{3}{4}(\alpha+\gamma)\varepsilon\right), 0, \mp\tfrac{1}{2}\varepsilon\sqrt{2}\right) + \mathcal{O}(\varepsilon^2),$$
$$v_{2,3}(P^\gamma_{1,2}) = \left(-\tfrac{1}{2}\alpha\varepsilon, 0, 1, \pm(1 + \tfrac{1}{4}\alpha\varepsilon)\right) + \mathcal{O}(\varepsilon^2);$$

- $\ell = 3 : \lambda_6(P^\gamma_{1,2}) < \lambda_5(P^\gamma_{1,2}) < \lambda_4(P^\gamma_{1,2}) < 0 < \lambda_3(P^\gamma_{1,2}) < \lambda_2(P^\gamma_{1,2}) < \lambda_1(P^\gamma_{1,2})$ *with*

$$\lambda_{1,6}(P^\gamma_1) = \pm\sqrt{2}\left(1 - \tfrac{3}{4}(\alpha+\beta-\gamma)\varepsilon + \mathcal{O}(\varepsilon^2)\right),$$
$$v_{1,6}(P^\gamma_1) = \left(1, \pm\sqrt{2}\left(1 - \tfrac{3}{4}(\alpha+\beta-\gamma)\varepsilon\right), 0, \mp\tfrac{1}{2}\varepsilon\sqrt{2}, 0, \mp\tfrac{1}{2D}\varepsilon\sqrt{2}\right) + \mathcal{O}(\varepsilon^2),$$
$$\lambda_{1,6}(P^\gamma_2) = \pm\sqrt{2}\left(1 - \tfrac{3}{4}(\alpha+\beta+\gamma)\varepsilon + \mathcal{O}(\varepsilon^2)\right),$$
$$v_{1,6}(P^\gamma_2) = \left(1, \pm\sqrt{2}\left(1 - \tfrac{3}{4}(\alpha+\beta+\gamma)\varepsilon\right), 0, \mp\tfrac{1}{2}\varepsilon\sqrt{2}, 0, \mp\tfrac{1}{2D}\varepsilon\sqrt{2}\right) + \mathcal{O}(\varepsilon^2),$$

$$\lambda_{2,5}(P^\gamma_{1,2}) = \pm\varepsilon\left(1 + \tfrac{\alpha}{4}\varepsilon + \mathcal{O}(\varepsilon^2)\right),$$
$$v_{2,5}(P^\gamma_{1,2}) = \left(-\tfrac{1}{2}\alpha\varepsilon, 0, 1, \pm(1 + \tfrac{1}{4}\alpha\varepsilon), \tfrac{\alpha}{2(D^2-1)}\varepsilon, \pm\tfrac{\alpha D}{2(D^2-1)}\varepsilon\right) + \mathcal{O}(\varepsilon^2),$$

$$\lambda_{3,4}(P^\gamma_{1,2}) = \pm\tfrac{\varepsilon}{D}\left(1 + \tfrac{\beta}{4}\varepsilon + \mathcal{O}(\varepsilon^2)\right),$$
$$v_{3,4}(P^\gamma_{1,2}) = \left(-\tfrac{1}{2}\beta\varepsilon, 0, -\tfrac{\beta D^2}{2(D^2-1)}\varepsilon, \mp\tfrac{\beta D}{2(D^2-1)}\varepsilon, 1, \pm(1 + \tfrac{1}{4}\beta\varepsilon)\right) + \mathcal{O}(\varepsilon^2).$$

Proof. This follows immediately from a straightforward computation, and note that we implicitly used that $D > 1$ to order the four intermediate eigenvalues $\lambda_{2,3,4,5}$ for $\ell = 3$. ∎

As a starting point for the analysis, we need a result on the existence of a heteroclinic or homoclinic orbit in the homogeneous versions of systems (4.7) and (1.9), i.e., we need to show that Hypothesis H2 is satisfied. There are two results in the literature that provide such a starting point.

Theorem 4.5. *Let $\gamma(\xi) \equiv 0$ and let $\varepsilon > 0$ be small enough. Then both ODE systems (4.7) and (1.9) support a heteroclinic 1-front orbit $\Gamma_{\text{het}}(\xi)$ that connects P^0_1 to P^0_2.*

Proof. This is a special case of results established in [9, 30, 31] on (families of) traveling 1-front solutions to the three-component system (1.2): fronts that travel with a speed $c = c(\gamma)$ with $c(0) = 0$. In these manuscripts, only the three-component models are considered explicitly. However, the result on the existence of 1-front solutions in the two-component system (4.6) follows immediately along identical lines; see also section 6 of [17]. We omit the details. ∎

In fact, the proof of Theorem 4.5 appears as a *side product* in our proof of Theorem 4.7 about the existence of defect solutions.

The second result in the literature is summarized in the following theorem.

Theorem 4.6. *Let $\gamma(\xi) \equiv \gamma$ and let $\varepsilon > 0$ be small enough. Moreover,*

- *for $\ell = 2$, let (α, γ) be such that $\alpha A = \gamma$ has K solutions with $A \in (0,1)$; and*
- *for $\ell = 3$, let $(\alpha, \beta, \gamma, D)$ be such that $\alpha A + \beta A^{\frac{1}{D}} = \gamma$ has K solutions with $A \in (0,1)$.*

If $K > 0$, then there are K homoclinic pulse, or 2-front, orbits $\Gamma_{\text{hom}}(\xi)$ to P_1^γ in system (4.7) ($\ell = 2$) or (1.9) ($\ell = 3$). Furthermore, $K \leq \ell - 1$.

Proof. As with Theorem 4.5, this result has been established only for the three-component case [17]. However, the two-component case is simpler and follows along identical lines; see also section 6 of [17]. We omit the details. ∎

The A of the above theorem corresponds to the leading order width x^* of the homoclinic pulse solution via $x^* = -\log A$, where $x^* := x_1 - x_2$ with $x_{1,2}$ corresponding to respectively the first and second zeros of the u-component of the pulse solution; see Figure 1. In particular, for the two-component case $K = 1$ if and only if α and γ have the same sign and $|\alpha| > |\gamma|$ and the leading order width of the pulse solution is given by $x^* = \log(\alpha/\gamma)$. Similarly, for the three-component case $K = 0$ if $|\alpha + \beta| < |\gamma|$ and it is necessary for α and β to have opposite signs for $K = 2$.

The symmetries

$$
\begin{array}{lll}
\ell = 2: & (u,p,v,q,\xi,\gamma(\xi) \equiv \gamma) \to (u,-p,v,-q,-\xi,\gamma) & \text{in (4.7)},\\
 & (u,p,v,q,\xi,\gamma(\xi) \equiv \gamma) \to (-u,p,-v,q,-\xi,-\gamma) & \text{in (4.7)},\\
\ell = 3: & (u,p,v,q,w,r,\xi,\gamma(\xi) \equiv \gamma) \to (u,-p,v,-q,w,-r,-\xi,\gamma) & \text{in (1.9)},\\
 & (u,p,v,q,w,r,\xi,\gamma(\xi) \equiv \gamma) \to (-u,p,-v,q,-w,r,-\xi,-\gamma) & \text{in (1.9)}
\end{array}
\tag{4.10}
$$

also immediately establish the existence of homoclinic pulse orbits to P_2^γ and, for $\gamma = 0$, of heteroclinic 1-front orbits connecting P_2^0 to P_1^0. We do not consider those orbits here, though.

4.2.2. Local defect solutions. Since both the ODE systems for $\xi \leq 0$ also depend on ε, we cannot distinguish between the equilibrium points $P^\pm$ for $\xi \leq 0$ and their perturbed versions for $\xi > 0$ by an ε-subscript, as in the preceding sections. Instead, we use $\tilde{P}^\pm$ for the perturbed equilibrium points. We first consider the possibility of having local defect solutions in (4.7)/(1.9) that are close to the heteroclinic 1-front $\Gamma_{\text{het}}(\xi)$ established in Theorem 4.5.

Theorem 4.7. *Let $\gamma(\xi)$ be as in (1.3) with $\gamma_1 = 0$ and let ε be small enough. Moreover, let $\Gamma_{\text{het}}(\xi)$ be the 1-front heteroclinic orbit that connects $P_1^0 \overset{\text{def}}{=} P^-$ to $P_2^0 \overset{\text{def}}{=} P^+$ in the homogeneous case $\gamma = 0$ (see Theorem 4.5), and let $\alpha, \beta, \gamma_2 \in \mathbb{R}$ be $\mathcal{O}(1)$ with respect to ε. Then,*

- *(4.7) supports a heteroclinic local defect solution $\Gamma_{\text{het,ld}}(\xi)$ near $\tilde{P}^+ = P_2^{\gamma_2}$ that connects P^- to $\tilde{P}^+$ if and only if $\alpha > 0$; and*
- *(1.9) supports a heteroclinic local defect solution $\Gamma_{\text{het,ld}}(\xi)$ near $\tilde{P}^+ = P_2^{\gamma_2}$ that connects P^- to $\tilde{P}^+$ for $\alpha, \beta > 0$.*

The orbit of the local defect solution $\Gamma_{\text{het,ld}}(\xi)$ in the 2ℓ-dimensional phase space of (4.7)/(1.9) is $\mathcal{O}(\varepsilon)$ close to the corresponding $\Gamma_{\text{het}}(\xi)$.

Hence, in this case we are able to *control* the twist condition necessary for an existence result on local defect solutions for which $\dim(\mathcal{W}^u(P^-)) = \dim(\mathcal{W}^u(P^+)) = k > 1$—with

$k = \ell$—and real eigenvalues; see Theorems 1.9, 3.9, and 3.11. Since this twist condition is in fact a condition on the global dynamics of $\mathcal{W}^u(P^-)$, this is in general a very hard condition to validate. Here, it is possible though by the singular perturbed nature of (4.7) and (1.9). Nevertheless, even with this additional structure, interpreting the twist condition explicitly in terms of the parameters in the problem is a far from trivial enterprise, as is shown in the upcoming proof. For that same reason, the statement of the above theorem in the $k = \ell = 3$ case is much less strong than the *if and only if* result established for $k = \ell = 2$. Moreover, we do not consider the possibility of having two distinct local defect solutions in the $\ell = 3$ case; see Theorem 3.11. See also Remark 4.9 for a brief discussion on these limitations of Theorem 4.7 in the $\ell = 3$ case.

The twist condition, i.e., the issue of controlling the orientation of $\mathcal{W}^u(P^-)$ as it passes along P^+, is the focus of the proof of Theorem 4.7. However, notice also that we cannot directly apply Theorems 1.9, 3.9, and 3.11 to establish the existence of local defect solutions in (4.7) and (1.9) under an *abstract* twist condition: these systems do not satisfy the general form (1.1) and the local character of the *unperturbed* $\xi \leq 0$ equilibrium points $P^\pm$ is determined by $\mathcal{O}(\varepsilon)$ small quantities; see Lemma 4.4. So, it is a priori not obvious that the $\mathcal{O}(\varepsilon)$ perturbations of the $\xi > 0$ system do not change the local character of the flows near $P^\pm/\tilde{P}^\pm$, which is a crucial ingredient of all arguments in the preceding sections. Nevertheless, it follows from Lemma 4.4 that the local flow near $\tilde{P}^+$ is not changed by the defect, which indicates that the geometry of the system is indeed as is necessary for the geometrical application of the arguments developed in the previous sections. For that same reason, we also do not have to go into the nasty details of bringing (4.7) and (1.9) into a normal form as is used in the previous sections. The normal form structure (3.1) significantly simplified the presentation of our arguments in section 3, but—unlike the geometric structure—it is not necessary for the derivation of our results in this section.

Proof. The proof of this theorem strongly builds on the geometric structure associated to the singularly perturbed systems (4.7) and (1.9); see [17] for more details on this. The $2(\ell-1)$-dimensional slow manifolds $\mathcal{M}^\pm$ to which the slow flow is restricted associated to the unperturbed $\xi \leq 0$-systems are given by

$$\begin{aligned}
&\ell = 2: \quad \mathcal{M}^\pm = \{u = \pm 1 + \varepsilon u_1^\pm(v,q), p = \varepsilon p_1^\pm(v,q)\} \\
&\qquad\quad \text{with } u_1^\pm = -\tfrac{1}{2}(\alpha v + \gamma_1) + \mathcal{O}(\varepsilon),\ p_1^\pm = \mathcal{O}(\varepsilon), \\
&\ell = 3: \quad \mathcal{M}^\pm = \{u = \pm 1 \varepsilon u_1^\pm(v,q,w,r), p = \varepsilon p_1^\pm(v,q,w,r)\} \\
&\qquad\quad \text{with } u_1^\pm = -\tfrac{1}{2}(\alpha v + \beta w + \gamma_1) + \mathcal{O}(\varepsilon),\ p_1^\pm = \mathcal{O}(\varepsilon);
\end{aligned} \tag{4.11}$$

see (2.8), (2.9) in [17] and [25, 26]. The manifolds $\mathcal{M}^\pm$ have $(2\ell-1)$-dimensional stable and unstable manifolds $\mathcal{W}^{s,u}(\mathcal{M}^\pm)$ that are $\mathcal{O}(\varepsilon)$ $\mathcal{C}^1$ close to the stable and unstable manifolds of the equilibrium points $(u,p) = (\pm 1, 0)$ of the $2(\ell-1)$ parameter family of fast reduced systems associated to (4.7) and (1.9), respectively,

$$\begin{aligned}
&u_\xi = p, p_\xi = -u + u^3, \\
&\ell = 2: v = v_0, q = q_0, \\
&\ell = 3: v = v_0, q = q_0, w = w_0, r = r_0,
\end{aligned} \tag{4.12}$$

within compact subsets of $\mathbb{R}^{2\ell}$ [25, 26]. The stable/unstable manifolds of (4.12) are given

analytically by the level set $\mathcal{H}(u,p)=0$ of the Hamiltonian

$$\mathcal{H}(u,p,v,q,w,r)) = \frac{1}{2}(u^2+p^2) - \frac{1}{4}(1+u^4).$$

It is important to note that $\mathcal{H}|_{\mathcal{M}^\pm} = \mathcal{O}(\varepsilon^2)$ [17]. The Hamiltonian becomes a slowly varying function in the full $\xi \leq 0$-flows (4.7), (1.9),

$$\begin{aligned} \ell = 2: &\quad \mathcal{H}_\xi(u,p,v,q) = \varepsilon\alpha p v, \\ \ell = 3: &\quad \mathcal{H}_\xi(u,p,v,q,w,r) = \varepsilon p(\alpha v + \beta w), \end{aligned} \tag{4.13}$$

where we recall that $\gamma(\xi) = \gamma_1 = 0$ for $\xi \leq 0$. The manifolds $\mathcal{W}^u(\mathcal{M}^-)$ and $\mathcal{W}^s(\mathcal{M}^+)$ are both $\mathcal{O}(\varepsilon)$ close to $\mathcal{H}=0$ and thus intersect the hyperplane $\{u=0\}$ transversally. In fact, a straightforward Melnikov argument based on (4.13) and the leading order description of p in (4.13) as the p-component of the heteroclinic solution of the fast reduced limit system (4.12) yields that the $\mathcal{H}$-coordinates of $\mathcal{W}^u(\mathcal{M}^-)\cap\{u=0\}$ and $\mathcal{W}^s(\mathcal{M}^+)\cap\{u=0\}$ are, up to higher order corrections, given by

(4.14)

$$\begin{aligned} \ell = 2: &\quad \mathcal{H}|_{\mathcal{W}^u(\mathcal{M}^-)\cap\{u=0\}} = 2\varepsilon\alpha v^-, && \mathcal{H}|_{\mathcal{W}^s(\mathcal{M}^+)\cap\{u=0\}} = -2\varepsilon\alpha v^+, \\ \ell = 3: &\quad \mathcal{H}|_{\mathcal{W}^u(\mathcal{M}^-)\cap\{u=0\}} = 2\varepsilon(\alpha v^- + \beta w^-), && \mathcal{H}|_{\mathcal{W}^s(\mathcal{M}^+)\cap\{u=0\}} = -2\varepsilon(\alpha v^+ + \beta w^+) \end{aligned}$$

with $v^\pm, w^\pm$ constants and where the p-coordinates of the intersections $\mathcal{W}^u(\mathcal{M}^-)\cap\{u=0\}$ and $\mathcal{W}^s(\mathcal{M}^+)\cap\{u=0\}$ are $\frac{1}{2}\sqrt{2}+\mathcal{O}(\varepsilon)$; see [17] for the details. Thus, $\mathcal{W}^u(\mathcal{M}^-)$ and $\mathcal{W}^s(\mathcal{M}^+)$ intersect in a $2(\ell-1)$-dimensional submanifold $\mathcal{W}^u(\mathcal{M}^-)\cap\mathcal{W}^s(\mathcal{M}^+)$. By (4.14), the $(2\ell-3)$-dimensional intersection $\mathcal{W}^u(\mathcal{M}^-)\cap\mathcal{W}^s(\mathcal{M}^+)\cap\{u=0\}$ is explicitly approximated by

$$\begin{aligned} &\mathcal{W}^u(\mathcal{M}^-)\cap\mathcal{W}^s(\mathcal{M}^+)\cap\{u=0\} \\ &= \begin{cases} \{(u,p,v,q)\,|\,u=0, p=\frac{1}{2}\sqrt{2}, v^- = -v^+\}, & \ell=2, \\ \{(u,p,v,q,w,r)\,|\,u=0, p=\frac{1}{2}\sqrt{2}, \alpha v^- + \beta w^- = -\alpha v^+ - \beta w^+\}, & \ell=3, \end{cases} \end{aligned} \tag{4.15}$$

up to $\mathcal{O}(\varepsilon)$ corrections. In Figure 17, the manifolds $\mathcal{W}^u(\mathcal{M}^-)$ and $\mathcal{W}^s(\mathcal{M}^+)$ of (4.7) and their intersections are sketched in a $3=(2\ell-1)$-dimensional setting ($\ell=2$) for two significantly different cases: $\alpha>0$ and $\alpha<0$. That is, (4.14) provides information not only on the existence and location of the intersection $\mathcal{W}^u(\mathcal{M}^-)\cap\mathcal{W}^s(\mathcal{M}^+)$, but also on the relative position of $\mathcal{W}^u(\mathcal{M}^-)$ with respect to $\mathcal{W}^s(\mathcal{M}^+)$. For $\alpha>0$, $\mathcal{W}^u(\mathcal{M}^-)$ is *outside* the span $\mathcal{W}^u(\mathcal{M}^+)\cup\mathcal{W}^s(\mathcal{M}^+)$ for $v_0>0$ ($\mathcal{H}|_{\mathcal{W}^u} > \mathcal{H}|_{\mathcal{W}^s}$) and *inside* $\mathcal{W}^u(\mathcal{M}^+)\cup\mathcal{W}^s(\mathcal{M}^+)$ for $v_0<0$; the situation is reversed for $\alpha<0$; see Figure 17. Note that $\mathcal{W}^{u,s}(\mathcal{M}^\pm)$ are of codimension one (both for $\ell=2,3$) and thus indeed define an inside and an outside. We refer to [18] for the introduction of this inside/outside distinction between intersecting stable and unstable manifolds of slow manifolds and its crucial implications for the associated flows. In the present setting, this distinction enables us to determine whether the twist condition can be satisfied.

Since $P^-\in\mathcal{M}^-$, respectively, $P^+\in\mathcal{M}^+$, it follows that the ℓ-dimensional unstable manifold $\mathcal{W}^u(P^-)$, respectively, stable manifold $\mathcal{W}^s(P^+)$, is a submanifold of the $(2\ell-1)$-dimensional manifold $\mathcal{W}^u(\mathcal{M}^-)$, respectively, $\mathcal{W}^s(\mathcal{M}^+)$; see Lemma 4.4. Hence, the heteroclinic orbit $\Gamma_{\text{het}}(\xi)$ of Theorem 4.5 must be part of a $(2\ell-3)$-parameter family of heteroclinic

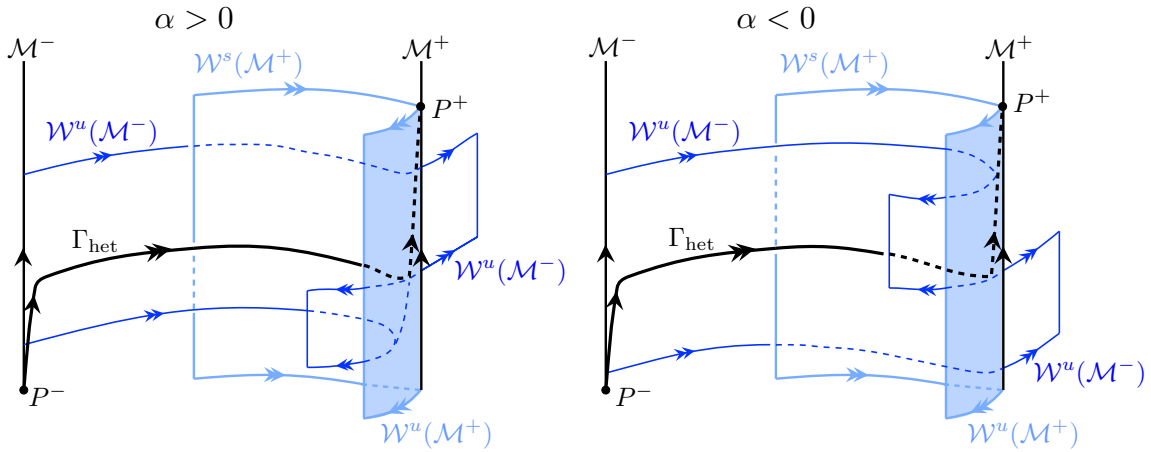

Figure 17. *The three-dimensional unstable manifold $\mathcal{W}^u(\mathcal{M}^-)$ and stable manifold $\mathcal{W}^s(\mathcal{M}^+)$ of the two-dimensional slow manifolds $\mathcal{M}^-$ and $\mathcal{M}^+$ in the four-dimensional phase space associated to (4.7), sketched as two-dimensional unstable and stable manifolds in $\mathbb{R}^3$. Left panel: $\alpha > 0$ and $\mathcal{W}^u(\mathcal{M}^-)$ is outside $\mathcal{W}^u(\mathcal{M}^+) \cup \mathcal{W}^s(\mathcal{M}^+)$ for $v_0 > 0$ and inside for $v_0 < 0$. Right panel: $\alpha < 0$ and the situation is reversed $\mathcal{W}^u(\mathcal{M}^-)$ is outside $\mathcal{W}^u(\mathcal{M}^+) \cup \mathcal{W}^s(\mathcal{M}^+)$ for $v_0 < 0$ and inside for $v_0 > 0$. The more subtle stretched and folded structure of $\mathcal{W}^u(\mathcal{M}^-)$ exponentially close to $\mathcal{W}^u(\mathcal{M}^-) \cap \mathcal{W}^s(\mathcal{M}^+)$ [18] is not shown.*

connections between $\mathcal{M}^-$ and $\mathcal{M}^+$. Since, for $\ell = 2$, the (v, q)-components of such a connection must remain constant to leading order during the *fast transition* from $\mathcal{M}^-$ to $\mathcal{M}^+$ (see (4.7)), it follows by (4.15) that these connecting orbits *take off* from $\mathcal{M}^-$ and *touch down* on $\mathcal{M}^+$ with $v = 0$; see once again [17] for the full geometric and analytic details. For $\ell = 3$, the (v, q, w, r)-components of such a connection must remain constant to leading order and in a similar fashion the jump condition becomes $\alpha v + \beta w = 0$. Clearly, the orbit $\Gamma_{\rm het}(\xi)$ must take off from $\mathcal{W}^u(P^-) \cap \mathcal{M}^-$ and touch down on $\mathcal{W}^s(P^+) \cap \mathcal{M}^+$. These intersections are determined by respectively the unstable manifold of $P^- \subset \mathcal{M}^-$ and the stable manifold of $P^+ \subset \mathcal{M}^+$, restricted to the slow flow on respectively $\mathcal{M}^-$ and $\mathcal{M}^+$. It follows from (4.7)/(1.9) and (4.11) that the flows on the slow manifolds $\mathcal{M}^\pm$ are to leading order linear and given by

$$\ell = 2: \quad \begin{cases} v_\xi = \varepsilon q\,, \\ q_\xi = \varepsilon(v \mp 1)\,, \end{cases} \qquad \ell = 3: \quad \begin{cases} v_\xi &= \varepsilon q\,, \\ q_\xi &= \varepsilon(v \mp 1)\,, \\ w_\xi &= \varepsilon r\,, \\ r_\xi &= \varepsilon(w \mp 1)\,. \end{cases}$$

Since the manifolds $\mathcal{M}^\pm$ are also linear (up to $\mathcal{O}(\varepsilon^2)$ corrections; see (4.11)), it follows from Lemma 4.4, with $\gamma = 0$, that

$$\begin{aligned} \ell = 2: \quad & \mathcal{W}^u(P^-) \cap \mathcal{M}^- = \operatorname{span}\{v_2(P^-)\}, \\ & \mathcal{W}^s(P^+) \cap \mathcal{M}^+ = \operatorname{span}\{v_3(P^+)\}, \\ \ell = 3: \quad & \mathcal{W}^u(P^-) \cap \mathcal{M}^- = \operatorname{span}\{v_2(P^-), v_3(P^-)\}, \\ & \mathcal{W}^s(P^+) \cap \mathcal{M}^+ = \operatorname{span}\{v_4(P^+), v_5(P^+)\} \end{aligned} \tag{4.16}$$

up to $\mathcal{O}(\varepsilon^2)$ corrections. Observe that the proof of Theorem 4.5 now indeed follows as a side product from this geometrical framework. In particular, from the combination of (4.15) and

(4.16) it follows that for $\ell = 2$, $\Gamma_{\text{het}}(\xi)$ is selected from the one-parameter family of orbits in $\mathcal{W}^u(\mathcal{M}^-) \cap \mathcal{W}^s(\mathcal{M}^+)$ by its (v, q)-coordinates during its *jump* from $\mathcal{M}^-$ to $\mathcal{M}^+$: $(v, q) = (0, 1)$ (to leading order). Similarly, for $\ell = 3$ it follows that $(v, q, w, r) = (0, 1, 0, 1)$. See [17] for a more polished version of these arguments.

Note that we may also conclude from the geometrical setting that $\mathcal{W}^u(P^-) \cap \mathcal{W}^s(P^+)$ is *minimally nontransversal* in the sense of Hypothesis H2: the intersection is one-dimensional and it contains only $\Gamma_{\text{het}}(\xi)$. Moreover, it follows the symmetries (4.10) of (4.7)/(1.9), with $\gamma = 0$, that Γ_{het} is an odd function of ξ.

To carefully trace the evolution of $\mathcal{W}^u(P^-)$ along/near $\Gamma_{\text{het}}(\xi)$, the central issue of this proof, we first consider the simpler case $\ell = 2$. Since we do not normalize the vector field of (4.7) as in section 3, we define the geometrical equivalent of the intersection L_δ as defined in Definitions 3.2 and 3.8 in section 3 by

$$
\begin{aligned}
L_\delta &= (\mathcal{W}^u(P^-) \cap \mathcal{V}_\delta) \cap B_{K\delta}(P^+) \\
&\overset{\text{def}}{=} (\mathcal{W}^u(P^-) \cap \{\delta v_3(P^+) + \text{ span}\,\{v_1(P^+), v_2(P^+), v_4(P^+)\}\}) \cap B_{K\delta}(P^+),
\end{aligned} \tag{4.17}
$$

where $0 < \varepsilon \ll \delta \ll 1$ and $B_{K\delta}(P^+)$ is a ball centered around P^+ with radius $K\delta$ large enough so that L_δ is of $\mathcal{O}(\delta)$ length. Thus, L_δ is the intersection of $\mathcal{W}^u(P^-)$ with the three-dimensional hyperplane $\mathcal{V}_\delta$. This hyperplane is an $\mathcal{O}(\delta)$ translation of the linear approximation of $\mathcal{W}^u(P^+)$ extended with the fast stable direction $v_4(P^+)$; see Lemma 4.4. This $\mathcal{O}(\delta)$ translation is in the direction of the slow stable eigenvector of P^+ (see Lemma 4.4 and (4.16)), i.e., in the direction of the orbit $\Gamma_{\text{het}}(\xi)$. Here, δ is assumed small enough such that the flow of (4.7) in an $\mathcal{O}(\delta)$ neighborhood of P^+ is dominated by its linearization (as in section 3). Note that L_δ is expected to be one-dimensional, since $\mathcal{W}^u(P^-)$ is two-dimensional.

By the strong separation of scales ($\mathcal{O}(1)$ versus $\mathcal{O}(\varepsilon)$) in the (linearized) flow near P^+ this implies that L_δ must be squeezed along (the δ translation of) the slow unstable eigenvector $v_2(P^+) \subset \mathcal{V}_\delta$. This insight can be deduced either analytically through the exchange lemma (with exponentially small errors with respect to ε) [38] or directly by the more geometrical arguments of [18]—which we employ here. Since $\Gamma_{\text{het}}(\xi)$ travels an $\mathcal{O}(1)$ distance with respect to ε along $\mathcal{M}^+$ after touching down, it must be exponentially close to $\mathcal{M}^+$ during its flight along $\mathcal{M}^+$. Hence, the component of L_δ in the fast stable $v_4(P^+)$ direction must already have become asymptotically small with respect to ε way before $\mathcal{W}^u(P^-)$ has reached $\mathcal{V}_\delta$. Orbits in $\mathcal{W}^u(P^-)$ that remain close to $\Gamma_{\text{het}}(\xi)$ up to an $\mathcal{O}(\delta)$ distance to P^+, i.e., orbits that pass through L_δ, must also be exponentially close with respect to ε to $\mathcal{M}^+$. Therefore, also the components of these orbits in the fast unstable direction associated to $v_1(P^+)$, which spans the leading order approximation of $\mathcal{W}^u(\mathcal{M}^+)$, can be at most exponentially small with respect to ε. That is, they can be bounded by $e^{-C/\varepsilon}$ for some $\mathcal{O}(1)$ $C > 0$.

In forward *time* ξ, orbits through L_δ spread out over $\mathcal{W}^u(P^+)$, an evolution that is dominated by the fast flow associated to $\lambda_1(P^+)$ and $v_1(P^+)$. As in the case of Theorems 1.9, 3.9, and 3.11 and Figures 4 and 12, $\mathcal{W}^u(P^-)$ will be *torn into pieces* along $\Gamma_{\text{het}}(\xi)$ as it passes along P^+. The question about when (or if) the *twist condition* for the existence of local defect solutions can be satisfied thus corresponds to understanding how $\mathcal{W}^u(P^-)$ gets torn apart and how it subsequently spreads along $\mathcal{W}^u(P^+)$.

By construction, orbits through L_δ are in $\mathcal{W}^u(P^-) \subset \mathcal{W}^u(\mathcal{M}^-)$ and in backward *time* ξ they are close to $\Gamma_{\text{het}}(\xi) = \mathcal{W}^u(P^-) \cap \mathcal{W}^s(P^+) \subset \mathcal{W}^u(\mathcal{M}^-) \cap \mathcal{W}^s(\mathcal{M}^+)$. Moreover, since L_δ

is exponentially close with respect to ε to $\mathcal{M}^+$, they are exponentially close to $\mathcal{W}^u(\mathcal{M}^+)$ in forward time ξ—at least, in compact, $\mathcal{O}(1)$ with respect to ε, neighborhoods of $\mathcal{M}^+$ [25, 26]. As a consequence, the nature of the tearing and spreading of $\mathcal{W}^u(P^-)$ is governed by the *inside/outside* distinction made in the intersection of $\mathcal{W}^u(\mathcal{M}^-)$ and $\mathcal{W}^s(\mathcal{M}^+)$ at $\{u=0\}$; see Figure 17. For $\alpha>0$, respectively, $\alpha<0$, the part of $\mathcal{W}^u(P^-)\subset\mathcal{W}^u(\mathcal{M}^-)$ that is outside the span $\mathcal{W}^u(\mathcal{M}^+)\cup\mathcal{W}^s(\mathcal{M}^+)$ at the intersection with $\{u=0\}$ has positive, respectively, negative, v-coordinates (4.14). The heteroclinic orbit $\Gamma_{\rm het}(\xi)=\mathcal{W}^u(P^-)\cap\mathcal{W}^s(P^+)$ touches down on $\mathcal{M}^+$ asymptotically close with respect to ε to

$$\{P^+ + \ \text{span}\,\{v_3(P^+)\}\}\cap\{v=0\};$$

see (4.15), (4.16). This implies that the part of $\mathcal{W}^u(P^-)$ that is outside $\mathcal{W}^u(\mathcal{M}^+)\cup\mathcal{W}^s(\mathcal{M}^+)$ has a positive coordinate in the $v_2(P^+)$-direction for $\alpha>0$ and points in the negative $v_2(P^+)$-direction for $\alpha<0$; see Lemma 4.4. This orientation cannot change as $\mathcal{W}^u(P^-)$ travels along $\mathcal{M}^+$ toward $\mathcal{V}_\delta$ (4.17). Recalling that L_δ is squeezed asymptotically close with respect to ε to $v_2(P^+)$, we define $L_\delta^\pm\subset L_\delta$ by

$$L_\delta^+=L_\delta\cap\{\mu v_2(P^+),\mu>0,\mu\gg\mathcal{O}(\varepsilon^2)\},\quad L_\delta^-=L_\delta\cap\{\mu v_2(P^+),\mu<0,|\mu|\gg\mathcal{O}(\varepsilon^2)\}.$$

Note that the above asymptotic analysis provides results only up to $\mathcal{O}(\varepsilon^2)$ corrections, and hence we cannot consider $\mu=\mathcal{O}(\varepsilon^2)$ or smaller, so that our definition leaves a subregion $L_\delta^0\subset L_\delta$ in between L_δ^- and L_δ^+ of length $\mu=\mathcal{O}(\varepsilon^2)$ for which we cannot decide whether it is inside or outside $\mathcal{W}^u(\mathcal{M}^-)\cup\mathcal{W}^s(\mathcal{M}^+)$ (recall that the length of L_δ is $\mathcal{O}(\delta)$ and that $\delta\gg\varepsilon$). We conclude that

$$\begin{array}{ll}\alpha>0: & L_\delta^+ \text{ is outside } \mathcal{W}^u(\mathcal{M}^+)\cup\mathcal{W}^s(\mathcal{M}^+);\ L_\delta^- \text{ is inside } \mathcal{W}^u(\mathcal{M}^+)\cup\mathcal{W}^s(\mathcal{M}^+);\\ \alpha<0: & L_\delta^+ \text{ is inside } \mathcal{W}^u(\mathcal{M}^+)\cup\mathcal{W}^s(\mathcal{M}^+);\ L_\delta^- \text{ is outside } \mathcal{W}^u(\mathcal{M}^+)\cup\mathcal{W}^s(\mathcal{M}^+).\end{array}$$

Outside $\mathcal{W}^u(\mathcal{M}^+)\cup\mathcal{W}^s(\mathcal{M}^+)$ the fast unstable flow near P^+ is in the direction of positive multiples of $v_1(P^+)$; inside $\mathcal{W}^u(\mathcal{M}^-)\cup\mathcal{W}^s(\mathcal{M}^+)$ it points in the negative $v_1(P^+)$-direction. Define for $|\mu_{1,2}|\gg\varepsilon^2$ the four (translated) $\mathcal{O}(\delta)$-sized planar half-cones,

$$\begin{aligned}\mathcal{C}_\delta^{+,+} &= \{P^+ +\mu_1 v_1(P^+)+\mu_2 v_2(P^+):\mu_1>0,\mu_2>0\}\cap B_{K\delta}(P^+),\\ \mathcal{C}_\delta^{+,-} &= \{P^+ +\mu_1 v_1(P^+)+\mu_2 v_2(P^+):\mu_1>0,\mu_2<0\}\cap B_{K\delta}(P^+),\\ \mathcal{C}_\delta^{-,+} &= \{P^+ +\mu_1 v_1(P^+)+\mu_2 v_2(P^+):\mu_1<0,\mu_2>0\}\cap B_{K\delta}(P^+),\\ \mathcal{C}_\delta^{-,-} &= \{P^+ +\mu_1 v_1(P^+)+\mu_2 v_2(P^+):\mu_1<0,\mu_2<0\}\cap B_{K\delta}(P^+)\end{aligned}$$

with $B_{K\delta}(P^+)$ and K as defined in (4.17). It thus follows from the local, linearly dominated, flow of (4.7) near P^+ (see Lemma 4.4) that the projection in the $v_3(P^+)$-direction of the orbits through L_δ on the linear approximation $\{P^+ + \ \text{span}\,\{v_1(P^+),v_2(P^+)\}\}$ of $\mathcal{W}^u(P^+)$ covers the union $\mathcal{C}_\delta^{+,+}\cup\mathcal{C}_\delta^{-,-}$ for $\alpha>0$ and $\mathcal{C}_\delta^{+,-}\cup\mathcal{C}_\delta^{-,+}$ for $\alpha<0$; see Figure 18. Note that this settles the issue of the *twist condition*: this result provides the necessary insight on how $\mathcal{W}^u(P^-)$ is torn into two parts and how these parts are spread over $\mathcal{W}^u(P^+)$ as $\mathcal{W}^u(P^-)$ passes near P^+.

The proof for $\ell=2$ is concluded by explicitly determining the intersection of $\mathcal{W}^u(P^+)$ and $\mathcal{W}^s(\tilde{P}^+)$, i.e., by determining the location of the unique trivial defect solution connecting

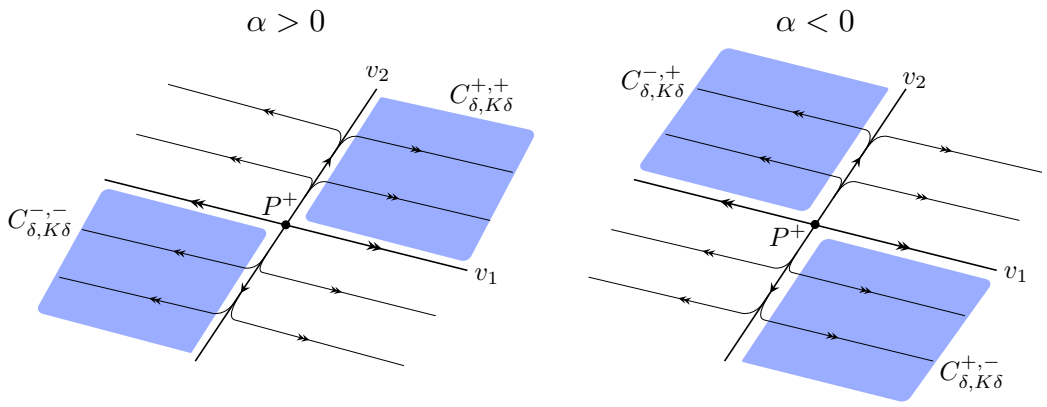

Figure 18. *The blue areas represent the projections in the $v_3(P^+)$-direction of the solutions of (4.7) which are in $\mathcal{W}^u(P^-)$ with initial conditions on L_δ on the linear approximation $\{P^+ + \text{ span}\{v_1(P^+), v_2(P^+)\}\}$ of $\mathcal{W}^u(P^+)$, restricted to $B_{K\delta}(P^+)$. Left panel: $\alpha > 0$. Right panel: $\alpha < 0$. Observe the $\mathcal{O}(\varepsilon^2)$ gap between the blue areas and the $v_{1,2}$ axes.*

P^+ to $\tilde{P}^+$; see Theorem 1.7. To leading order, this follows from the intersection of the approximations of the linear flow near P^+ and $\tilde{P}^+$:

$$\begin{aligned}
&\begin{pmatrix} 1-\frac{1}{2}\varepsilon\alpha \\ 0 \\ 1-\frac{1}{2}\varepsilon\alpha \\ 0 \end{pmatrix} + \mu_1 \begin{pmatrix} 1 \\ \sqrt{2}(1-\frac{3}{4}\varepsilon\alpha) \\ 0 \\ -\frac{1}{2}\sqrt{2}\varepsilon \end{pmatrix} + \mu_2 \begin{pmatrix} -\frac{1}{2}\varepsilon\alpha \\ 0 \\ 1 \\ 1+\frac{1}{4}\varepsilon\alpha \end{pmatrix} \\
&= \begin{pmatrix} 1-\frac{1}{2}\varepsilon(\alpha+\gamma_2) \\ 0 \\ 1-\frac{1}{2}\varepsilon(\alpha+\gamma_2) \\ 0 \end{pmatrix} + \nu_1 \begin{pmatrix} 1 \\ -\sqrt{2}(1-\frac{3}{4}\varepsilon(\alpha+\gamma_2)) \\ 0 \\ \frac{1}{2}\sqrt{2}\varepsilon \end{pmatrix} + \nu_2 \begin{pmatrix} -\frac{1}{2}\varepsilon\alpha \\ 0 \\ 1 \\ -1-\frac{1}{4}\varepsilon\alpha \end{pmatrix}
\end{aligned} \tag{4.18}$$

up to $\mathcal{O}(\varepsilon^2)$ corrections; see (4.8), (4.9) and Lemma 4.4. Hence,

$$\mu_1 = -\frac{1}{4}\varepsilon\gamma_2 + \mathcal{O}(\varepsilon^2),\ \mu_2 = -\frac{1}{4}\varepsilon\gamma_2 + \mathcal{O}(\varepsilon^2),\ \nu_1 = \frac{1}{4}\varepsilon\gamma_2 + \mathcal{O}(\varepsilon^2),\ \nu_2 = \frac{1}{4}\varepsilon\gamma_2 + \mathcal{O}(\varepsilon^2).$$

Note that it thus follows that the projection of $\mathcal{W}^u(P^+) \cap \mathcal{W}^s(\tilde{P}^+)$ on the linear approximation of $\mathcal{W}^u(P^+)$ is in $\mathcal{C}_\delta^{-,-}$ for $\gamma_2 > 0$ and in $\mathcal{C}_\delta^{+,+}$ for $\gamma_2 < 0$, respectively. Thus we may conclude that $\mathcal{W}^u(P^+) \cap \mathcal{W}^s(\tilde{P}^+)$ is covered by $\mathcal{W}^u(P^-)$ for $\alpha > 0$, independent of the sign of γ_2, and cannot be reached by $\mathcal{W}^u(P^-)$ if $\alpha < 0$. Since the intersection $\mathcal{W}^u(P^+) \cap \mathcal{W}^s(\tilde{P}^+) \in \mathcal{C}_\delta^{-,-}$ is transversal under an $\mathcal{O}(1)$ angle and since $|P^+ - \tilde{P}^+| = \mathcal{O}_s(\varepsilon)$, the existence of the local defect solution $\Gamma_{\text{het,ld}}(\xi)$ follows, for $\ell = 2$, from the singular slow/fast nature of the almost linear flow of (4.7) $\mathcal{O}(\delta)$ near P^+ and $\tilde{P}^+$. The statement of the distance in phase space between the orbits $\Gamma_{\text{het,ld}}(\xi)$ and $\Gamma_{\text{het}}(\xi)$ is a direct consequence of the construction of $\Gamma_{\text{het,ld}}(\xi)$ from $\Gamma_{\text{het}}(\xi)$.

The proof of the theorem in the $\ell = 3$ case runs along the same lines as for $\ell = 2$. First, we define the $\ell = 3$-version of L_δ,

$$L_\delta = \mathcal{W}^u(P^-) \cap \{\delta v_4(P^+) + \text{ span}\{v_1(P^+), v_2(P^+), v_3(P^+), v_5(P^+)v_6(P^+)\}\} \cap B_{K\delta}(P^+)$$

with $B_{K\delta}(P^+)$ and K as defined in the $\ell = 2$ case. That is, L_δ is the intersection of $\mathcal{W}^u(P^-)$ with a five-dimensional hyperplane that is an $O(\delta)$ translation in the direction $v_4(P^+)$, the slowest stable eigenvalue along which $\Gamma_{\text{het}}(\xi)$ approaches P^+. The hyperplane is spanned by an extension of the linear approximation of $\mathcal{W}^u(P^+)$ in directions independent of the translation (compare to (4.17) and see Lemma 4.4). Note that L_δ is two-dimensional. It follows from exactly the same arguments as in the $\ell = 2$ case, either based on [18] or on [38], that L_δ must be squeezed asymptotically close to the δ translation of the two-dimensional linear space spanned by the slow unstable eigenvectors $v_2(P^+)$ and $v_3(P^+)$.

In the $\ell = 2$ case, the next crucial step was to observe that the distinction between the inside and outside parts of $\mathcal{W}^u(P^-)$ with respect to the span $\mathcal{W}^s(\mathcal{M}^+) \cup \mathcal{W}^u(\mathcal{M}^+)$ can be directly related to the direction of the slow unstable vector $v_2(P^+)$ as $\mathcal{W}^u(P^-)$ travels along $\mathcal{M}^+$. The main difference between the $\ell = 2$ and $\ell = 3$ cases is that for $\ell = 3$ this relation in general cannot be made in a similar straightforward fashion: the distinction between parts of $\mathcal{W}^u(P^-)$ being inside or outside of $\mathcal{W}^s(\mathcal{M}^+) \cup \mathcal{W}^u(\mathcal{M}^+)$ is now determined by the sign of $\alpha v + \beta w$ at the intersection with $\{u = 0\}$ (4.14), as well as when $\Gamma_{\text{het}}(\xi)$ touches down on $\mathcal{M}^+$; see (4.15) and (4.16). This is a sum of v- and w-components and thus does not directly yield information on the individual $v_2(P^+)$- and $v_3(P^+)$-directions of $\mathcal{W}^u(P^-)$ as it flows along $\mathcal{M}^+$. However, the $\ell = 2$ arguments can be followed directly if we assume that both α and β are positive (as assumed in the theorem). In that case, we may indeed conclude that the part of L_δ that is close to the planar half-cone spanned by positive multiples, respectively, negative multiples, of the slow unstable vectors $v_2(P^+)$ and $v_3(P^+)$ must be outside, respectively, inside, the span $\mathcal{W}^s(\mathcal{M}^+) \cup \mathcal{W}^u(\mathcal{M}^+)$. As in the $\ell = 2$ case, our asymptotic analysis only provides results up to $\mathcal{O}(\varepsilon^2)$ corrections, so the inside/outside statements are valid only for elements in L_δ that are at a distance $\gg \varepsilon^2$ from the combined boundaries of the half-cones, $\text{span}\{v_2(P^+)\} \cup \text{span}\{v_3(P^+)\}$. The fast unstable flow of (1.9) near P^+ is in the direction of positive, respectively, negative, multiples of $v_1(P^+)$ outside, respectively, inside, $\mathcal{W}^u(\mathcal{M}^+) \cup \mathcal{W}^s(\mathcal{M}^+)$. Therefore, we define, for $|\mu_{1,2,3}| \gg \varepsilon^2$, the two $\mathcal{O}(\delta)$-sized three-dimensional half-cones,

(4.19)
$$\begin{aligned}
\mathcal{C}_\delta^{+,+,+} &= \{P^+ + \mu_1 v_1(P^+) + \mu_2 v_2(P^+) + \mu_3 v_3(P^+) : \mu_1 > 0, \mu_2 > 0, \mu_3 > 0\} \cap B_{K\delta}(P^+),\\
\mathcal{C}_\delta^{-,-,-} &= \{P^+ + \mu_1 v_1(P^+) + \mu_2 v_2(P^+) + \mu_3 v_3(P^+) : \mu_1 < 0, \mu_2 < 0, \mu_3 < 0\} \cap B_{K\delta}(P^+)
\end{aligned}$$

with $B_{K\delta}(P^+)$ and K as defined before. Like for $\ell = 2$, it follows from the characteristics of the flow of (1.9) near P^+ that the projection in the $v_4(P^+)$-direction of the orbits through L_δ on the linear approximation $\{P^+ + \text{span}\{v_1(P^+), v_2(P^+), v_3(P^+)\}\}$ of $\mathcal{W}^u(P^+)$ covers the union $\mathcal{C}_\delta^{+,+,+} \cup \mathcal{C}_\delta^{-,-,-}$. Note that the difference with the $\ell = 2$ case is that this is not a complete description of how $\mathcal{W}^u(P^-)$ spreads over $\mathcal{W}^u(P^+)$: $\mathcal{W}^u(P^-)$ also covers other parts of $\mathcal{W}^u(P^+)$. However, these parts of the cover originate from subsets of L_δ for which the present arguments do not provide insight on whether these are inside or outside of $\mathcal{W}^u(\mathcal{M}^+) \cup \mathcal{W}^s(\mathcal{M}^+)$. Such insight is not needed for $\alpha, \beta > 0$.

Next, we again determine the intersection of $\mathcal{W}^u(P^+)$ and $\mathcal{W}^s(\tilde{P}^+)$ (as in (4.18) for $\ell = 2$). With $\mu_{1,2,3}$ as defined in (4.19), i.e., similar to (4.18), we again find

$$\mu_1 = -\frac{1}{4}\varepsilon\gamma_2 + \mathcal{O}(\varepsilon^2),\ \mu_2 = -\frac{1}{4}\varepsilon\gamma_2 + \mathcal{O}(\varepsilon^2),\ \mu_3 = -\frac{1}{4}\varepsilon\gamma_2 + \mathcal{O}(\varepsilon^2).$$

Hence, it again follows that the projection of $\mathcal{W}^u(P^+) \cap \mathcal{W}^s(\tilde{P}^+)$ on the linear approximation of $\mathcal{W}^u(P^+)$ is in $\mathcal{C}_\delta^{+,+,+} \cup \mathcal{C}_\delta^{-,-,-}$, independent of the sign of γ_2. The statement of the theorem now follows by exactly the same final arguments as for $\ell = 2$. ∎

Due to the reversibility symmetry (4.10) of systems (4.7) and (1.9), the formulation of the equivalent of Theorem 4.7 for the homoclinic 2-front orbits of Theorem 4.6 is very similar to that of Theorem 4.7.

Theorem 4.8. *Let $\gamma(\xi)$ be as in (1.3) and let ε be small enough. Moreover, let $\alpha, \beta, \gamma_{1,2} \in \mathbb{R}$ be $\mathcal{O}(1)$ with respect to ε such that the homogeneous version of (1.2) (that is, (1.2) with $\gamma(\xi) = \gamma_1$) supports a homoclinc 2-front orbit $\Gamma_{\mathrm{hom}}(\xi)$ to $P_1^{\gamma_1} \overset{\mathrm{def}}{=} P^- = P^+$ (see Theorem 4.6 with $\gamma = \gamma_1$).*

- *$\ell = 2$: Then, there exists a local defect homoclinic 2-front orbit $\Gamma_{\mathrm{hom,defect}}(\xi)$ to (4.7) that connects P^- to $\tilde{P}^- \overset{\mathrm{def}}{=} P_1^{\gamma_2}$ if and only if in $\alpha > 0$.*
- *$\ell = 3$: Then, there exists a local defect heteroclinic orbit $\Gamma_{\mathrm{hom,defect}}(\xi)$ to (1.9) that connects P^- to $\tilde{P}^-$ for $\alpha, \beta > 0$.*

The orbit of the local defect $\Gamma_{\mathrm{hom,defect}}(\xi)$ in the 2ℓ-dimensional phase space of (4.7)/(1.9) is $\mathcal{O}(\varepsilon)$ close to that $\Gamma_{\mathrm{hom}}(\xi)$.

Note that since we assume that $\alpha, \beta > 0$ for $\ell = 3$, we have implicitly assumed that γ_1 is also positive for $\ell = 3$; see the statement of Theorem 4.6.

Proof. To prove this theorem, we may concentrate on the structure and orientation of $\mathcal{W}^u(P^-)$ as it jumps back from $\mathcal{M}^+$ to $\mathcal{M}^-$, touches down on $\mathcal{M}^-$, and flows back toward P^-; see [17] and especially Figure 4 therein for the full details of the geometric setting. The proof of Theorem 4.7 is crucially based on the fact that $\mathcal{W}^u(P^-) \subset \mathcal{W}^u(\mathcal{M}^-)$, which enables us to study the character of the intersection $\mathcal{W}^u(\mathcal{M}^-) \cap \mathcal{W}^s(\mathcal{M}^+)$ to distinguish between parts of $\mathcal{W}^u(P^-)$ that are inside or outside the span $\mathcal{W}^u(\mathcal{M}^+) \cup \mathcal{W}^s(\mathcal{M}^+)$. Since $\mathcal{W}^u(P^-)$ is not a subset of $\mathcal{W}^u(\mathcal{M}^+)$ we cannot directly copy these arguments to the jump-back case associated to the intersection $\mathcal{W}^u(\mathcal{M}^+) \cap \mathcal{W}^s(\mathcal{M}^-)$ and its relation to being inside or outside the span $\mathcal{W}^u(\mathcal{M}^-) \cup \mathcal{W}^s(\mathcal{M}^-)$. However, since $\mathcal{W}^u(P^-)$ is exponentially close with respect to ε to $\mathcal{M}^+$ during its passage along $\mathcal{M}^+$, $\mathcal{W}^u(P^-)$ must also be exponentially close with respect to ε to $\mathcal{W}^u(\mathcal{M}^-)$ during its jump back to $\mathcal{M}^-$. The intersection of $\mathcal{W}^u(\mathcal{M}^+)$ with $\mathcal{W}^s(\mathcal{M}^-)$ is transversal with an $\mathcal{O}(\varepsilon)$ angle. So, on second thought, we indeed can apply the same arguments as in the proof of Theorem 4.7: in the context of our geometric arguments there is no relevant distinction between $\mathcal{W}^u(P^-)$ being a subset of $\mathcal{W}^u(\mathcal{M}^-)$ or being exponentially close with respect to ε to $\mathcal{W}^u(\mathcal{M}^-)$.

We can now prove the theorem by copying the arguments in the proof of Theorem 4.7 or directly conclude the validity of Theorem 4.7 by applying and interpreting the reversibility symmetry (4.10). ∎

Remark 4.9. The results on the three-component model (1.2) as formulated in Theorems 4.7 and 4.8 only consider the case $\alpha, \beta > 0$. From the mathematical point of view this is quite a restriction, since only for this case we have been able to obtain sufficient "control" over the way $\mathcal{W}^u(P^-)$ "spreads out" over $\mathcal{W}^u(P^+)$—see the proof of Theorem 4.7. If $\mathrm{sign}(\alpha) \neq \mathrm{sign}(\beta)$, the geometrical structure of $\mathcal{W}^u(P^-)$ as it passes along P^+ is expected to be more intricate and the approach in the proof of Theorem 4.7 does not yield sufficiently accurate information. This calls for a nontrivial extension of the approach developed in the proof of

Theorem 4.7, which we do not go into here. For similar reasons, the proof of Theorem 4.7 also does not provide a statement on the possible existence of two distinct local defect solutions, as can be expected from Theorem 3.11 since all $k = 3$ unstable eigenvalues are real. It is natural to expect that this may indeed be the case if $\text{sign}(\alpha) \neq \text{sign}(\beta)$ in (1.2). However, note that from the modeling point of view, i.e., with the background of (1.2) as model for gas-discharge dynamics in mind, both α and β must be positive [50, 55, 58].

5. Outlook. In this manuscript, we investigated the *existence* of localized defect patterns in PDE systems with a small heterogeneity of jump-type, assuming that the unperturbed homogeneous stationary ODE reduction has a heteroclinic orbit connecting two hyperbolic equilibrium points $P^{\pm}$ corresponding to a localized structure in the PDE context. We distinguished between three types of defect solutions: *global defect solutions* in which the jump occurs away from the endpoints P^- and P^+ of the heteroclinic orbit (see Definition 1.4, the left panel of Figure 1 and the right panel of Figure 3), (two kinds of) *local defect solutions* in which the jump occurs asymptotically close to one of the endpoints (see Definition 1.4, the center panel and right panel of Figure 1, and the middle two panels of Figure 3), and *trivial defect solutions* in which the jump occurs asymptotically close to both of the endpoints (see Definition 1.4 and the left panel of Figure 3). The existence of a unique trivial defect solution is straightforward and follows directly from the *local stable and unstable manifold theorem.* The remainder of the manuscript focused entirely on local defect solutions, the far simpler case compared to global defect solutions since the core of the analysis takes place near an equilibrium point and the ODE near this equilibrium point behaves, to leading order, as a linear system. Consequently, the geometry of the flow is very well understood. We established the persistence, or nonpersistence, of the original heteroclinic orbit into various kinds of heteroclinic connections in the discontinuous, nonautonomous ODE reduction associated with the heterogeneous PDE. The persistence result is richer than a priori could be expected, especially in the most interesting, and perhaps most relevant, case in which the dimension of the unstable manifold $\mathcal{W}^u(P^-)$ of P^- equals the dimension of the unstable manifold $\mathcal{W}^u(P^+)$ of P^+—which is by definition the case if the original localized structure is of pulse type so that the connecting orbit in the ODE reduction is a homoclinic orbit to $P^- = P^+$. We have shown that the local defect solution may be unique, or that there can be a well-defined finite number (which may be asymptotically large) of local defect solutions, or that there can be countably many local defect solutions. We provided an explicit example of the latter in the context of a heterogeneous eFK equation. Finally, we applied the general theory to the setting of the three-component FHN system (1.2) that originally motivated this research, thereby explicitly connecting the existence of the local defect solutions plotted in the center panel and right panel of Figure 1 to the signs of some of the parameters in the model.

The pinned stationary local defect solutions considered here are the most simple defect solutions and we only considered PDE systems with very simple spatial heterogeneities. Consequently, the theory developed in this manuscript is only the very first step toward understanding (the dynamics of) local defect patterns. Apart from considering defects that differ from the small simple (single) jump-type defects studied here, there are at least three next steps to be taken:

- Throughout this manuscript, we assumed that there exists a heteroclinic orbit Γ in the unperturbed system (1.4),

$$\dot{u} = f(u), \qquad u(t) : \mathbb{R} \to \mathbb{R}^n. \tag{5.1}$$

  Thus, Γ corresponds to a stationary localized solution in the homogeneous PDE. However, one may also expect pinned stationary defect solutions in heterogeneous PDEs for which the homogeneous limit does not have a corresponding stationary localized pattern. Typically, there does exist a *traveling* localized structure in the homogeneous limit in such cases, which indeed gets pinned by the defect and thus corresponds to the stationary solution of the heterogeneous system; see, for example, [15, 16, 31, 41]. As a very explicit example we mention the pinned *global* defect solutions of (1.2) with $\gamma_1 \neq \gamma_2$ and both $\gamma_{1,2} \neq 0$ in (1.3) that travel with nonzero speed—but $\mathcal{O}(\varepsilon)$ slow—in the homogeneous limit $\gamma(x) \equiv \gamma_1$; see [31]. Thus, instead of assuming the existence of a heteroclinic orbit in (5.1), one should in this case base the existence of local defect solutions on the assumption that there exists a heteroclinic orbit in a perturbed version of (5.1),

$$\dot{u} = f(u;\varepsilon) + \varepsilon c(u;\varepsilon), \qquad u(t) : \mathbb{R} \to \mathbb{R}^n \tag{5.2}$$

  (cf. Remark 1.13), where the smooth function $c(u;\varepsilon)$ may model the (linear) effect of traveling with a certain (asymptotically small) speed, but it may also directly relate to $g(u)$ in the case that one wants to study the existence of local defect solutions near P^- by inverting time and under the assumption that there is a homoclinic orbit in (5.1); see Remark 1.12. It can be expected that most existence results of the present manuscript persist in this case.
- An existence theory like in the present manuscript should necessarily be followed by a PDE analysis of the stability of the defect patterns. This is in general a much harder problem and has already been considered for specific PDEs in a number of articles in the literature, e.g., [15, 16, 31, 37, 40, 41, 45, 46]. In future research, we will consider this problem in a general setting by assuming that the linearized spectral problem associated to the localized structure that corresponds to the unperturbed heteroclinic orbit of (5.1) only has stable spectrum bounded away from the imaginary axis, except for the zero eigenvalue associated to the translational symmetry of the homogeneous PDE. A small spatial heterogeneity is expected to have at most an $\mathcal{O}(\varepsilon)$ effect on this eigenvalue—which thus will decide about the stability of the defect pattern. Note that the *derivative of the wave* is, in general, not an eigenfunction of the spectral problem in the heterogeneous case since it is nonsmooth; hence $\lambda = 0$ is in general not expected to be an eigenvalue of the defect pattern. The perturbation analysis developed here is expected to form a foundation of an asymptotic analysis by which one can explicitly approximate this $\mathcal{O}(\varepsilon)$ small eigenvalue; see for instance, [15, 16, 31, 40, 41].
- The pinned stationary defect patterns represent the limit states of an interaction process between one or more localized states and the heterogeneity in the PDE model; see, for instance, the simulations shown in [31]. In [22, 23, 54, 56], a mathematical framework has been developed by which the weak interactions between localized structures

such as pulses or fronts can be described in the form of low-dimensional ODEs. As a next step in understanding defect solutions in systems with small jump-type heterogeneities, one would like to use these methods to obtain an explicit reduction of the interaction between localized structures and the defect into a similar low-dimensional ODE. Since the implicit assumption underlying the methods of [22, 23, 54, 56] is that the distance between *weakly interacting* structures does not become *too small*, it is unlikely that the entire process—with the stationary pinned defect as limit state—can be described by these methods. However, as with the FHN example of section 4.2, it is expected that it is possible to obtain such an analytical control over the full localized structure-defect interaction process in the setting of singularly perturbed models. In such systems, the interaction between localized structures typically is of semi-strong type [19], and it is to be expected that the methods developed in [1, 20, 30] can be extended to also incorporate the semi-strong interactions between a localized state—that may be either stationary or slowly traveling in the homogeneous limit—and a defect. The renormalization group method of [1, 20, 30], which is based on [54], needs both the existence and the stability analysis as *input*, hence this step can be taken only after the preceding ones.

REFERENCES

[1] T. Bellsky, A. Doelman, T. J. Kaper, and K. Promislow, *Adiabatic stability under semi-strong interactions: The weakly damped regime*, Indiana Univ. Math. J., 62 (2013), pp. 1809–1859.

[2] D. L. Benson, J. A. Sherrat, and P. K. Maini, *Diffusion driven instability in an inhomogeneous domain*, Bull. Math. Biol., 55 (1993), pp. 365–384.

[3] M. di Bernardo, C. Budd, and A. Champneys, *Grazing, skipping and sliding: Analysis of the non-smooth dynamics of the DC/DC buck converter*, Nonlinearity, 11 (1998), pp. 859–890.

[4] P. K. Brazhnik and J. J. Tyson, *Steady-state autowave patterns in a two-dimensional excitable medium with a band of different excitability*, Phys. D, 102 (1997), pp. 300–312.

[5] M. Bode, A. W. Liehr, C. P. Schenk, and H.-G. Purwins, *Interaction of dissipative solitons: Particle-like behaviour of localized structures in a three-component reaction-diffusion system*, Phys. D, 161 (2002), pp. 45–66.

[6] Ch.-N. Chen and Y. S. Choi, *Standing pulse solutions to FitzHugh–Nagumo equations*, Arch. Ration. Mech. Anal., 206 (2012), pp. 741–777.

[7] Ch.-N. Chen and X. Hu, *Stability analysis for standing pulse solutions to FitzHugh–Nagumo equations*, Calc. Var. Partial Differential Equations, 49 (2014), pp. 827–845.

[8] Ch.-N. Chen, S.-Y. Kung, and Y. Morita, *Planar Standing Wavefronts in the FitzHugh–Nagumo Equations*, SIAM J. Math. Anal., 46 (2014), pp. 657–690.

[9] M. Chirilus-Bruckner, A. Doelman, P. van Heijster, and J. D. M. Rademacher, *Butterfly catastrophe for fronts in a three-component reaction-diffusion system*, J. Nonlinear Sci., 25 (2015), pp. 87–129.

[10] J. Cortes, *Discontinuous dynamical systems*, IEEE Trans. Control Systems, 28 (2008), pp. 36–73.

[11] P. Coullet, C. Elphick, and D. Repaux, *Nature of spatial chaos*, Phys. Rev. Lett., 58 (1987), pp. 431–434.

[12] G. T. Dee and W. van Saarloos, *Bistable systems with propagating fronts leading to pattern formation*, Phys. Rev. Lett., 60 (1988), pp. 2641–2644.

[13] B. Deng, *Exponential expansion with principal eigenvalues. Nonlinear dynamics, bifurcations and chaotic behavior*, Internat. J. Bifu. Chaos Appl. Sci. Engrg. 6 (1996), pp. 1161–1167.

[14] G. Derks, *Stability of fronts in inhomogeneous wave equations*, Acta Appl. Math., 137 (2014), pp. 61–78.

[15] G. Derks, A. Doelman, C. J. K. Knight, and H. Susanto, *Pinned fluxons in a Josephson junction with a finite-length inhomogeneity*, European J. Appl. Math., 23 (2012), pp. 201–244.
[16] G. Derks, A. Doelman, S. A. van Gils, and H. Susanto, *Stability analysis of π-kinks in a $0-\pi$ Josephson junction*, SIAM J. Appl. Dyn. Syst., 6 (2007), pp. 99–141.
[17] A. Doelman, P. van Heijster, and T. J. Kaper, *Pulse dynamics in a three-component system: Existence analysis*, J. Dynam. Differential Equations, 21 (2009), pp. 73–115.
[18] A. Doelman and P. Holmes, *Homoclinic explosions and implosions*, Philos. Trans. R. Soc. Lond. Ser. A Math. Phys. Eng. Sci., 354 (1996), pp. 845–893.
[19] A. Doelman and T. J. Kaper, *Semistrong pulse interactions in a class of coupled reaction-diffusion equations*, SIAM J. Appl. Dyn. Syst., 2 (2003), pp. 53–96.
[20] A. Doelman, T. J. Kaper, and K. Promislow, *Nonlinear asymptotic stability of the semistrong pulse dynamics in a regularized Gierer-Meinhardt model*, SIAM J. Math. Anal., 38 (2007), pp. 1760–1787.
[21] N. Dirr and N. K. Yip, *Pinning and de-pinning phenomena in front propagation in heterogeneous media*, Interface. Free Bound., 8 (2006), pp. 79–109.
[22] S.-I. Ei, *The motion of weakly interacting pulses in reaction-diffusion systems*, J. Dynam. Differential Equations, 14 (2002), pp. 85–137.
[23] S.-I. Ei, M. Mimura, and M. Nagayama, *Pulse-pulse interaction in reaction-diffusion systems*, Phys. D, 165 (2002), pp. 176–198.
[24] E. Goldobin, K. Vogel, O. Crasser, R. Walser, W. P. Schleich, D. Koelle, and R. Kleiner, *Quantum tunneling of semifluxons in a 0-π-0 long Josephson junction*, Phys. Rev. B, 72 (2005), 054527.
[25] N. Fenichel, *Persistence and smoothness of invariant manifolds for flows*, Indiana Univ. Math. J., 21 (1971), pp. 193–226.
[26] N. Fenichel, *Geometric singular perturbation theory for ordinary differential equations*, J. Differential Equations, 31 (1979), pp. 53–98.
[27] A. F. Filippov, *Differential Equations with Discontinuous Righthand Sides*, Kluwer, Norwell, MA, 1988.
[28] R. A. Fisher, *The wave of advance of advantageous genes*, Ann. Eugenic., 7 (1937), pp. 355–369.
[29] P. van Heijster, A. Doelman, and T. J. Kaper, *Pulse dynamics in a three-component system: Stability and bifurcations*, Phys. D, 237 (2008), pp. 3335–3368.
[30] P. van Heijster, A. Doelman, T. J. Kaper, and K. Promislow, *Front interactions in a three-component system*, SIAM J. Appl. Dyn. Syst., 9 (2010), pp. 292–332.
[31] P. van Heijster, A. Doelman, T. J. Kaper, Y. Nishiura, and K.-I. Ueda, *Pinned fronts in heterogeneous media of jump type*, Nonlinearity, 24 (2011), pp. 127–157.
[32] P. van Heijster, H. Hardway, T. J. Kaper, and C. A. Bradham, *A computational model for BMP movement in sea urchin embryos*, J. Theoret. Biol., 363 (2014), pp. 277–289.
[33] P. van Heijster and B. Sandstede, *Planar radial spots in a three-component FitzHugh–Nagumo system*, J. Nonlinear Sci., 21 (2011), pp. 705–745.
[34] P. van Heijster and B. Sandstede, *Bifurcations to travelling planar spots in a three-component FitzHugh–Nagumo system*, Phys. D, 275 (2014), pp. 19–34.
[35] A. J. Homburg and B. Sandstede, *Homoclinic and heteroclinic bifurcations in vector fields*, in Handbook of Dynamical Systems, Vol. 3, North-Holland, Amsterdam, 2010, pp. 379–524.
[36] H. Ikeda and S.-I. Ei, *Front dynamics in heterogeneous diffusive media*, Physica D, 239 (2010), pp. 1637–1649.
[37] R. K. Jackson, R. Marangell, and H. Susanto, *An instability criterion for nonlinear standing waves on nonzero backgrounds*, J. Nonlinear Sci., 24 (2014), pp. 1177–1196.
[38] C. K. R. T. Jones, T. J. Kaper, and N. Kopell, *Tracking invariant manifolds up to exponentially small errors*, SIAM J. Math. Anal., 27 (1996), pp. 558–577.
[39] W. D. Kalies and R. C. A. M. van der Vorst, *Multitransition homoclinic and heteroclinic solutions of the extended Fisher–Kolmogorov equation*, J. Differential Equations, 131 (1996), pp. 209–228.
[40] C. J. K. Knight and G. Derks, *A stability criterion for the non-linear wave equation with spatial inhomogeneity*, J. Differential Equations, 259 (2015), pp. 4745–4762.
[41] C. J. K. Knight, G. Derks, A. Doelman, and H. Susanto, *Stability of stationary fronts in a nonlinear wave equation with spatial inhomogeneity*, J. Differential Equations, 254 (2013), pp. 408–468.

[42] R. Kollár and A. Scheel, *Coherent structures generated by inhomogeneities in oscillatory media*, SIAM J. Appl. Dyn. Syst., 6 (2007), pp. 236–262.
[43] A. N. Kolmogorov, I. G. Petrovsky, and N. S. Piskunov, *Etude de l'eq́uation de la diffusion avec croissance de la quantité de matière et son application à un problème biologique*, Moscow Univ. Math. Bull., 1 (1937), pp. 1–25.
[44] A. C. J. Luo, *Discontinuous Dynamical Systems*, Springer, Berlin, 2012.
[45] R. Marangell, C. K. R. T. Jones, and H. Susanto, *Localized standing waves in inhomogeneous Schrödinger equations*, Nonlinearity, 23 (2010), pp. 2059–2080.
[46] R. Marangell, H. Susanto, and C. K. R. T. Jones, *Unstable gap solitons in inhomogeneous nonlinear Schrödinger equations*, J. Differential Equations, 253 (2012), pp. 1191–1205
[47] D. W. McLaughlin and A. C. Scott, *Perturbation analysis of fluxon dynamics*, Phys. Rev. A, 18 (1978), pp. 1652–1680.
[48] J. D. Meiss, *Differential Dynamical Systems*, Math. Model. Comput., 14, SIAM, Philidelphia, 2007.
[49] Y. Nishiura, T. Teramoto, and K.-I. Ueda, *Scattering and separators in dissipative systems*, Phys. Rev. E, 67 (2003), 056210.
[50] M. Or-Guil, M. Bode, C. P. Schenk, and H.-G. Purwins, *Spot bifurcations in three-component reaction- diffusion systems: The onset of propagation*, Phys. Rev. E, 57 (1998), pp. 6432–6437.
[51] C. M. Pegrum, *Can a fraction of a quantum be better than a whole one?* Science, 312 (2006), pp. 1483–1484.
[52] L. A. Peletier and W. C. Troy, *A topological shooting method and the existence of kinks of the extended Fisher–Kolmogorov equation*, Topol. Methods Nonlinear Anal. 6 (1995), pp. 331–355.
[53] L. A. Peletier and W. C. Troy, *Spatial Patterns: Higher Order Models in Physics and Mechanics*, Birkhäuser, Boston, 2001.
[54] K. Promislow, *A renormalization method for modulational stability of quasi-steady patterns in dispersive systems*, SIAM J. Math. Anal., 33 (2002), pp. 1455–1482.
[55] H.-G. Purwins and L. Stollenwerk, *Synergetic aspects of gas-discharge: Lateral patterns in DC systems with a high ohmic barrier*, Plasma Phys. Contr. F., 56 (2014), 123001.
[56] B. Sandstede, *Stability of travelling waves*, in Handbook of Dynamical Systems, Vol. 3, North-Holland, Amsterdam, 2002, pp. 983–1055.
[57] B. Sandstede and A. Scheel, *Defects in oscillatory media: towards a classification*, SIAM J. Appl. Dyn. Syst., 3 (2004), pp. 1–68.
[58] C. P. Schenk, M. Or-Guil, M. Bode, and H.-G. Purwins, *Interacting pulses in three-component reaction-diffusion systems on two-dimensional domains*, Phys. Rev. Lett., 78 (1997), pp. 3781–3784.
[59] L. P. Shilnikov, A. L. Shilnikov, D. V. Turaev, and L. O. Chua, *Methods of Qualitative Theory in Nonlinear Dynamics. Part I*, Ser. Nonlinear Sci. Ser. A 4, World Scientific, Hackensak, NJ, 1998.
[60] H. Susanto, E. Goldobin, D. Koelle, R. Kleiner, and S. A. van Gils, *Controllable plasma energy bands in a one-dimensional crystal of fractional Josephson vortices*, Phys. Rev. B, 71 (2005), 174510.
[61] K. R. Swanson, E. C. Alvord, and J. D. Murray, *A quantitative model for differential motility of gliomas in grey and white matter*, Cell Proliferat., 33 (2000), pp. 317–329.
[62] D. M. Umulis, O. Shimmi, M. B. O'Conner, and H. G. Othmer, *Organism-scale modeling of early drosophila patterning via bone morphogenetic proteins*, Dev. Cell, 18 (2010), pp. 260–274.
[63] V. K. Vanag and I. R. Epstein, *Localized patterns in reaction-diffusion systems*, Chaos, 17 (2007), 037110.
[64] X. Yuan, T. Teramoto, and N. Nishiura, *Heterogeneity-induced defect bifurcation and pulse dynamics for a three-component reaction-diffusion system*, Phys. Rev. E, 75 (2007), 036220.
[65] W. Zimmerman, *Propagating fronts near a Lifshitz point*, Phys. Rev. Lett., 66 (1991), 1546.